ETSI TR 138 922 V19.3.0 (2026-02)

TECHNICAL REPORT

5G;
Study on International Mobile Telecommunications (IMT) parameters for 4400 - 4800 MHz, 7125 - 8400 MHz and 14800 - 15350 MHz
(3GPP TR 38.922 version 19.3.0 Release 19)

Reference
RTR/TSGR-0438922vj30

Keywords
5G

ETSI

650 Route des Lucioles
F-06921 Sophia Antipolis Cedex - FRANCE

Tel.: +33 4 92 94 42 00 Fax: +33 4 93 65 47 16

Siret N° 348 623 562 00017 - APE 7112B
Association à but non lucratif enregistrée à la
Sous-Préfecture de Grasse (06) N° w061004871

Intellectual Property Rights

Essential patents

IPRs essential or potentially essential to normative deliverables may have been declared to ETSI. The declarations pertaining to these essential IPRs, if any, are publicly available for **ETSI members and non-members**, and can be found in ETSI SR 000 314: *"Intellectual Property Rights (IPRs); Essential, or potentially Essential, IPRs notified to ETSI in respect of ETSI standards"*, which is available from the ETSI Secretariat. Latest updates are available on the ETSI IPR online database.

Pursuant to the ETSI Directives including the ETSI IPR Policy, no investigation regarding the essentiality of IPRs, including IPR searches, has been carried out by ETSI. No guarantee can be given as to the existence of other IPRs not referenced in ETSI SR 000 314 (or the updates on the ETSI Web server) which are, or may be, or may become, essential to the present document.

Trademarks

The present document may include trademarks and/or tradenames which are asserted and/or registered by their owners. ETSI claims no ownership of these except for any which are indicated as being the property of ETSI, and conveys no right to use or reproduce any trademark and/or tradename. Mention of those trademarks in the present document does not constitute an endorsement by ETSI of products, services or organizations associated with those trademarks.

DECT™, **PLUGTESTS™**, **UMTS™** and the ETSI logo are trademarks of ETSI registered for the benefit of its Members. **3GPP™**, **LTE™** and **5G™** logo are trademarks of ETSI registered for the benefit of its Members and of the 3GPP Organizational Partners. **oneM2M™** logo is a trademark of ETSI registered for the benefit of its Members and of the oneM2M Partners. **GSM**® and the GSM logo are trademarks registered and owned by the GSM Association.

Legal Notice

This Technical Report (TR) has been produced by ETSI 3rd Generation Partnership Project (3GPP).

The present document may refer to technical specifications or reports using their 3GPP identities. These shall be interpreted as being references to the corresponding ETSI deliverables.

The cross reference between 3GPP and ETSI identities can be found at 3GPP to ETSI numbering cross-referencing.

Modal verbs terminology

In the present document "**should**", "**should not**", "**may**", "**need not**", "**will**", "**will not**", "**can**" and "**cannot**" are to be interpreted as described in clause 3.2 of the ETSI Drafting Rules (Verbal forms for the expression of provisions).

"**must**" and "**must not**" are **NOT** allowed in ETSI deliverables except when used in direct citation.

Contents

Foreword

This Technical Report has been produced by the 3rd Generation Partnership Project (3GPP).

The contents of the present document are subject to continuing work within the TSG and may change following formal TSG approval. Should the TSG modify the contents of the present document, it will be re-released by the TSG with an identifying change of release date and an increase in version number as follows:

Version x.y.z

where:

- x the first digit:
  - 1 presented to TSG for information;
  - 2 presented to TSG for approval;
  - 3 or greater indicates TSG approved document under change control.
- y the second digit is incremented for all changes of substance, i.e. technical enhancements, corrections, updates, etc.
- z the third digit is incremented when editorial only changes have been incorporated in the document.

In the present document, modal verbs have the following meanings:

shall indicates a mandatory requirement to do something

shall not indicates an interdiction (prohibition) to do something

The constructions "shall" and "shall not" are confined to the context of normative provisions, and do not appear in Technical Reports.

The constructions "must" and "must not" are not used as substitutes for "shall" and "shall not". Their use is avoided insofar as possible, and they are not used in a normative context except in a direct citation from an external, referenced, non-3GPP document, or so as to maintain continuity of style when extending or modifying the provisions of such a referenced document.

should indicates a recommendation to do something

should not indicates a recommendation not to do something

may indicates permission to do something

need not indicates permission not to do something

The construction "may not" is ambiguous and is not used in normative elements. The unambiguous constructions "might not" or "shall not" are used instead, depending upon the meaning intended.

can indicates that something is possible

cannot indicates that something is impossible

The constructions "can" and "cannot" are not substitutes for "may" and "need not".

will indicates that something is certain or expected to happen as a result of action taken by an agency the behaviour of which is outside the scope of the present document

will not indicates that something is certain or expected not to happen as a result of action taken by an agency the behaviour of which is outside the scope of the present document

might indicates a likelihood that something will happen as a result of action taken by some agency the behaviour of which is outside the scope of the present document

might not indicates a likelihood that something will not happen as a result of action taken by some agency the behaviour of which is outside the scope of the present document

In addition:

is (or any other verb in the indicative mood) indicates a statement of fact

is not (or any other negative verb in the indicative mood) indicates a statement of fact

The constructions "is" and "is not" do not indicate requirements.

1 Scope

The present document is a technical report for the study item on IMT parameters for 4400 to 4800 MHz, 7125 to 8400 MHz and 14800 to 15350 MHz frequency ranges. It covers the study on transmitter and receiver characteristics for both NR BS and NR UE, and related parameters, including co-existence studies, AAS antenna models, and responses to the ITU-R W5PD's requests as well as three additional questions.

Findings and evaluations captured in this technical report are based on the Rel-18 version of the NR specifications, unless otherwise stated.

Related LS replies for each of the frequency ranges in question were sent out to ITU-R W5PD in [4, 5, 6].

2 References

The following documents contain provisions which, through reference in this text, constitute provisions of the present document.

- References are either specific (identified by date of publication, edition number, version number, etc.) or non-specific.
- For a specific reference, subsequent revisions do not apply.
- For a non-specific reference, the latest version applies. In the case of a reference to a 3GPP document (including a GSM document), a non-specific reference implicitly refers to the latest version of that document *in the same Release as the present document*.

[1] 3GPP TR 21.905: "Vocabulary for 3GPP Specifications".

[2] (Void)

[3] (Void)

[4] (Void)

[5] (Void)

[6] (Void)

[7] (Void)

[8] (Void)

[9] 3GPP TS 38.104: "NR; Base Station (BS) radio transmission and reception"

[10] 3GPP TS 36.104: "Evolved Universal Terrestrial Radio Access (E-UTRA); Base Station (BS) radio transmission and reception"

[11] 3GPP TS 38.101-3: "NR; User Equipment (UE) radio transmission and reception; Part 3: Range 1 and Range 2 Interworking operation with other radios"

[12] 3GPP TS 38.101-1: "NR; User Equipment (UE) radio transmission and reception; Part 1: Range 1 Standalone"

[13] ITU-R Recommendation SM.329: "Unwanted emissions in the spurious domain"

[14] 3GPP TR 38.921: "Study on International Mobile Telecommunications (IMT) parameters for 6.425 – 7.025 GHz, 7.025 – 7.125 GHz and 10.0. – 10.5 GHz"

[15] C A Balanis, "Antenna Theory Analysis and Design", John Wiley and sons

[16] H. Jin et al., "Massive MIMO Evolution Toward 3GPP Release 18," in IEEE Journal on Selected Areas in Communications, vol. 41, no. 6, pp. 1635-1654, June 2023

[17] Christopher Mollen, Ulf Gustavsson, Thomas Eriksson, Erik G Larsson, “Out of Band radiation Measure for MIMO arrays with beamformed transmission “, Proc. IEEE Int. Conf. Commun., May 2016.

[18] Erik Larsson, Liesbet Van der Perre, “Out of band Radiation for Antenna arrays Clarified”, arXiv : 1802.02745v1, Feb 2018

[19] E. Sienkiewicz, N. McGowan, B. Göransson, T. Chapman and T. Elfström, "Spatially dependent ACLR modelling," 2014 IEEE Conference on Antenna Measurements & Applications (CAMA), Antibes Juan-les-Pins, France, 2014, pp. 1-4,

[20] A. S. Tehrani, H. Cao, S. Afsardoost, T. Eriksson, M. Isaksson and C. Fager, "A Comparative Analysis of the Complexity/Accuracy Trade off in Power Amplifier Behavioural Models," in IEEE Transactions on Microwave Theory and Techniques, vol. 58, no. 6, pp. 1510-1520, June 2010

[21] C. Mollén, U. Gustavsson, T. Eriksson and E. G. Larsson, "Spatial Characteristics of Distortion Radiated From Antenna Arrays With Transceiver Nonlinearities," in IEEE Transactions on Wireless Communications, vol. 17, no. 10, pp. 6663-6679, Oct. 2018.

[22] Y. Zou et al., "Impact of Power Amplifier Nonlinearities in Multi-User Massive MIMO Downlink,” 2015 IEEE Globecom Workshops, San Diego, CA, USA, 2015, pp. 1-7.

[23] P Nandin et al, “Web Lab: A Web based set up for PA digital distortion and Characterisation”, IEEE Microwave Magazine, vol 16, no1, p 138- 140, Feb 2015

[24] (Void)

[25] (Void)

[26] (Void) [27] (Void)

[28] ITU-R Recommendation M.2101: " Modelling and simulation of IMT networks and systems for use in sharing and compatibility studies"[29] (Void)

[30] (Void)

[31] (Void)

[32] (Void)

[33] (Void)

[34] (Void)

3 Definitions of terms, symbols and abbreviations

3.1 Terms

For the purposes of the present document, the terms given in TR 21.905 [1] and the following apply. A term defined in the present document takes precedence over the definition of the same term, if any, in TR 21.905 [1].

array element: subdivision of a passive *antenna array*, consisting of a single radiating element or a group of radiating elements, with a fixed radiation pattern

basic limit: emissions limit relating to the power supplied by a single transmitter to a single antenna transmission line in ITU-R SM.329 [13] used for the formulation of unwanted emission requirements for FR1.

beam: beam (of the antenna) is the main lobe of the radiation pattern of an *antenna array*

NOTE: For certain BS *antenna array*, there may be more than one beam.

beamwidth: beam which has a half-power contour that is essentially elliptical, the half-power beamwidths in the two pattern cuts that respectively contain the major and minor axis of the ellipse

BS type 1-C: NR base station operating at FR1 with requirements set consisting only of conducted requirements defined at individual *antenna connectors*

BS type 1-H: NR base station operating at FR1 with a *requirement set* consisting of conducted requirements defined at individual *TAB connectors* and OTA requirements defined at RIB

BS type 1-O: NR base station operating at FR1 with a *requirement set* consisting only of OTA requirements defined at the RIB

front-to-back ratio: ratio of maximum directivity of an antenna to its directivity in a specified rearward direction

gain: ratio of the radiation intensity, in a given direction, to the radiation intensity that would be obtained if the power accepted by the antenna were radiated in an isotropic manner.

NOTE: If the direction is not specified, the direction of maximum radiation intensity is implied.

operating band: frequency range in which NR operates (paired or unpaired), that is defined with a specific set of technical requirements

radiated interface boundary: *operating band* specific radiated requirements reference where the radiated requirements apply

NOTE: For requirements based on EIRP/EIS, the *radiated interface boundary* is associated to the far-field region

TAB connector: *transceiver array boundary* connector

total radiated power: is the total power radiated by the antenna

NOTE: The *total radiated power* is the power radiating in all direction for two orthogonal polarizations. *Total radiated power* is defined in both the near-field region and the far-field region

transceiver array boundary: conducted interface between the transceiver unit array and the composite antenna

transmission bandwidth: RF Bandwidth of an instantaneous transmission from a UE or BS, measured in resource block units

3.2 Symbols

For the purposes of the present document, the following symbols apply:

A_A	Composite *antenna array* pattern in dBi
A_E	*Array element* pattern in dBi
A_m	Front to back ratio in dB
d_h	Horizontal element separation in meters
d_v	Vertical element separation in meters
$G_{E,max}$	Array element peak gain in dBi
SLA_v	Side lobe suppression in dB
φ_{3dB}	Horizonal half power beamwidth
θ_{3dB}	Vertical half power beamwidth
θ_{etilt}	Electrical down-tilt angle in degrees (defined from antenna array normal and downwards)
φ_{escan}	Electrical scan angle in degrees
φ	Horizontal angle (defined between -180° and 180°).
θ	Vertical angle of the signal direction (defined between -0° and 180°,90° represents the direction perpendicular to the antenna array
N_{RB}	Transmission bandwidth configuration, expressed in resource blocks
$BW_{Channel}$	*BS channel bandwidth*
BW_{Config}	*Transmission bandwidth configuration*, where $BW_{Config} = N_{RB}$ x SCS x 12
Δf	Separation between the *channel edge* frequency and the nominal -3 dB point of the measuring filter closest to the carrier frequency
Δf_{max}	f_offset_{max} minus half of the bandwidth of the measuring filter
Δf_{OBUE}	Maximum offset of the *operating band* unwanted emissions mask from the downlink *operating band* edge
Δf_{OOB}	Maximum offset of the out-of-band boundary from the uplink *operating band* edge

F_C	*RF reference frequency* on the channel raster, given in table 5.4.2.2-1
f_offset	Separation between the *channel edge* frequency and the centre of the measuring
f_offset_{max}	The offset to the frequency Δf_{OBUE} outside the downlink *operating band*
$F_{UL,low}$	The lowest frequency of the uplink *operating band*
$F_{UL,high}$	The highest frequency of the uplink *operating band*
$P_{REFSENS}$	Conducted Reference Sensitivity power level

3.3 Abbreviations

For the purposes of the present document, the abbreviations given in TR 21.905 [1] and the following apply. An abbreviation defined in the present document takes precedence over the definition of the same abbreviation, if any, in TR 21.905 [1].

AAS	Active Antenna System
ACIR	Adjacent Channel Interference Ratio
ACLR	Adjacent Channel Leakage Ratio
ACS	Adjacent Channel Selectivity
AWGN	Additive White Gaussian Noise
BS	Base Station
BW	Bandwidth
EIRP	Effective Isotropic Radiated Power
FDD	Frequency Division Duplex
FR	Frequency Range
FRC	Fixed Reference Channel
IMT	International Mobile Telecommunications
ITU-R	Radiocommunication Sector of the International Telecommunication Union
LA	Local Area
LOS	Line-Of-Sight
MMSE	Minimum Mean Squared Error
MR	Medium Range
MU-MIMO	Multi User- Multiple Input Multiple Output
NLOS	Non-Line-Of-Sight
NR	New Radio
OCNG	OFDMA Channel Noise Generator
OTA	Over The Air
O-to-I	Outdoor-to-Indoor
RB	Resource Block
RF	Radio Frequency
SBFD	Sub-Band Full Duplex
SCS	Sub-Carrier Spacing
TAB	Transceiver Array Boundary
TDD	Time division Duplex
TRP	Total Radiated Power
WA	Wide Area
ZF	Zero Forcing

4 4400 - 4800 MHz frequency range

4.1 General parameters

The general parameters can be extracted from requirements defined for NR operating band n79.

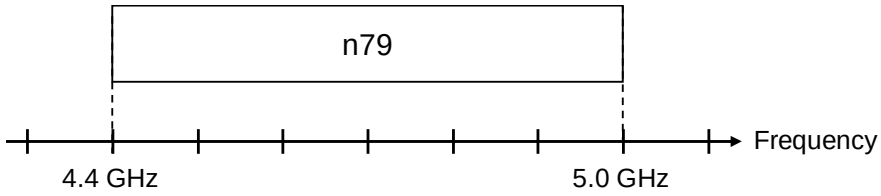

Figure 4.1-1: NR band definition in the 4.4 – 5.0 GHz frequency range

4.1.1 Duplex mode

RAN4 considered TDD as the current duplexing candidate. An enhancement of TDD duplexing, via allowing the simultaneous existence of non-overlapping downlink and uplink sub-band at the BS side within a TDD carrier in a conventional TDD band (i.e., sub-band non-overlapping full duplex), was studied in Rel-18. RAN4 Rel-19 normative work for SBFD operation at the BS side within a TDD carrier is on-going and the requirements and conformance aspects for Rel-19 SBFD work item can be tracked through the list of impacted specifications captured in the respective Work Item description.

4.1.2 Channel Bandwidth

While a number of channel bandwidth would be specified for this frequency range, 100 MHz has been considered as a representative channel bandwidth that is expected to be used.

Channel bandwidths supported by n79 in Rel-18 are listed in Table 4.1.2-1.

Table 4.1.2-1: *BS channel bandwidths* for band n79

NR Band	SCS (kHz)	*BS channel bandwidth* (MHz)															
		3	5	10	15	20	25	30	35	40	45	50	60	70	80	90	100
n79	15			10		20		30		40		50					
	30			10		20		30		40		50	60	70	80	90	100
	60			10		20		30		40		50	60	70	80	90	100

4.1.3 Signal Bandwidth

The signal bandwidth for a NR channel bandwidth signal is calculated based on the NR spectrum utilization for the associated SCS:

$$\text{Signal bandwidth} = N_{RB} \times \text{SCS} \times 12$$

where N_{RB} is the number of resource blocks for particular bandwidth and the associated SCS, as specified in TS 38.104 [9], clause 5.3.2.

4.2 BS parameters

4.2.1 Transmitter characteristics

4.2.1.1 Power dynamic range

There is no power control in downlink and fixed power per resource block is assumed during the study phase. Hence 0 dB power dynamic range was agreed.

4.2.1.2 Spectral mask

The requirement limits applicable for band n79 are re-used. Refer to TS 38.104 [9], clause 6.6.4 for conducted requirements and TS 38.104 [9] Clause 9.7.4.2 for radiated requirements applicable for this range.

4.2.1.3 ACLR

The ACLR limit applicable for band n79 are re-used. Related extracts from TS 38.104 [9], clause 6.6.3 are listed in Table 4.2.1.3-1.

Table 4.2.1.3-1: Base station ACLR limit

***BS channel bandwidth* of *lowest/highest carrier* transmitted $BW_{Channel}$ (MHz)**	**BS adjacent channel centre frequency offset below the lowest or above the highest carrier centre frequency transmitted**	**Assumed adjacent channel carrier (informative)**	**Filter on the adjacent channel frequency and corresponding filter bandwidth**	**ACLR limit**
10, 20, 30, 40, 50, 60, 70, 80, 90,100	$BW_{Channel}$	NR of same BW (Note 2)	Square (BW_{Config})	45 dB
	2 x $BW_{Channel}$	NR of same BW (Note 2)	Square (BW_{Config})	45 dB
NOTE 1: $BW_{Channel}$ and BW_{Config} are the *BS channel bandwidth* and *transmission bandwidth configuration* of the *lowest/highest carrier* transmitted on the assigned channel frequency. NOTE 2: With SCS that provides largest transmission bandwidth configuration (BW_{Config}).				

4.2.1.4 Spurious emissions

The spurious emission limits applicable for band n79 are re-used. Related extracts from TS 38.104 [9] are listed in Table 4.2.1.4-1 and Table 4.2.1.4-2. for conducted requirements.

Table 4.2.1.4-1: General BS transmitter spurious emission limits in FR1, Category A

Spurious frequency range	**Limit**	***Measurement bandwidth***	**Notes**
9 kHz – 150 kHz	-13 dBm	1 kHz	Note 1, Note 4
150 kHz – 30 MHz		10 kHz	Note 1, Note 4
30 MHz – 1 GHz		100 kHz	Note 1
1 GHz 12.75 GHz		1 MHz	Note 1, Note 2
12.75 GHz – 5th harmonic of the upper frequency edge of the DL *operating band* in GHz		1 MHz	Note 1, Note 2, Note 3
NOTE 1: *Measurement bandwidth*s as in ITU-R SM.329, s4.1. NOTE 2: Upper frequency as in ITU-R SM.329, s2.5 table 1. NOTE 3: Applies for Band for which the upper frequency edge of the DL *operating band* is greater than 2.55 GHz and less than or equal to 5.2 GHz. NOTE 4: This spurious frequency range applies only to *BS type 1-C* and *BS type 1-H*.			

Table 4.2.1.4-2: General BS transmitter spurious emission limits in FR1, Category B

Spurious frequency range	Limit	*Measurement bandwidth*	Notes
9 kHz – 150 kHz	-36 dBm	1 kHz	Note 1, Note 4
150 kHz – 30 MHz		10 kHz	Note 1, Note 4
30 MHz – 1 GHz		100 kHz	Note 1
1 GHz – 12.75 GHz	-30 dBm	1 MHz	Note 1, Note 2
12.75 GHz – 5th harmonic of the upper frequency edge of the DL *operating band* in GHz		1 MHz	Note 1, Note 2, Note 3
NOTE 1: *Measurement bandwidth*s as in ITU-R SM.329, s4.1. NOTE 2: Upper frequency as in ITU-R SM.329, s2.5 table 1. NOTE 3: Applies for Band for which the upper frequency edge of the DL *operating band* is greater than 2.55 GHz and less than or equal to 5.2 GHz. NOTE 4: This spurious frequency range applies only to *BS type 1-C* and *BS type 1-H*.			

Additional spurious emissions requirements relevant for band n79 can be found in TS 38.104 [9], clause 6.6.5.2.3 and clause 6.6.5.2.4. Refer to TS 38.104 [9] Clause 9.7.5 for radiated requirements applicable for this range.

4.2.1.5 Maximum output power

The maximum base station output power/ sector (e.i.r.p.) was provided as extracted in Table 4.2.1.5-1. It was agreed to be aligned with antenna characteristics.

Table 4.2.1.5-1: Maximum BS output power in 1710 to 4990 MHz

	Rural	Macro suburban	Macro urban	Small cell outdoor/ Micro urban	Small cell indoor/ Indoor urban
Maximum base station output power/sector (e.i.r.p.) (dBm)	72.2	72.2	72.2	61.5	N/A

The Total Radiated Power (TRP) for two polarizations was agreed as shown in Table 4.2.1.5-2 below.

Table 4.2.1.5-2: Total Radiated Power

Parameter	Rural	Macro Sub-urban	Macro Urban	Micro Urban
Total Radiated Power for two polarizations (dBm)	46	46	46	37

4.2.1.6 Average output power

It was agreed the average output power won't be mentioned in the reply LS.

4.2.2 Receiver characteristics

4.2.2.1 Noise figure

The BS noise figure is listed in Table 4.2.2.1-1.

Table 4.2.2.1-1: Noise figure

BS class	Noise figure (dB)
Wide Area	5
Medium Range	10
Local Area	13

4.2.2.2 Sensitivity

The BS reference sensitivity levels are listed in Table 4.2.2.2-1, Table 4.2.2.2-2 and Table 4.2.2.2-3, as re-used from TS 38.104 [9].

Table 4.2.2.2-1: NR Wide Area BS reference sensitivity levels

BS channel bandwidth **(MHz)**	**Sub-carrier spacing (kHz)**	**Reference measurement channel**	**Reference sensitivity power level, $P_{REFSENS}$ (dBm)**
3	15	G-FR1-A1-7 (Note 1)	-103.6
		G-FR1-A1-21 (Note 6)	-103.6
5, 10, 15	15	G-FR1-A1-1 (Note 1)	-101.7
		G-FR1-A1-10 (Note 3)	-101.7 (Note 2)
10, 15	30	G-FR1-A1-2 (Note 1)	-101.8
10, 15	60	G-FR1-A1-3 (Note 1)	-98.9
20, 25, 30, 35, 40, 45, 50	15	G-FR1-A1-4 (Note 1)	-95.3
		G-FR1-A1-11 (Note 4)	-95.3 (Note 2)
20, 25, 30, 35, 40, 45, 50, 60, 70, 80, 90, 100	30	G-FR1-A1-5 (Note 1)	-95.6
20, 25, 30, 35, 40, 45, 50, 60, 70, 80, 90, 100	60	G-FR1-A1-6 (Note 1)	-95.7

NOTE 1: $P_{REFSENS}$ is the power level of a single instance of the reference measurement channel. This requirement shall be met for each consecutive application of a single instance of the reference measurement channel mapped to disjoint frequency ranges with a width corresponding to the number of resource blocks of the reference measurement channel each, except for one instance that might overlap one other instance to cover the full *BS channel bandwidth*.

NOTE 2: The requirements apply to BS that supports NB-IoT operation in NR in-band.

NOTE 3: $P_{REFSENS}$ is the power level of a single instance of the reference measurement channel. This requirement shall be met for a single instance of G-FR1-A1-10 mapped to the 24 NR resource blocks adjacent to the NB-IoT PRB, and for each consecutive application of a single instance of G-FR1-A1-1 mapped to disjoint frequency ranges with a width of 25 resource blocks each.

NOTE 4: $P_{REFSENS}$ is the power level of a single instance of the reference measurement channel. This requirement shall be met for a single instance of G-FR1-A1-11 mapped to the 105 NR resource blocks adjacent to the NB-IoT PRB, and for each consecutive application of a single instance of G-FR1-A1-4 mapped to disjoint frequency ranges with a width of 106 resource blocks each.

NOTE 6: $P_{REFSENS}$ is the power level of a single instance of the reference measurement channel. This requirement shall be met for a single instance of G-FR1-A1-21 mapped to the 12 NR resource blocks adjacent to the NB-IoT PRB, and for each consecutive application of a single instance of G-FR1-A1-7 mapped to disjoint frequency ranges with a width of 15 resource blocks each.

Table 4.2.2.2-2: NR Medium Range BS reference sensitivity levels

BS channel bandwidth **(MHz)**	**Sub-carrier spacing (kHz)**	**Reference measurement channel (Note 5)**	**Reference sensitivity power level, $P_{REFSENS}$ (dBm)**
3	15	G-FR1-A1-7 (Note 1)	-98.6
		G-FR1-A1-21 (Note 6)	-98.6

5, 10, 15	15	G-FR1-A1-1 (Note 1)	-96.7
		G-FR1-A1-10 (Note 3)	-96.7 (Note 2)
10, 15	30	G-FR1-A1-2 (Note 1)	-96.8
10, 15	60	G-FR1-A1-3 (Note 1)	-93.9
20, 25, 30, 35, 40, 45, 50	15	G-FR1-A1-4 (Note 1)	-90.3
		G-FR1-A1-11 (Note 4)	-90.3 (Note 2)
20, 25, 30, 35, 40, 45, 50, 60, 70, 80, 90, 100	30	G-FR1-A1-5 (Note 1)	-90.6
20, 25, 30, 35, 40, 45, 50, 60, 70, 80, 90, 100	60	G-FR1-A1-6 (Note 1)	-90.7

Note 1: $P_{REFSENS}$ is the power level of a single instance of the reference measurement channel. This requirement shall be met for each consecutive application of a single instance of the reference measurement channel mapped to disjoint frequency ranges with a width corresponding to the number of resource blocks of the reference measurement channel each, except for one instance that might overlap one other instance to cover the full *BS channel bandwidth*.

Note 2: The requirements apply to BS that supports NB-IoT operation in NR in-band.

Note 3: $P_{REFSENS}$ is the power level of a single instance of the reference measurement channel. This requirement shall be met for a single instance of G-FR1-A1-10 mapped to the 24 NR resource blocks adjacent to the NB-IoT PRB, and for each consecutive application of a single instance of G-FR1-A1-1 mapped to disjoint frequency ranges with a width of 25 resource blocks each.

Note 4: $P_{REFSENS}$ is the power level of a single instance of the reference measurement channel. This requirement shall be met for a single instance of G-FR1-A1-11 mapped to the 105 NR resource blocks adjacent to the NB-IoT PRB, and for each consecutive application of a single instance of G-FR1-A1-4 mapped to disjoint frequency ranges with a width of 106 resource blocks each.

Note 5: These reference measurement channels are not applied for band n46, n96 and n102.

Note 6: $P_{REFSENS}$ is the power level of a single instance of the reference measurement channel. This requirement shall be met for a single instance of G-FR1-A1-21 mapped to the 12 NR resource blocks adjacent to the NB-IoT PRB, and for each consecutive application of a single instance of G-FR1-A1-7 mapped to disjoint frequency ranges with a width of 15 resource blocks each.

Table 4.2.2.2-3: NR Local Area BS reference sensitivity levels

BS channel bandwidth **(MHz)**	**Sub-carrier spacing (kHz)**	**Reference measurement channel (Note 5)**	**Reference sensitivity power level, $P_{REFSENS}$ (dBm)**
3	15	G-FR1-A1-7 (Note 1)	-95.6
		G-FR1-A1-21 (Note 6)	-95.6

5, 10, 15	15	G-FR1-A1-1 (Note 1)	-93.7
		G-FR1-A1-10 (Note 3)	-93.7 (Note 2)
10, 15	30	G-FR1-A1-2 (Note 1)	-93.8
10, 15	60	G-FR1-A1-3 (Note 1)	-90.9
20, 25, 30, 35, 40, 45, 50	15	G-FR1-A1-4 (Note 1)	-87.3
		G-FR1-A1-11 (Note 4)	-87.3 (Note 2)
20, 25, 30, 35, 40, 45, 50, 60, 70, 80, 90, 100	30	G-FR1-A1-5 (Note 1)	-87.6
20, 25, 30, 35, 40, 45, 50, 60, 70, 80, 90, 100	60	G-FR1-A1-6 (Note 1)	-87.7

Note 1: $P_{REFSENS}$ is the power level of a single instance of the reference measurement channel. This requirement shall be met for each consecutive application of a single instance of the reference measurement channel mapped to disjoint frequency ranges with a width corresponding to the number of resource blocks of the reference measurement channel each, except for one instance that might overlap one other instance to cover the full *BS channel bandwidth*.

Note 2: The requirements apply to BS that supports NB-IoT operation in NR in-band.

Note 3: $P_{REFSENS}$ is the power level of a single instance of the reference measurement channel. This requirement shall be met for a single instance of G-FR1-A1-10 mapped to the 24 NR resource blocks adjacent to the NB-IoT PRB, and for each consecutive application of a single instance of G-FR1-A1-1 mapped to disjoint frequency ranges with a width of 25 resource blocks each.

Note 4: $P_{REFSENS}$ is the power level of a single instance of the reference measurement channel. This requirement shall be met for a single instance of G-FR1-A1-11 mapped to the 105 NR resource blocks adjacent to the NB-IoT PRB, and for each consecutive application of a single instance of G-FR1-A1-4 mapped to disjoint frequency ranges with a width of 106 resource blocks each.

Note 5: These reference measurement channels are not applied for band n46, n96 and n102.

Note 6: $P_{REFSENS}$ is the power level of a single instance of the reference measurement channel. This requirement shall be met for a single instance of G-FR1-A1-21 mapped to the 12 NR resource blocks adjacent to the NB-IoT PRB, and for each consecutive application of a single instance of G-FR1-A1-7 mapped to disjoint frequency ranges with a width of 15 resource blocks each.

4.2.2.3 Blocking response

The BS blocking characteristics listed in Table 4.2.2.3-1, Table 4.2.2.3-2, Table 4.2.2.3-3, Table 4.2.2.3-4, Table 4.2.2.3-5, and Table 4.2.2.3-6 are re-used from TS 38.104 [9].

The in-band blocking requirement applies from $F_{UL,low}$ - Δf_{OOB} to $F_{UL,high}$ + Δf_{OOB}. The Δf_{OOB} for *BS type 1-C* and *BS type 1-H* is defined in Table 4.2.2.3-1.

Table 4.2.2.3-1: Δf_{OOB} offset for NR *operating bands*

BS type	***Operating band* characteristics**	**Δf_{OOB} (MHz)**
BS type 1-C	$F_{UL,high} - F_{UL,low} \leq 200$ MHz	20
	200 MHz < $F_{UL,high} - F_{UL,low} \leq 900$ MHz	60
BS type 1-H	$F_{UL,high} - F_{UL,low} < 100$ MHz	20
	100 MHz ≤ $F_{UL,high} - F_{UL,low} \leq 900$ MHz	60

Table 4.2.2.3-2: Base station general blocking requirement

***BS channel bandwidth* of the *lowest/highest carrier* received (MHz)**	**Wanted signal mean power (dBm) (Note 2)**	**Interfering signal mean power (dBm)**	**Interfering signal centre frequency minimum offset from the lower/upper *Base Station RF Bandwidth edge* or *sub-block* edge inside a *sub-block gap* (MHz)**	**Type of interfering signal**
3	PREFSENS + x dB	Wide Area BS: -43 Medium Range BS: -38 Local Area BS: -35	±4.5	3 MHz DFT-s-OFDM NR signal 15 kHz SCS, 15 RBs
5, 10, 15, 20	$P_{REFSENS}$ + x dB	Wide Area BS: -43 Medium Range BS: -38 Local Area BS: -35	±7.5	5 MHz DFT-s-OFDM NR signal 15 kHz SCS, 25 RBs
25, 30, 35, 40, 45, 50, 60, 70, 80, 90, 100	$P_{REFSENS}$ + x dB	Wide Area BS: -43 Medium Range BS: -38 Local Area BS: -35	±30	20 MHz DFT-s-OFDM NR signal 15 kHz SCS, 100 RBs
NOTE 1: $P_{REFSENS}$ depends on the RAT. For NR, $P_{REFSENS}$ depends also on the *BS channel bandwidth* as specified in tables 7.2.2-1, 7.2.2-2 and 7.2.2-3. For band n104, $P_{REFSENS}$ depends on the *BS channel bandwidth* as specified in tables 7.2.2-1a, 7.2.2-2c, and 7.2.2-3c. For NB-IoT, $P_{REFSENS}$ depends also on the *sub-carrier spacing* as specified in tables 7.2.1-5, 7.2.1-5a and 7.2.1-5c of TS 36.104 [10]. NOTE 2: For a BS capable of single band operation only, "x" is equal to 6 dB. For a BS capable of multi-band operation, "x" is equal to 6 dB in case of interfering signals that are in the in-band blocking frequency range of the operating band where the wanted signal is present or in the in-band blocking frequency range of an adjacent or overlapping operating band. For other in-band blocking frequency ranges of the interfering signal for the supported operating bands, "x" is equal to 1.4 dB.				

Table 4.2.2.3-3: Base Station narrowband blocking requirement

***BS channel bandwidth* of the *lowest/highest carrier* received (MHz)**	**Wanted signal mean power (dBm)**	**Interfering signal mean power (dBm)**
3, 5, 10, 15, 20, 25, 30, 35, 40, 45, 50, 60, 70, 80,90, 100 (Note 1)	$P_{REFSENS}$ + 6 dB	Wide Area BS: -49 Medium Range BS: -44 Local Area BS: -41
NOTE 1: The SCS for the *lowest/highest carrier* received is the lowest SCS supported by the BS for that *BS channel bandwidth* NOTE 2: $P_{REFSENS}$ depends on the *BS channel bandwidth* as specified in tables 7.2.2-1, 7.2.2-2 and 7.2.2-3. NOTE 3: 7.5 kHz shift is not applied to the wanted signal.		

Table 4.2.2.3-4: Base Station narrowband blocking interferer frequency offsets

***BS channel bandwidth* of the *lowest/highest carrier* received (MHz)**	**Interfering RB centre frequency offset to the lower/upper *Base Station RF Bandwidth edge* or *sub-block* edge inside a *sub-block gap* (kHz) (Note 2)**	**Type of interfering signal**
3	±(255+m*180), m=0, 1, 2, 3, 4, 7, 10, 13	3 MHz DFT-s-OFDM NR signal, 15 kHz SCS, 1 RB
5	±(350+m*180), m=0, 1, 2, 3, 4, 9, 14, 19, 24	5 MHz DFT-s-OFDM NR signal, 15 kHz SCS, 1 RB
10	±(355+m*180), m=0, 1, 2, 3, 4, 9, 14, 19, 24	
15	±(360+m*180), m=0, 1, 2, 3, 4, 9, 14, 19, 24	
20	±(350+m*180), m=0, 1, 2, 3, 4, 9, 14, 19, 24	
25	±(565+m*180), m=0, 1, 2, 3, 4, 29, 54, 79, 99	20 MHz DFT-s-OFDM NR signal, 15 kHz SCS, 1 RB
30	±(570+m*180), m=0, 1, 2, 3, 4, 29, 54, 79, 99	
35	±(560+m*180), m=0, 1, 2, 3, 4, 29, 54, 79, 99	
40	±(565+m*180), m=0, 1, 2, 3, 4, 29, 54, 79, 99	
45	±(570+m*180), m=0, 1, 2, 3, 4, 29, 54, 79, 99	
50	±(560+m*180), m=0, 1, 2, 3, 4, 29, 54, 79, 99	
60	±(570+m*180), m=0, 1, 2, 3, 4, 29, 54, 79, 99	
70	±(565+m*180), m=0, 1, 2, 3, 4, 29, 54, 79, 99	
80	±(560+m*180), m=0, 1, 2, 3, 4, 29, 54, 79, 99	
90	±(570+m*180), m=0, 1, 2, 3, 4, 29, 54, 79, 99	
100	±(565+m*180), m=0, 1, 2, 3, 4, 29, 54, 79, 99	
NOTE 1: Interfering signal consisting of one resource block positioned at the stated offset, the *channel bandwidth* of the interfering signal is located adjacently to the lower/upper *Base Station RF Bandwidth edge* or *sub-block* edge inside a *sub-block gap*. NOTE 2: The centre of the interfering RB refers to the frequency location between the two central subcarriers.		

The out-of-band blocking requirements defined in TS 38.104 [9] clause 7.5.2 Table 7.5.2-1a for non-AAS and defined in TS 38.104 [9] clause 10.6.2.1 for AAS BS apply from 1 MHz to $F_{UL,low} - \Delta f_{OOB}$ and from $F_{UL,high} + \Delta f_{OOB}$ up to 12750 MHz.

Table 4.2.2.3-5: Void

The blocking requirement for co-location with BS in other bands is listed in Table 4.2.2.3-6.

Table 4.2.2.3-6: Blocking performance requirement for NR BS when co-located with BS in other frequency bands.

Frequency range of interfering signal	Wanted signal mean power (dBm)	Interfering signal mean power for WA BS (dBm)	Interfering signal mean power for MR BS (dBm)	Interfering signal mean power for LA BS (dBm)	Type of interfering signal
Frequency range of co-located downlink *operating band*	$P_{REFSENS}$ +6dB (Note 1)	+16	+8	x (Note 2)	CW carrier
NOTE 1: $P_{REFSENS}$ depends on the *BS channel bandwidth* as specified in Table 7.2.2-1, 7.2.2-2, and 7.2.2-3. NOTE 2: x = -7 dBm for NR BS co-located with Pico GSM850 or Pico CDMA850 x = -4 dBm for NR BS co-located with Pico DCS1800 or Pico PCS1900 x = -6 dBm for NR BS co-located with UTRA bands or E-UTRA bands or NR bands NOTE 3: The requirement does not apply when the interfering signal falls within any of the supported uplink *operating band(s)* or in Δf_{OOB} immediately outside any of the supported uplink *operating band(s)*. NOTE 4: For unsynchronized base stations (except in band n46, n96 and n102), special co-location requirements may apply that are not covered by the 3GPP specifications.					

4.2.2.4 ACS

The BS ACS is listed in Table 4.2.2.4-1 and Table 4.2.2.4-2, as re-used from TS 38.104 [9].

Table 4.2.2.4-1: Base station ACS requirement

BS channel bandwidth **of the lowest/*highest carrier* received (MHz)**	**Wanted signal mean power (dBm)**	**Interfering signal mean power (dBm)**
3	$P_{REFSENS}$ + 8 dB	Wide Area BS: -52 Medium Range BS: -47 Local Area BS: -44
5, 10, 15, 20, 25, 30, 35, 40, 45, 50, 60, 70, 80, 90, 100 (Note 1)	$P_{REFSENS}$ + 6 dB	
NOTE 1: The SCS for the lowest/highest carrier received is the lowest SCS supported by the BS for that bandwidth. NOTE 2: $P_{REFSENS}$ depends on the RAT. For NR, $P_{REFSENS}$ depends also on the *BS channel bandwidth* as specified in tables 7.2.2-1, 7.2.2-2, 7.2.2-3. For NB-IoT, $P_{REFSENS}$ depends also on the *sub-carrier spacing* as specified in tables 7.2.1-5, 7.2.1-5a and 7.2.1-5c of TS 36.104 [10].		

Table 4.2.2.4-2: Base Station ACS interferer frequency offset values

***BS channel bandwidth* of the *lowest/highest carrier* received (MHz)**	**Interfering signal centre frequency offset from the lower/upper *Base Station RF Bandwidth edge* or *sub-block* edge inside a *sub-block gap* (MHz)**	**Type of interfering signal**
3	±1.5075	3 MHz DFT-s-OFDM NR signal 15 kHz SCS, 15 RBs
5	±2.5025	5 MHz DFT-s-OFDM NR signal 15 kHz SCS, 25 RBs
10	±2.5075	
15	±2.5125	
20	±2.5025	
25	±9.4675	20 MHz DFT-s-OFDM NR signal 15 kHz SCS, 100 RBs
30	±9.4725	
35	±9.4625	
40	±9.4675	
45	±9.4725	
50	±9.4625	
60	±9.4725	
70	±9.4675	
80	±9.4625	
90	±9.4725	
100	±9.4675	

4.3 UE parameters

4.3.1 Transmitter characteristics

4.3.1.1 Power dynamic range

The minimum controlled output power of the UE is defined as the power in the channel bandwidth for all transmit bandwidth configurations (resource blocks) when the power is set to a minimum value. For Rel-18 FR1 bands, the minimum output power is -33 dBm for 100 MHz channel bandwidth. Hence, the power dynamic range is 56 dB for 100 MHz channel bandwidth with power class 3 (i.e. 23 dBm maximum output power) UE.

4.3.1.2 Spectral mask

The UE spectral mask is described in Table 4.3.1.2-1.

Table 4.3.1.2-1: General NR spectrum emission mask

Δf_{OOB} (MHz)	**Channel bandwidth (MHz) / Spectrum emission limit (dBm)**				**Measurement bandwidth**
	3	**5**	**10, 15, 20, 25, 30, 35, 40, 45**	**50, 60, 70, 80, 90, 100**	
± 0-1	-13	-13	-13		1 % of channel BW
± 0-1				-24	30 kHz
± 1-5	-10	-10	-10		1 MHz
± 5-6	-25	-13			
± 6-10		-25			
± 5-$BW_{Channel}$			-13		
± $BW_{Channel}$-($BW_{Channel}$+5)			-25		

4.3.1.3 ACLR

The UE ACLR requirement is listed in Table 4.3.1.3-1.

Table 4.3.1.3-1: NR ACLR requirement

	Power class 1	Power class 1.5	Power class 2	Power class 3
NR ACLR	37 dB	31 dB	31 dB	30 dB

4.3.1.4 Spurious emissions

The UE spurious emission requirement is captured in Table 4.3.1.4-1 and Table 4.3.1.4-2.

Table 4.3.1.4-1: Boundary between NR out of band and general spurious emission domain

Channel bandwidth	OOB boundary F_{OOB} (MHz)
3	6
5, 10, 15, 20, 25, 30, 35, 40, 45, 50, 60, 70, 80, 90, 100	$BW_{Channel}$ + 5

Table 4.3.1.4-2: Requirement for general spurious emissions limits

Frequency Range	Maximum Level	Measurement bandwidth	NOTE
9 kHz ≤ f < 150 kHz	-36 dBm	1 kHz	
150 kHz ≤ f < 30 MHz	-36 dBm	10 kHz	
30 MHz ≤ f < 1000 MHz	-36 dBm	100 kHz	
1 GHz ≤ f < 12.75 GHz	-30 dBm	1 MHz	4
	-25 dBm	1 MHz	3
12.75 GHz ≤ f < 5th harmonic of the upper frequency edge of the UL operating band in GHz	-30 dBm	1 MHz	1
12.75 GHz < f < 26 GHz	-30 dBm	1 MHz	2

NOTE 1: Applies for Band for which the upper frequency edge of the UL Band is greater than 2.55 GHz and less than or equal to 5.2 GHz
NOTE 2: Applies for Band that the upper frequency edge of the UL Band more than 5.2 GHz
NOTE 3: Applies for Band n41, CA configurations including Band n41, and EN-DC configurations that include n41 specified in clause 5.2B of TS 38.101-3 [11] when NS_04 is signalled.
NOTE 4: Does not apply for Band n41, CA configurations including Band n41, and EN-DC configurations that include n41 specified in subclause 5.2B of TS 38.101-3 [11] when NS_04 is signalled.

4.3.1.5 Maximum output power

The UE maximum output power requirement is listed in Table 4.3.1.5-1.

Table 4.3.1.5-1: UE Power Class

NR band	Class 1 (dBm)	Tolerance (dB)	Class 1.5 (dBm)	Tolerance (dB)	Class 2 (dBm)	Tolerance (dB)	Class 3 (dBm)	Tolerance (dB)
n79			29[5]	+2/-3	26	+2/-3	23	+2/-3

NOTE 1: $P_{PowerClass}$ is the maximum UE power specified without taking into account the tolerance
NOTE 2: Power class 3 is default power class unless otherwise stated
NOTE 3: Refers to the transmission bandwidths confined within F_{UL_low} and F_{UL_low} + 4 MHz or F_{UL_high} – 4 MHz and F_{UL_high}, the maximum output power requirement is relaxed by reducing the lower tolerance limit by 1.5 dB.
NOTE 4: The maximum output power requirement is relaxed by reducing the lower tolerance limit by 0.3 dB
NOTE 5: Achieved via dual Tx
NOTE 6: Generally, PC1 UE is not targeted for smartphone form factor.

4.3.1.6 Average output power

It was agreed the average output power won't be mentioned in the reply LS to WP5D.

4.3.2 Receiver characteristics

4.3.2.1 Noise figure

The UE noise figure is 9 dB.

4.3.2.2 Sensitivity

The UE sensitivity requirement limits applicable for band n79 are re-used. Related extracts from TS 38.101-1 [12] are listed in Table 4.3.2.2-1.

Table 4.3.2.2-1: Two antenna port reference sensitivity QPSK $P_{REFSENS}$ for TDD, SDL and FDD with variable duplex operation bands

Operating band / SCS / Channel bandwidth / REFSENS				
Operating band	**SCS kHz**	**Channel bandwidth (MHz)**	**REFSENS (dBm)**	**Duplex Mode**
n79	15	10, 20, 30, 40, 50	$-95.8 + 10\log_{10}(N_{RB}/52)$	TDD
	30	10, 20, 30, 40, 50, 60, 70, 80, 90, 100	$-96.1 + 10\log_{10}(N_{RB}/24)$	
	60	10, 20, 30, 40, 50, 60, 70, 80, 90, 100	$-96.5 + 10\log_{10}(N_{RB}/11)$	

4.3.2.3 Blocking response

The UE blocking requirement is listed in Table 4.3.2.3-1, Table 4.3.2.3-2, Table 4.3.2.3-3 and Table 4.3.2.3-4, as re-used from TS 38.101-1 [12].

Table 4.3.2.3-1: In-band blocking parameters for NR bands with $F_{DL\_low} \geq 3300$ MHz and $F_{UL\_low} \geq 3300$ MHz

RX parameter	Units	Channel bandwidth (MHz)
		10, 15, 20, 25, 30, 35, 40, 45, 50, 60, 70, 80, 90, 100
Power in transmission bandwidth configuration	dBm	REFSENS + 6 dB[3]
$BW_{interferer}$	MHz	$BW_{Channel}$
$F_{Ioffset,\ case\ 1}$	MHz	$(3/2)*BW_{Channel}$
$F_{Ioffset,\ case\ 2}$	MHz	$(5/2)*BW_{Channel}$
NOTE 1: The transmitter shall be set to 4 dB below $P_{CMAX\_L,f,c}$ at the minimum UL configuration specified in Table 7.3.2-3 with $P_{CMAX\_L,f,c}$ defined in clause 6.2.4.		
NOTE 2: The interferer consists of the RMC specified in Annexes A.3.2.2 and A.3.3.2 with one sided dynamic OCNG Pattern OP.1 FDD/TDD for the DL-signal as described in Annex A.5.1.1/A.5.2.1		
NOTE 3: For Band n104, the power in transmission bandwidth configuration is REFSENS + 9 dB		

Table 4.3.2.3-2: In-band blocking for NR bands with F_{DL_low} ≥ 3300 MHz and F_{UL_low} ≥ 3300 MHz

NR band	Parameter	Unit	Case 1	Case 2
	$P_{interferer}$	dBm	-56	-44
n77, n78, n79, n104	$F_{interferer}$ (offset)	MHz	$-BW_{Channel}/2 - F_{loffset,\ case\ 1}$ and $BW_{Channel}/2 + F_{loffset,\ case\ 1}$	≤ $-BW_{Channel}/2 - F_{loffset,\ case\ 2}$ and ≥ $BW_{Channel}/2 + F_{loffset,\ case\ 2}$
	$F_{interferer}$		NOTE 2	$F_{DL\_low} - 3*BW_{Channel}$ to $F_{DL\_high} + 3*BW_{Channel}$
NOTE 1: The absolute value of the interferer offset Finterferer (offset) shall be further adjusted to $(\lceil F_{interferer} / SCS \rceil + 0.5) SCS$ MHz with SCS the sub-carrier spacing of the wanted signal in MHz. The interferer is an NR signal with an SCS equal to that of the wanted signal. NOTE 2: For each carrier frequency, the requirement applies for two interferer carrier frequencies: a: $-BW_{Channel}/2 - F_{loffset,\ case\ 1}$; b: $BW_{Channel}/2 + F_{loffset,\ case\ 1}$ NOTE 3: $BW_{Channel}$ denotes the channel bandwidth of the wanted signal				

Table 4.3.2.3-3: Out-of-band blocking parameters for NR bands with F_{DL_low} ≥ 3300 MHz and F_{UL_low} ≥ 3300 MHz

RX parameter	Units	Channel bandwidth (MHz)		
		10	15	20, 25, 30, 35, 40, 45, 50, 60, 70, 80, 90, 100
Power in transmission bandwidth configuration	dBm	REFSENS + 6 dB	REFSENS + 7 dB	REFSENS + 9 dB
NOTE: The transmitter shall be set to 4 dB below $P_{CMAX\_L,f,c}$ at the minimum UL configuration specified in Table 7.3.2-3 with $P_{CMAX\_L,f,c}$ defined in clause 6.2.4.				

Table 4.3.2.3-4: Out of-band blocking for NR bands with F_{DL_low} ≥ 3300 MHz and F_{UL_low} ≥ 3300 MHz

NR band	Parameter	Unit	Range1	Range 2	Range 3
n79 (NOTE 4)	$F_{interferer}$ (CW)	MHz	N/A	$-150 < f - F_{DL\_low} \le -MAX(60,3*BW_{Channel})$ or $MAX(60,3*BW_{Channel}) \le f - F_{DL\_high} < 150$	$1 \le f \le F_{DL\_low} - MAX(150,3*BW_{Channel})$ or $F_{DL\_high} + MAX(150,3*BW_{Channel}) \le f \le 12750$
NOTE 1: The power level of the interferer ($P_{Interferer}$) for Range 3 shall be modified to -20 dBm for $F_{Interferer}$ > 6000 MHz. NOTE 2: $BW_{Channel}$ denotes the channel bandwidth of the wanted signal NOTE 3: The power level of the interferer ($P_{Interferer}$) for Range 3 shall be modified to -20 dBm, for $F_{Interferer}$ > 2700 MHz and $F_{Interferer}$ < 4800 MHz. For $BW_{Channel}$ > 15 MHz, the requirement for Range 1 is not applicable and Range 2 applies from the frequency offset of $3*BW_{Channel}$ from the band edge. For $BW_{Channel}$ larger than 60 MHz, the requirement for Range 2 is not applicable and Range 3 applies from the frequency offset of $3*BW_{Channel}$ from the band edge. NOTE 4: The power level of the interferer ($P_{Interferer}$) for Range 3 shall be modified to -20 dBm, for $F_{Interferer}$ > 3650 MHz and $F_{Interferer}$ < 5750 MHz. For $BW_{Channel}$ ≥ 40 MHz, the requirement for Range 2 is not applicable and Range 3 applies from the frequency offset of $3*BW_{Channel}$ from the band edge. NOTE 5: The power level of the interferer ($P_{Interferer}$) for Range 3 shall be modified to -20 dBm, for $F_{Interferer}$ > 5175 MHz. For $BW_{Channel}$ > 60 MHz, the requirement for Range 2 is not applicable and Range 3 applies from the frequency offset of $3*BW_{Channel}$ from the band edge. The power level of the interferer ($P_{Interferer}$) for Range 2 shall be modified to -33 dBm for the range $5925 - MAX(60,3*CBW) \le f < F_{DL\_low} - MAX(60,3*CBW)$.					

4.3.2.4 ACS

The UE ACS requirement is listed in Table 4.3.2.4-1 and Table 4.3.2.4-2, as re-used from TS 38.101-1 [12].

Table 4.3.2.4-1: Test parameters for NR bands with F_{DL_low} ≥ 3300 MHz and F_{UL_low} ≥ 3300 MHz, case 1

RX parameter	Units	Channel bandwidth (MHz)
		10, 15, 20, 25, 30, 35, 40, 45, 50, 60, 70, 80, 90, 100
Power in transmission bandwidth configuration	dBm	REFSENS + 14 dB
$P_{interferer}$	dBm	REFSENS + 45.5 dB
$BW_{interferer}$	MHz	$BW_{Channel}$
$F_{interferer}$ (offset)	MHz	$BW_{Channel}$ / -$BW_{Channel}$
NOTE 1: The transmitter shall be set to 4 dB below $P_{CMAX\_L,f,c}$ at the minimum UL configuration specified in Table 7.3.2-3 with $P_{CMAX\_L,f,c}$ defined in clause 6.2.4.		
NOTE 2: The absolute value of the interferer offset $F_{interferer}$ (offset) shall be further adjusted to $\left(\left\lceil \left| F_{\text{interferer}} \right| / SCS \right\rceil + 0.5\right) SCS$ MHz with SCS the sub-carrier spacing of the wanted signal in MHz. The interferer is an NR signal with an SCS equal to that of the wanted signal.		
NOTE 3: The interferer consists of the RMC specified in Annexes A.3.2.2 and A.3.3.2 with one sided dynamic OCNG Pattern OP.1 FDD/TDD for the DL-signal as described in Annex A.5.1.1/A.5.2.1.		

Table 4.3.2.4-2: Test parameters for NR bands with F_{DL_low} ≥ 3300 MHz and F_{UL_low} ≥ 3300 MHz, case 2

RX parameter	Units	Channel bandwidth (MHz)
		10, 15, 20, 25, 30, 35, 40, 45, 50, 60, 70, 80, 90, 100
Power in transmission bandwidth configuration	dBm	-56.5
$P_{interferer}$	dBm	-25
$BW_{interferer}$	MHz	$BW_{Channel}$
$F_{interferer}$ (offset)	MHz	$BW_{Channel}$ / -$BW_{Channel}$
NOTE 1: The transmitter shall be set to 24 dB below $P_{CMAX\_L,f,c}$ at the minimum UL configuration specified in Table 7.3.2-3 with $P_{CMAX\_L,f,c}$ defined in clause 6.2.4.		
NOTE 2: The absolute value of the interferer offset $F_{interferer}$ (offset) shall be further adjusted to $\left(\left\lceil \left| F_{\text{interferer}} \right| / SCS \right\rceil + 0.5\right) SCS$ MHz with SCS the sub-carrier spacing of the wanted signal in MHz. The interferer is an NR signal with an SCS equal to that of the wanted signal.		
NOTE 3: The interferer consists of the RMC specified in Annexes A.3.2.2 and A.3.3.2 with one sided dynamic OCNG Pattern OP.1 FDD/TDD for the DL-signal as described in Annex A.5.1.1/A.5.2.1.		

4.4 Antenna characteristics

4.4.1 BS antenna characteristics

4.4.1.1 Antenna model

The antenna model is described in clause 7.1.

4.4.1.2 Antenna parameters

The BS antenna parameters are listed in Table 4.4.1.2-1.

Table 4.4.1.2-1: IMT parameters relevant for 1710 to 4990 MHz

Parameter	Macro Rural	Macro suburban	Macro urban	Micro urban
A_m	30 dB	30 dB	30 dB	30 dB
SLA_v	30 dB	30 dB	30 dB	30 dB
φ_{3dB}	90 deg.	90 deg.	90 deg.	90 deg.
θ_{3dB}	65 deg.	65 deg.	65 deg.	65 deg.
$G_{E,max}$	6.4 dBi	6.4 dBi	6.4 dBi	6.4 dBi
M_{sub}	3	3	3	N/A
$d_{v,sub}$	0.7λ m	0.7λ m	0.7λ m	N/A
$\theta_{subtilt}$	3 deg.	3 deg.	3 deg.	N/A
M	4	4	4	8
N	8	8	8	8
d_h	0.5λ m	0.5λ m	0.5λ m	0.5λ m
d_v	2.1λ m	2.1λ m	2.1λ m	0.7λ m
θ_{etilt}	$90 \leq \theta_{escan} \leq 100$ deg.	$90 \leq \theta_{escan} \leq 100$ deg.	$90 \leq \theta_{escan} \leq 100$ deg.	$90 \leq \theta_{escan} \leq 120$ deg.
φ_{escan}	$-60 \leq \varphi_{escan} \leq 60$ deg.	$-60 \leq \varphi_{escan} \leq 60$ deg.	$-60 \leq \varphi_{escan} \leq 60$ deg.	$-60 \leq \varphi_{escan} \leq 60$ deg.
ρ	1	1	1	1
P_{tx}	46 dBm	46 dBm	46 dBm	37 dBm
θ_{mech}	3 deg.	6 deg.	6 deg.	N/A

4.4.2 UE antenna characteristics

The UE is expected to have a conducted interface assuming an isotropic radiation pattern antenna and without beamforming.

5 7125 - 8400 MHz frequency range

5.1 General parameters

5.1.1 Duplex mode

Even though FDD is not precluded, most likely TDD will be used in this frequency range. This frequency range is adjacent to existing TDD bands, e.g. n104 (6425 – 7125 MHz) and n79 (4400 – 5000 MHz), making also SBFD as a candidate duplexing method. The core requirements for Rel-19 SBFD work item can be tracked through the list of impacted specifications captured in the respective Work Item description.

5.1.2 Channel Bandwidth

While a number of channel bandwidth will be specified for this frequency range, 100 MHz is considered as a typical channel bandwidth. Higher channel bandwidths compared to 100MHz are not precluded for this range. Annex A entails additional information on the impact of higher channel bandwidth on different RF parameters.

5.1.3 Signal Bandwidth

The signal bandwidth for a 100 MHz typical channel bandwidth signal is calculated based on the NR spectrum utilization:

$$\text{Signal bandwidth} = N_{RB} \times SCS \times 12$$

with N_{RB}: Number of Resource block for 100 MHz channel bandwidth and the associated SCS, as specified in TS 38.104 [9], clause 5.3.2.

5.2 BS parameters

5.2.1 Transmitter characteristics

5.2.1.1 Power dynamic range

There is no power control in downlink and fixed power per resource block is assumed during the study phase. Hence 0 dB power dynamic range was agreed for the LS reply.

5.2.1.2 Spectral mask

Both Category A and B spectral mask are specified. Since the frequency range 7125 to 8400 MHz is just adjacent to existing NR band n104, it is proposed that existing spectral mask (Category B) for band n104 in TS 38.104 subclause 6.6.4 for conducted requirements and subclause 9.7.4.2 for radiated requirements are applicable for the range. Category A limits for Wide Area BS are specified in Table 5.2.1.2-1 for non-AAS BS and in Table 5.2.1.2-2 for AAS BS in macro cell scenarios.

Table 5.2.1.2-1: Wide Area BS operating band unwanted emission limits for non-AAS BS (Category A)

Frequency offset of measurement filter -3dB point from the carrier frequency, Δf	Limits	Measurement Bandwidth
0 MHz ≤ Δf < 20MHz	$-7\text{dBm} - \frac{7}{20}\left(\frac{f\_offset}{MHz} - 0.05\right)$	100 kHz
20 MHz ≤ Δf < min(40 MHz, Δf_{max})	-14 dBm	100 kHz
40 MHz ≤ Δf ≤ Δf_{max}	-13 dBm	1 MHz
NOTE: Δf_{max} is equal to f_offset_{max} minus half of the bandwidth of the measuring filter, where f_offset_{max} is the offset to the frequency Δf_{OBUE} = 40 MHz outside the downlink operating band.		

Table 5.2.1.2-2: Wide Area BS operating band unwanted emission limits for AAS BS (Category A)

Frequency offset of measurement filter -3dB point from the carrier frequency, Δf	Limits	Measurement Bandwidth
0 MHz ≤ Δf < 50MHz	$2\text{dBm} - \frac{7}{50}\left(\frac{f\_offset}{MHz} - 0.05\right)$	100 kHz
50 MHz ≤ Δf < min(100 MHz, Δf_{max})	-5 dBm	100 kHz
100 MHz ≤ Δf ≤ Δf_{max}	-4 dBm	1 MHz
NOTE: Δf_{max} is equal to f_offset_{max} minus half of the bandwidth of the measuring filter, where f_offset_{max} is the offset to the frequency Δf_{OBUE} = 100 MHz outside the downlink operating band.		

5.2.1.3 ACLR

It is agreed to re-use n104 ACLR. The ACLR should be higher than the value specified in Table 5.2.1.3-1.

Table 5.2.1.3-1: Base station ACLR limit

BS channel bandwidth **of *lowest/highest carrier*** **transmitted $BW_{Channel}$ (MHz)**	**BS adjacent channel centre frequency offset below the lowest or above the highest carrier centre frequency transmitted**	**Assumed adjacent channel carrier (informative)**	**Filter on the adjacent channel frequency and corresponding filter bandwidth**	**ACLR limit**
20, 25, 30, 35, 40, 45, 50, 60, 70, 80, 90,100	$BW_{Channel}$	NR of same BW (Note 2)	Square (BW_{Config})	38 dB
	2 x $BW_{Channel}$	NR of same BW (Note 2)	Square (BW_{Config})	38 dB
NOTE 1: $BW_{Channel}$ and BW_{Config} are the *BS channel bandwidth* and *transmission bandwidth configuration* of the *lowest/highest carrier* transmitted on the assigned channel frequency. NOTE 2: With SCS that provides largest transmission bandwidth configuration (BW_{Config}).				

5.2.1.4 Spurious emissions

The general spurious emissions in TS 38.104 subclause 6.6.5 are applicable for the frequency range 7125 to 8400 MHz. It is agreed to adopt Δf_{OBUE} = 40 MHz for non-AAS BS and Δf_{OBUE} = 100 MHz for AAS BS.

5.2.1.5 Maximum output power

The maximum base station output power/ sector (e.i.r.p.) was provided as extracted in Table 5.2.1.5-1. It was agreed to be aligned with antenna characteristics.

Table 5.2.1.5-1: Maximum BS output power in 7125 to 8400 MHz

	Macro suburban	**Macro urban**	**Small cell outdoor/ Micro urban**
Maximum base station output power/sector (e.i.r.p.) (dBm)	78.3	78.3	61.5

The Total Radiated Power (TRP) for two polarizations was agreed as shown in Table 5.2.1.5-2 below.

Table 5.2.1.5-2: Total Radiated Power

Parameter	**Macro Sub-urban**	**Macro Urban**	**Micro Urban**	
Total Radiated Power for two polarizations (dBm)	46	46	37	

5.2.1.6 Average output power

It was agreed the average output power won't be mentioned in the reply LS.

5.2.2 Receiver characteristics

5.2.2.1 Noise figure

The BS typical noise figure is listed in Table 5.2.2.1-1.

Table 4.2.2.1-1: Noise figure

BS class	**Noise figure (dB)**
Wide Area	6
Medium Range	11
Local Area	14

5.2.2.2 Sensitivity

The sensitivity is not a critical parameter for sharing and compatibility studies. It was agreed to not mention any value for this parameter.

5.2.2.3 Blocking response

The in-band blocking requirement applies from $F_{UL,low}$ - Δf_{OOB} to $F_{UL,high}$ + Δf_{OOB}, excluding the downlink frequency range of the FDD *operating band*. It is agreed to adopt Δf_{OOB} = 60 MHz for non-AAS BS and Δf_{OOB} = 100 MHz for AAS BS. The in-band blocking levels are reused from existing FR1 requirements, as listed in Table 5.2.2.3-1 for non-AAS and requirements defined in TS 38.104 [9] clause 10.5.2.2 for AAS BS.

Table 5.2.2.3-1: Base station general blocking requirement

BS channel bandwidth of the lowest/highest carrier received (MHz)	Wanted signal mean power (dBm)	Interfering signal mean power (dBm)	Interfering signal centre frequency minimum offset from the lower/upper Base Station RF Bandwidth edge or sub-block edge inside a sub-block gap (MHz)	Type of interfering signal
20, 25, 30, 40, 50, 60, 70, 80, 90, 100	$P_{REFSENS}$ + 6 dB	Wide Area BS: -43 Medium Range BS: -38 Local Area BS: -35	±30	20 MHz DFT-s-OFDM NR signal 15 kHz SCS, 100 RBs
NOTE: $P_{REFSENS}$ depends on the RAT.				

The out-of-band blocking requirement applies from 1 MHz to 12.75 GHz, excluding the in-band blocking frequency range, but including the downlink frequency range in case of an FDD operating band. It is agreed to use n104 out-of-band levels as defined in TS 38.104 [9] clause 7.5.2 Table 7.5.2-1a for non-AAS and requirements defined in TS 38.104 [9] clause 10.6.2.1 for AAS BS.

5.2.2.4 ACS

It is agreed to specify 42 dB.

5.3 UE parameters

5.3.1 Transmitter characteristics

5.3.1.1 Power dynamic range

The minimum controlled output power of the UE is defined as the power in the channel bandwidth for all transmit bandwidth configurations (resource blocks), when the power is set to a minimum value. For existing FR1 bands, the minimum output power is -33 dBm for 100 MHz channel bandwidth. The minimum output power can be reused for 7.125 – 8.4 GHz, i.e. power dynamic range is 56 dB for 100 MHz channel bandwidth with power class 3 (i.e. 23 dBm maximum output power) UE.

5.3.1.2 Spectral mask

The UE spectral mask is described in Table 5.3.1.2-1.

Table 5.3.1.2-1: General NR spectrum emission mask

Δf_{OOB} (MHz)	Channel bandwidth (MHz) / Spectrum emission limit (dBm)				Measurement bandwidth
	3	5	10, 15, 20, 25, 30, 35, 40, 45	50, 60, 70, 80, 90, 100	
± 0-1	-13	-13	-13		1 % of channel BW
± 0-1				-24	30 kHz
± 1-5	-10	-10	-10		1 MHz
± 5-6	-25	-13			
± 6-10		-25			
± 5-$BW_{Channel}$			-13		
± $BW_{Channel}$-($BW_{Channel}$+5)			-25		

5.3.1.3 ACLR

According to the previous studies and simulation results in TR 38.921 [14] sub-clause 4.3, it was concluded that 26 dB ACLR would be sufficient for 6.425 - 7.125 GHz. Thus, ACLR of 26dB can be considered for the frequency range 7.125 – 8.4 GHz.

The actual ACLR for this frequency range or parts there-of should be further studied in the WI phase.

5.3.1.4 Spurious emissions

The general spurious emissions defined in TS 38.101-1 [12] clause 6.5.3.1 can apply to the frequency range 7.125 – 8.4 GHz.

5.3.1.5 Maximum output power

The UE maximum output power for the considered frequency ranges could be 23 dBm. Other UE power classes, e.g. 20dBm, 26dBm and 29dBm, are not precluded (corresponding ACLR limit will be adapted accordingly to avoid additional interference). Annex A entails additional information on the impact of higher output power on ACIR.

5.3.1.6 Average output power

This parameter was not mentioned in the previous response to ITU-R WP5D in [5].

5.3.2 Receiver characteristics

5.3.2.1 Noise figure

A noise figure in the [9, 13] dB interval was agreed for 6.425 - 7.125 GHz in the previous response to ITU-R WP5D sharing studies. The noise figure of 12 dB was assumed for the 3GPP band n104. For the frequency range 7.125 – 8.4 GHz noise figure of 13dB can be assumed.

The actual noise figure for this frequency range or parts there-of to define RF requirements should be further studied in the WI phase.

5.3.2.2 Sensitivity

The sensitivity is not a critical parameter for sharing and compatibility studies. It was agreed to not mention any value for this parameter.

5.3.2.3 Blocking response

The blocking characteristic specified in clause 7.6 of TS 38.101-1 [12] for frequency larger than 3300 MHz could be applied for the frequency range 7.125 – 8.4 GHz.

The actual requirements for this frequency range or parts there-of may differ depending on the band plan and possible re-use of RF hardware components.

5.3.2.4 ACS

According to the previous studies and simulation results in TR 38.921 [14] sub-clause 4.3, adjacent channel selectivity (ACS) is agreed as 32 dBc for 6425 – 7125 MHz. Thus, ACS of 32dB can be considered for the frequency range 7.125 – 8.4 GHz.

The actual ACS for this frequency range or parts there-of should be further studied in the WI phase.

5.4 Antenna characteristics

5.4.1 BS antenna characteristics

5.4.1.1 Antenna model

The BS antenna model is described in subclause 7.1.

5.4.1.2 Antenna parameters

The BS antenna parameters are listed in Table 5.4.1.2-1.

Table 5.4.1.2-1: IMT parameters relevant for 7125 to 8400 MHz

Parameter	Macro suburban	Macro urban	Micro urban
A_m	30 dB	30 dB	30 dB
SLA_v	30 dB	30 dB	30 dB
φ_{3dB}	90 deg.	90 deg.	90 deg.
θ_{3dB}	65 deg.	65 deg.	65 deg.
$G_{E,max}$	6.4 dBi	6.4 dBi	6.4 dBi
M_{sub}	3	3	N/A
$d_{v,sub}$	0.7λ m	0.7λ m	N/A
$\theta_{subtilt}$	3 deg.	3 deg.	N/A
M	8	8	8
N	16	16	8
d_h	0.5λ m	0.5λ m	0.5λ m
d_v	2.1λ m	2.1λ m	0.7λ m
θ_{etilt}	$90 \leq \theta_{escan} \leq 100$ deg.	$90 \leq \theta_{escan} \leq 100$ deg.	$90 \leq \theta_{escan} \leq 120$ deg.
φ_{escan}	$-60 \leq \varphi_{escan} \leq 60$ deg.	$-60 \leq \varphi_{escan} \leq 60$ deg.	$-60 \leq \varphi_{escan} \leq 60$ deg.
ρ	1	1	1
P_{tx}	46 dBm	46 dBm	37 dBm
θ_{mech}	6 deg.	6 deg.	N/A

5.4.2 UE antenna characteristics

The outcome of the RAN WG4 study for collecting technical background information relevant for the frequency range 7 to 24 GHz indicated that the frequency range 7.125 - [10-13] GHz would have "FR1 like" requirements. Therefore, the UE is expected to have a conducted interface assuming an isotropic radiation pattern antenna and without beamforming.

6 14800 - 15350 MHz frequency range

6.1 Co-existence study

6.1.1 Co-existence simulation scenarios

Table 6.1.1-1 summarizes the proposed simulation scenarios for 14800 - 15350 MHz.

Table 6.1.1-1: Summary of simulation scenarios for 14800 - 15350 MHz

No.	Usage scenario	Aggressor	Victim	Direction	Simulation frequency	Deployment Scenario	Priority
1	eMBB	NR, 100/200 MHz	Same as aggressor	DL to DL	15 GHz	Indoor hotspot	Down-prioritized
2	eMBB	NR, 100/200 MHz	Same as aggressor	DL to DL	15 GHz	Urban macro	
3	eMBB	NR, 100/200 MHz	Same as aggressor	DL to DL	15 GHz	Dense urban	Down-prioritized
4	eMBB	NR, 100/200 MHz	Same as aggressor	UL to UL	15 GHz	Indoor hotspot	Down-prioritized
5	eMBB	NR, 100/200 MHz	Same as aggressor	UL to UL	15 GHz	Urban macro	
6	eMBB	NR, 100/200 MHz	Same as aggressor	UL to UL	15 GHz	Dense urban	Down-prioritized
Note: It is agreed to down-prioritize the dense urban and indoor hotspot scenarios in this coexistence study, as urban macro scenario is the worst case among the three simulated scenarios and will drive the ACIR requirements.							

6.1.2 Co-existence simulation assumption

6.1.2.1 Network layout model

6.1.2.1.1 Urban macro

Details on urban macro network layout model are listed in Table 6.1.2.1.1-1 and 6.1.2.1.1-2.

Table 6.1.2.1.1-1: Single operator layout for urban macro

Parameters		Values	Remark
Network layout		hexagonal grid, 19 macro sites, 3 sectors per site with wrap around	
Inter-site distance		450 m	
BS antenna height		25 m	
UE location	Outdoor/indoor	Outdoor and indoor	
	Indoor UE ratio	20/0%	
	Low/high Penetration loss ratio	50% low loss, 50% high loss	
	LOS/NLOS	LOS and NLOS	
	UE antenna height	Same as 3D-UMa in TR 36.873	
UE distribution (horizontal)		Uniform	
Minimum BS - UE distance (2D)		35 m	
Channel model		UMa	
Shadowing correlation		Between cells: 1.0 Between sites: 0.5	

Table 6.1.2.1.1-2: Multi operators layout for urban macro

Parameters	Values	Remark
Multi operators layout	Coordinated operation (0% Grid Shift) and Un-coordinated operation (100% Grid Shift)	

Coordinated Operation: each network with co-location of sites	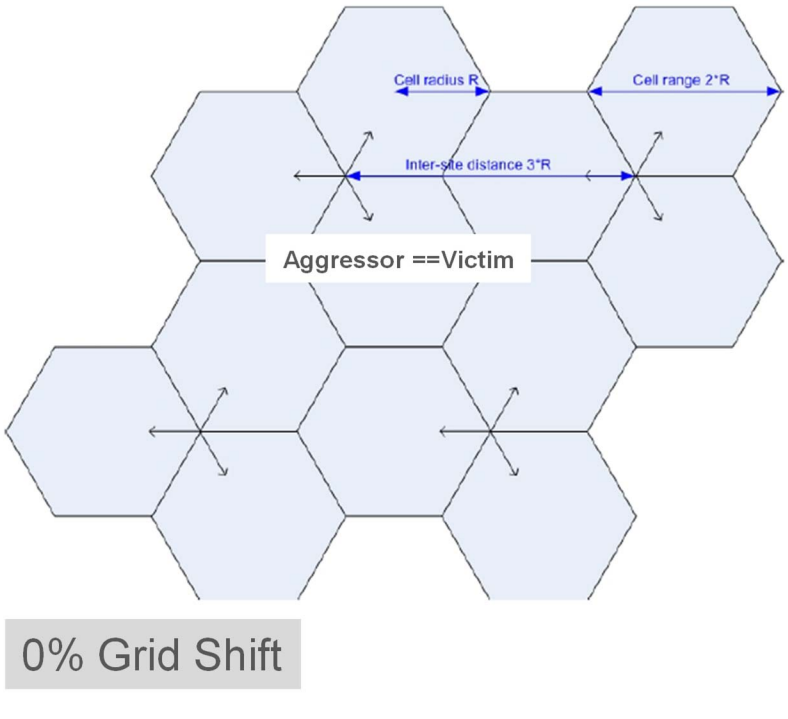

Figure 6.1.2.1.1-1: Coordinated operation

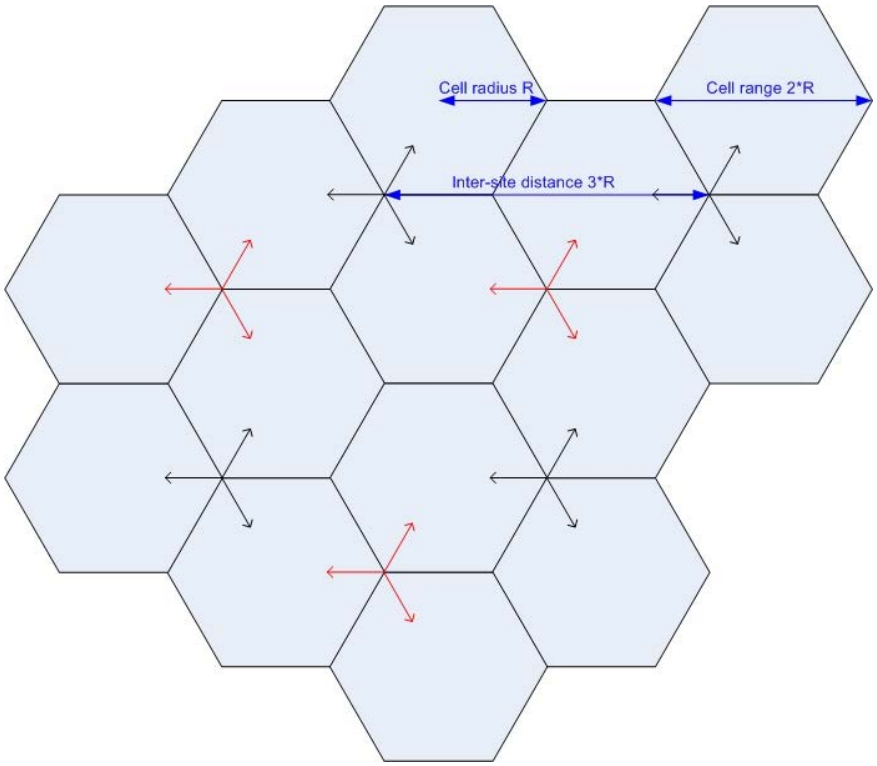

Figure 6.1.2.1.1-2: Uncoordinated operation

6.1.2.1.2 Dense urban

Details on dense urban network layout model are listed in Table 6.1.2.1.2-1 and 6.1.2.1.2-2.

Table 6.1.2.1.2-1: Single operator layout for dense urban

Parameters		Values	Remark
Network layout		Fixed cluster circle within a macro cell.	note1
Number of micro BSs per macro cell		3	3 cluster circles are in a macro cell. 1 cluster circle has 1 micro BS.
Radius of UE dropping within a micro cell		< 64.95 m	$\sqrt{3} \div 4 \times \mathrm{ISD} \div 3$
BS antenna height		10 m	
UE location	Outdoor/indoor	Outdoor and indoor	
	Indoor UE ratio	80 %	
	50% low loss, 50% high loss	Low/high Penetration loss ratio	
	LOS/NLOS	LOS and NLOS	
	UE antenna height	Same as 3D-UMi in TR 36.873	
UE distribution (horizontal)		Uniform	
Minimum BS - UE distance (2D)		3m	
Channel model		UMi	
Shadowing correlation		Between cite: 0.5	
Note 1: Micro BS is randomly dropped on an edge of the cluster circle. All UEs communicate with micro BS, i.e. macro cell is only used for determining position of micro BS. As a layout of macro cell, hexagonal grid, 19 macro sites, 3 sectors per site model with wrap around with ISD = 450 m is assumed.			

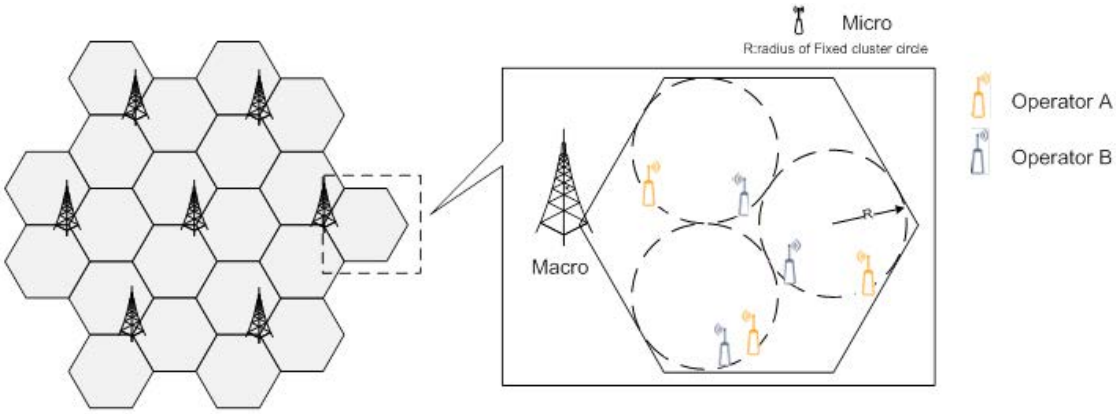

Figure 6.1.2.1.2-1: Network layout for dense urban

Table 6.1.2.1.2-2: Multi operators layout for dense urban

Parameters	Values	Remark
Multi operator layout	Cluster circle is coordinated	Note 1
Minimum distance between micro BSs in different operator	10 m	
Note 1: Macro cell is collocated. Micro BS itself is randomly dropped.		

6.1.2.1.3 Indoor

Details on indoor network layout model are listed in Table 6.1.2.1.3-1 and 6.1.2.1.3-2.

Table 6.1.2.1.3-1: Single operator layout for indoor

Parameters		Values	Remark
Network layout		50m x 120m, 12BSs	
Inter-site distance		20m	Single sector per site
BS antenna height		3 m	Mounted on ceiling
UE location	Outdoor/indoor	Indoor	
	LOS/NLOS	LOS and NLOS	
	UE antenna height	1 m	
UE distribution (horizontal)		Uniform	
Minimum BS - UE distance (2D)		0 m	
Channel model		Indoor Office	
Shadowing correlation		NA	

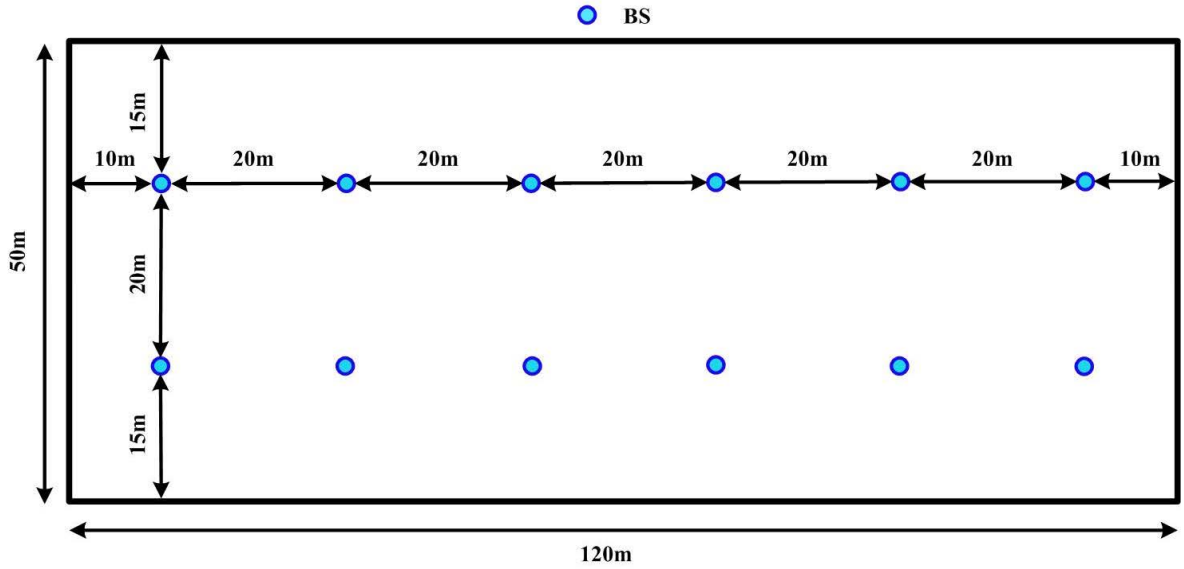

Figure 6.1.2.1.3-1: Network layout for indoor

Table 6.1.2.1.3-2: Multi operators layout for indoor

Parameters	Values	Remark
Multi operator layout	Coordinated operation (0% Grid Shift)	

6.1.2.2 Propagation model

6.1.2.2.1 Pathloss

The pathloss models are summarized in Table 6.1.2.2.1-1 and the distance definitions are indicated in Figure 6.1.2.2.1-1 and Figure 6.1.2.2.1-2. Note that the distribution of the shadow fading is log-normal, and its standard deviation for each scenario is given in Table 6.1.2.2.1-1.

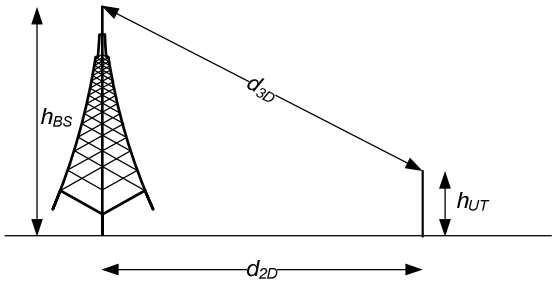

Figure 6.1.2.2.1-1: Definition of d_{2D} and d_{3D} for outdoor UTs

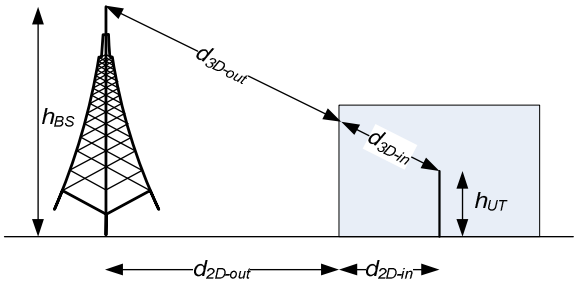

Figure 6.1.2.2.1-2: Definition of $d_{2D\text{-}out}$, $d_{2D\text{-}in}$ and $d_{3D\text{-}out}$, $d_{3D\text{-}in}$ for indoor UTs.

Note that

$$d_{3D-out} + d_{3D-in} = \sqrt{\left(d_{2D-out} + d_{2D-in}\right)^2 + \left(h_{BS} - h_{UT}\right)^2} \quad (6.1.2.2\text{-}1)$$

Table 6.1.2.2.1-1: Pathloss models

Scenario	LOS/NLOS	Pathloss [dB], f_c is in GHz and d is in meters, see note 6	Shadow fading std [dB]	Applicability range, antenna height default values
UMa	LOS	$PL_{\text{UMa-LOS}} = \begin{cases} PL_1 & 10\text{m} \le d_{2D} \le d'_{BP} \\ PL_2 & d'_{BP} \le d_{2D} \le 5\text{km} \end{cases}$, see note 1 $PL_1 = 28.0 + 22\log_{10}(d_{3D}) + 20\log_{10}(f_c)$ $PL_2 = 28.0 + 40\log_{10}(d_{3D}) + 20\log_{10}(f_c) - 9\log_{10}((d'_{BP})^2 + (h_{BS} - h_{UT})^2)$	$\sigma_{SF} = 4$	$1.5\text{m} \le h_{UT} \le 22.5\text{m}$ $h_{BS} = 25\text{m}$
	NLOS	$PL_{\text{UMa-NLOS}} = \max(PL_{\text{UMa-LOS}}, PL'_{\text{UMa-NLOS}})$ for $10\,\text{m} \le d_{2D} \le 5\,\text{km}$ $PL'_{\text{UMa-NLOS}} = 13.54 + 39.08\log_{10}(d_{3D}) + 20\log_{10}(f_c) - 0.6(h_{UT} - 1.5)$	$\sigma_{SF} = 6$	$1.5\text{m} \le h_{UT} \le 22.5\text{m}$ $h_{BS} = 25\text{m}$ Explanations: see note 3
		Optional $PL = 32.4 + 20\log_{10}(f_c) + 30\log_{10}(d_{3D})$	$\sigma_{SF} = 7.8$	
UMi - Street Canyon	LOS	$PL_{\text{UMi-LOS}} = \begin{cases} PL_1 & 10\text{m} \le d_{2D} \le d'_{BP} \\ PL_2 & d'_{BP} \le d_{2D} \le 5\text{km} \end{cases}$, see note 1 $PL_1 = 32.4 + 21\log_{10}(d_{3D}) + 20\log_{10}(f_c)$ $PL_2 = 32.4 + 40\log_{10}(d_{3D}) + 20\log_{10}(f_c) - 9.5\log_{10}((d'_{BP})^2 + (h_{BS} - h_{UT})^2)$	$\sigma_{SF} = 4$	$1.5\text{m} \le h_{UT} \le 22.5\text{m}$ $h_{BS} = 10\text{m}$
	NLOS	$PL_{\text{UMi-NLOS}} = \max(PL_{\text{UMi-LOS}}, PL'_{\text{UMi-NLOS}})$ for $10\,\text{m} \le d_{2D} \le 5\,\text{km}$ $PL'_{\text{UMi-NLOS}} = 35.3\log_{10}(d_{3D}) + 22.4 + 21.3\log_{10}(f_c) - 0.3(h_{UT} - 1.5)$	$\sigma_{SF} = 7.82$	$1.5\text{m} \le h_{UT} \le 22.5\text{m}$ $h_{BS} = 10\text{m}$ Explanations: see note 4
		Optional $PL = 32.4 + 20\log_{10}(f_c) + 31.9\log_{10}(d_{3D})$	$\sigma_{SF} = 8.2$	
InH - Office	LOS	$PL_{\text{InH-LOS}} = 32.4 + 17.3\log_{10}(d_{3D}) + 20\log_{10}(f_c)$	$\sigma_{SF} = 3$	$1\text{m} \le d_{3D} \le 150\text{m}$
	NLOS	$PL_{\text{InH-NLOS}} = \max(PL_{\text{InH-LOS}}, PL'_{\text{InH-NLOS}})$ $PL'_{\text{InH-NLOS}} = 38.3\log_{10}(d_{3D}) + 17.30 + 24.9\log_{10}(f_c)$	$\sigma_{SF} = 8.03$	$1\text{m} \le d_{3D} \le 150\text{m}$
		Optional $PL'_{\text{InH-NLOS}} = 32.4 + 20\log_{10}(f_c) + 31.9\log_{10}(d_{3D})$	$\sigma_{SF} = 8.29$	$1\text{m} \le d_{3D} \le 150\text{m}$

Scenario	LOS/NLOS	Pathloss [dB], f_c is in GHz and d is in meters, see note 6	Shadow fading std [dB]	Applicability range, antenna height default values
Note 1:		Breakpoint distance $d'_{BP} = 4\,h'_{BS}\,h'_{UT}\,f_c/c$, where f_c is the centre frequency in Hz, $c = 3.0\times10^8$ m/s is the propagation velocity in free space, and h'_{BS} and h'_{UT} are the effective antenna heights at the BS and the UT, respectively. The effective antenna heights h'_{BS} and h'_{UT} are computed as follows: $h'_{BS} = h_{BS} - h_E$, $h'_{UT} = h_{UT} - h_E$, where h_{BS} and h_{UT} are the actual antenna heights, and h_E is the effective environment height. For UMi $h_E = 1.0$m. For UMa h_E=1m with a probability equal to 1/(1+C(d_{2D}, h_{UT})) and chosen from a discrete uniform distribution uniform(12,15,…,(h_{UT}-1.5)) otherwise. With C(d_{2D}, h_{UT}) given by $$C(d_{2D}, h_{UT}) = \begin{cases} 0 & , h_{UT} < 13\text{m} \\ \left(\frac{h_{UT}-13}{10}\right)^{1.5} g(d_{2D}) & ,13\text{m} \le h_{UT} \le 23\text{m} \end{cases},$$ where $$g(d_{2D}) = \begin{cases} 0 & , d_{2D} \le 18\text{m} \\ \frac{5}{4}\left(\frac{d_{2D}}{100}\right)^3 \exp\left(\frac{-d_{2D}}{150}\right) & ,18\text{m} < d_{2D} \end{cases}.$$ Note that h_E depends on d_{2D} and h_{UT} and thus needs to be independently determined for every link between BS sites and UTs. A BS site may be a single BS or multiple co-located BSs.		
Note 2:		The applicable frequency range of the PL formula in this table is $0.5 < f_c < f_H$ GHz, where f_H = 30 GHz for RMa and f_H = 100 GHz for all the other scenarios. It is noted that RMa pathloss model for >7 GHz is validated based on a single measurement campaign conducted at 24 GHz.		
Note 3:		UMa NLOS pathloss is from TR36.873 with simplified format and $PL_{UMa\text{-}LOS}$ = Pathloss of UMa LOS outdoor scenario.		
Note 4:		$PL_{UMi\text{-}LOS}$ = Pathloss of UMi-Street Canyon LOS outdoor scenario.		
Note 5:		Break point distance $d_{BP} = 2\pi\, h_{BS}\, h_{UT}\, f_c/c$, where f_c is the centre frequency in Hz, $c = 3.0 \times 10^8$ m/s is the propagation velocity in free space, and h_{BS} and h_{UT} are the antenna heights at the BS and the UT, respectively.		
Note 6:		f_c denotes the center frequency normalized by 1GHz, all distance related values are normalized by 1m, unless it is stated otherwise.		

6.1.2.2.2 LOS probability

The Line-Of-Sight (LOS) probabilities are given in Table 6.1.2.2.2-1.

Table 6.1.2.2.2-1: LOS probability

Scenario	LOS probability (distance is in meters)
UMi – Street canyon	Outdoor users: $P_{LOS} = \min(18/d_{2D},1)(1-\exp(-d_{2D}/36)) + \exp(-d_{2D}/36)$ Indoor users: Use $d_{2D\text{-}out}$ in the formula above instead of d_{2D}
UMa	Outdoor users: $P_{LOS} = \min(18/d_{2D},1)(1-\exp(-d_{2D}/63)) + \exp(-d_{2D}/63)(1+C(d_{2D},h_{UT}))$ where $C(d_{2D},h_{UT}) = \begin{cases} 0 & ,h_{UT} < 13\text{m} \\ \left(\frac{h_{UT}-13}{10}\right)^{1.5} g(d_{2D}) & ,13\text{m} \le h_{UT} \le 23\text{m} \end{cases}$ and $g(d_{2D}) = \begin{cases} 0 & ,d_{2D} \le 18\text{m} \\ (1.25e-6)(d_{2D})^3 \exp(-d_{2D}/150) & ,18\text{m} < d_{2D} \end{cases}$ Indoor users: Use $d_{2D\text{-}out}$ in the formula above instead of d_{2D}
Indoor – Open office	$P_{LOS}^{Open\_office} = \begin{cases} 1, & d_{2D} \le 5 \\ \exp(-(d_{2D}-5)/70.8), & 5 < d_{2D} \le 49 \\ \exp(-(d_{2D}-49)/211.7)\cdot 0.54, & d_{2D} > 49 \end{cases}$
Note: The LOS probability is derived with assuming antenna heights of 3m for indoor, 10m for UMi, and 25m for UMa	

6.1.2.2.3 O-to-I penetration loss

The Path loss incorporating O-to-I building penetration loss is modelled as in the following:

$PL = PL_b + PL_{tw} + PL_{in} + N(0, \sigma_P^2)$

where PL_b is the basic outdoor path loss given in Section 6.1.2.2.1. PL_{tw} is the building penetration loss through the external wall, PL_{in} is the inside loss dependent on the depth into the building, and σ_P is the standard deviation for the penetration loss.

PL_{tw} is characterized as:

$$PL_{tw} = PL_{npi} - 10\log_{10}\sum_{i=1}^{N}\left(p_i \times 10^{\frac{L_{material\_i}}{-10}}\right)$$

PL_{npi} is an additional loss is added to the external wall loss to account for non-perpendicular incidence;

$L_{material\_i} = a_{material\_i} + b_{material\_i} \cdot f$, is the penetration loss of material *i*, example values of which can be found in Table 6.1.2.2.3-1.

p_i is proportion of i-th materials, where $\sum_{i=1}^{N} p_i = 1$; and

N is the number of materials.

Table 6.1.2.2.3-1: Material penetration losses

Material	Penetration loss [dB]
Standard multi-pane glass	$L_{glass} = 2 + 0.2 \cdot f$
IRR glass	$L_{IRRglass} = 23 + 0.3 \cdot f$
Concrete	$L_{concrete} = 5 + 4 \cdot f$
Wood	$L_{wood} = 4.85 + 0.12 \cdot f$
Note: f is in GHz	

Table 6.1.2.2.3-2 gives PL_{tw}, PL_{in} and σ_P for two O-to-I penetration loss models. The O-to-I penetration is UT-specifically generated, and is added to the SF realization in the log domain.

Table 6.1.2.2.3-2 O-to-I penetration loss model

	Path loss through external wall: PL_{tw} [dB]	Indoor loss: PL_{in} [dB]	Standard deviation: σ_P [dB]
Low-loss model	$5 - 10\log_{10}(0.3 \cdot 10^{-L_{glass}/10} + 0.7 \cdot 10^{-L_{concrete}/10})$	$0.5d_{2D\text{-}in}$	4.4
High-loss model	$5 - 10\log_{10}(0.7 \cdot 10^{-L_{IRRglass}/10} + 0.3 \cdot 10^{-L_{concrete}/10})$	$0.5d_{2D\text{-}in}$	6.5

$d_{2D\text{-}in}$ is minimum of two independently generated uniformly distributed variables between 0 and 25 m for RMa, UMa and UMi-Street Canyon. $d_{2D\text{-}in}$ shall be UT-specifically generated.

Both low-loss and high-loss models are applicable to UMa and UMi-Street Canyon.

Only the low-loss model is applicable to RMa.

The composition of low and high loss is a simulation parameter that should be determined by the user of the channel models, and is dependent on the use of metal-coated glass in buildings and the deployment scenarios. Such use is expected to differ in different markets and regions of the world and also may increase over years to new regulations and energy saving initiatives. Furthermore, the use of such high-loss glass currently appears to be more predominant in commercial buildings than in residential buildings in some regions of the world.

The pathloss incorporating O-to-I car penetration loss is modelled as in the following:

$$PL = PL_b + N(\mu, \sigma_P^2)$$

where PL_b is the basic outdoor path loss given in Section 6.1.2.2.1. $\mu = 9$, and $\sigma_P = 5$. Optionally, for metallized car windows, $\mu = 20$ can be used. The O-to-I car penetration loss models are applicable for at least 0.6-60 GHz.

6.1.2.3 Antenna and beam forming pattern modelling

6.1.2.3.1 BS antenna modelling

The antenna model for AAS BS is described in subclause 7.1.

In Table 6.1.2.3.1-1, representable parameter sets relevant for an AAS base station operating within 14800 - 15350 MHz are provided.

Table 6.1.2.3.1-1: Antenna array parameters

Parameter	Indoor	Urban macro	Dense urban
Element gain (dBi) (Note 2)	5	6.4	6.4
Horizontal/vertical 3 dB beam width of single element (degree)	90º for H 90º for V	90º for H 65º for V	90º for H 65º for V
Horizontal/vertical front-to-back ratio (dB)	30 for both H/V	30 for both H/V	30 for both H/V
Antenna polarization	Linear ±45º	Linear ±45º	Linear ±45º
Antenna array configuration (Row × Column) (Note 4)	4 x 4	16 x 24	16 x 24
Horizontal/Vertical radiating sub-array spacing	0.5 of wavelength for H, 0.5 of wavelength for V	0.5 of wavelength for H, 2.8 of wavelength for V (Note 5)	0.5 of wavelength for H, 2.8 of wavelength for V (Note 5)
Number of element rows in sub-array	N/A	4	4
Vertical element separation in sub-array ($d_{v,sub}$)	0.5 of wavelength of V	0.7 of wavelength of V	0.7 of wavelength of V
Pre-set sub-array down-tilt (degrees)	N/A	3	3
Array Ohmic loss (dB) (Note 2)	2	2	2
Conducted power (before Ohmic loss) per sub-array or element (dBm) (Note 3)	8	17.2	7.2
Base station horizontal coverage range (degrees)	+/-90	+/-60	+/-60
Base station vertical coverage range (degrees) (Note 1)	0-180	90-100	90-100
Mechanical down-tilt (degrees)	N/A(Note 6)	6	6
Note 1: The vertical coverage range is given for the elevation angle θ, defined between 0° and 180° i.e. 90° being at the horizon Note 2: The element gain includes the loss and is per polarization. Note 3: The conducted power per sub-array assumes 16 × 24 sub-arrays and 2 polarizations for urban macro and dense urban cases; the conducted power per element assumes 4 x 4 elements and 2 polarizations for indoor case Note 4: 16 × 24 means there are 16 vertical and 24 horizontal radiating sub-arrays for urban macro and dense urban cases; 4 x 4 means there are 4 vertical and 4 horizontal radiating elements for indoor case. Note 5: For the case of 4 elements per sub array, dv will be 2.8 wavelengths. Note 6: Roof mounted equipment with antenna boresight pointing downward			

6.1.2.3.3 UE antenna modelling

For the FR1-like RF design, the UE is expected to have a conducted interface assuming an isotropic radiation pattern antenna and without beamforming (only for simulation and not reflecting deployment, coverage, implementation, or requirement aspects).

6.1.2.4 Other simulation parameters

Table 6.1.2.4-1: Other simulation parameters

Parameters	Indoor	Urban macro	Dense urban
Channel bandwidth	100/200 MHz	100/200 MHz	100/200 MHz
Scheduled channel bandwidth per UE (DL)	100/200 MHz	100/200 MHz	100/200 MHz
Scheduled channel bandwidth per UE (UL)	100/200 MHz	100/200 MHz	100/200 MHz
The number of active UE (DL)	Same as the number of BS beam	Same as the number of BS beam	Same as the number of BS beam
The number of active UE (UL)	1 UE per slot (first priority) 3 UE per slot (second priority)	1 UE per slot (first priority) 3 UE per slot (second priority)	1 UE per slot (first priority) 3 UE per slot (second priority)
Traffic model	Full buffer	Full buffer	Full buffer
DL power control	NO	NO	NO
UL power control	YES	YES	YES
BS max TX power in dBm (2 polarizations)	23dBm	46dBm	36dBm
UE max TX power in dBm	23dBm	23dBm	23dBm
UE min TX power in dBm	-40dBm	-40dBm	-40dBm
BS Noise figure in dB	16	8	13
UE Noise figure in dB	13	13	13
Handover margin	3dB	3dB	3dB

6.1.2.5 Transmission power control model

For downlink scenario, no power control scheme is applied.

For uplink scenario, TPC model specified in clause 9.1 TR 36.942 is applied with following parameters.

- $CL_{x\text{-}ile} = 88 + 10*\log10(200/X) + 11 – Y$, where X is UL transmission BW (MHz) and Y is the BS noise figure
- $\gamma = 1$

6.1.3 Co-existence simulation results

6.1.3.1 Urban Macro scenario

6.1.3.1.1 Downlink

For Urban macro scenarios, simulation results for DL throughput loss with baseline assumption ACLR = 45 dBc at BS and ACS = 33 dBc at UE are summarized in Table 6.1.3.1.1-1/2/3/4/5. The following results are based on the FR1 like UE with omni-directional antenna and no beamforming.

Table 6.1.3.1.1-1: DL throughput loss for 14800 – 15350 MHz [Relative ACIR value]

Company	Throughput loss	Relative ACIR offset									
		0	**-2**	**-3**	**-4**	**-6**	**-8**	**-9**	**-10**	**-12**	**-15**
Nokia	Average throughput loss in % (15 GHz)	0.17		0.28		0.45		0.70		1.06	1.55
	5%-tile throughput loss in % (15 GHz)	0.00		0.18		0.35		1.00		1.38	3.53
ZTE	Average throughput loss in % (15 GHz)	0.33	0.41		0.52	0.67	0.85		1.09		
	5%-tile throughput loss in % (15 GHz)	2.50	2.75		3.41	4.38	4.97		5/89		

Table 6.1.3.1.1-2: DL throughput loss for 14800 – 15350 MHz [Absolute ACIR value]

	ACIR (dB)	5	10	15	17	18	19	20	21	25	30	32
Apple	Average throughput loss in %			0.47				0.232			0.49	0.026
	5%-tile throughput loss in %			0.623				0.247			0.054	0.006
CATT	Average throughput loss in %	0.043	0.026	0.015				0.0082		0.0042	0.0023	
	5%-tile throughput loss in %	0.16	0.15	0.14				0.11		0.10	0.046	
MediaTek	Average throughput loss in %	7.41	4.61	2.74		1.97			1.39	0.86	0.44	
	5%-tile throughput loss in %	35.10	22.03	12.45		8.57			5.90	3.78	1.70	
Vivo	Average throughput loss in %		3.11	1.79				0.91		0.46	0.24	
	5%-tile throughput loss in %		17.71	10.13				6.21		2.67	1.49	
Qualcomm	Average throughput loss in %	6.4	3.8	2.2				1.2		0.7	0.4	
	5%-tile throughput loss in %	34.5	20.4	10				5.4		2.5	1.5	
Ericsson	Average throughput loss in %				0.0134	0.0121	0.01	0.009	0.008			
	5%-tile throughput loss in %				8	7	6.24	5.25	4.6			
Huawei	Average throughput loss in %	5.63	3.29	1.83				0.97		0.49	0.23	
	5%-tile throughput loss in %	25.58	16.08	9.49				5.24		2.64	1.21	
Samsung	Average throughput loss in %	4	3	2				1		0	0	
	5%-tile throughput loss in %	34	20	12				7		3	2	

In addition, coexistence simulation results for 3 active UEs and Indoor Probability 0% are summarized in Table 6.1.3.1.1-3. and 6.1.3.1.1-4 below.

Table 6.1.3.1.1-3: DL throughput loss for 14800 – 15350 MHz [Relative ACIR with 3 active UEs]

Company	Throughput loss	Relative ACIR offset									
		0	-2	-3	-4	-6	-8	-9	-10	-12	-15
Nokia	Average throughput loss in % (15 GHz)	0.31		0.51		0.82		1.29		2.00	3.02
	5%-tile throughput loss in % (15 GHz)	0		0		2.11		2.11		2.99	4.86

Table 6.1.3.1.1-4: DL throughput loss for 14800 – 15350 MHz [Absolute ACIR with Indoor Probability 0%]

Company	Throughput loss	Absolute ACIR						
		17	18	19	20	21	22	23
Ericsson	Average throughput loss in % (15 GHz)	0.015	0.014	0.0125	0.01	0.01	0.009	0.008
	5%-tile throughput loss in % (15 GHz)	11	10	8	7.5	7.2	6.7	5.5

Based on the above simulation results, the required DL ACIR for 14800 – 15350 MHz for urban macro scenarios are in summarized in Table 6.1.3.1.1-5. The range of ACIR is derived as 20-26 dB, and the range of 22-24 dB by excluding the highest/lowest.

Table 6.1.3.1.1-5: DL simulation results for 14800 – 15350 MHz

	ACIR (dB)
Company	**Urban macro**
Nokia	-12 dB (relative)
Apple	28-30
CATT	24
MediaTek	23-24
Vivo	22
Qualcomm	22
Ericsson	20-24
ZTE	-8 dB (relative)
Huawei	21
Samsung	24-25
[Average in range]	20-26
[Excluding the highest/lowest]	22-24

6.1.3.1.2 Uplink

For Urban macro scenarios, simulation results for UL throughput loss with baseline assumption ACLR = 30 dBc at UE and ACS = 45 dBc at BS are summarized in Table 6.1.3.1.2-1/2/3/4/5. The following results are based on the FR1 like UE with omni-directional antenna and no beamforming.

Table 6.1.3.1.2-1: UL throughput loss for 14800 – 15350 MHz [Relative ACIR value]

Company	Throughput loss	Relative ACIR offset									
		0	-2	-3	-4	-6	-8	-9	-10	-12	-15
Nokia	Average throughput loss in % (15 GHz)	0.07		0.12		0.20		0.30		0.46	0.68
	5%-tile throughput loss in % (15 GHz)	1.14		2.21		3.52		3.55		3.61	3.73
ZTE	Average throughput loss in % (15 GHz)	0.26	0.30		0.34	0.39	0.46		0.55		
	5%-tile throughput loss in % (15 GHz)	6.36	7.20		8.95	9.10	9.36		10.98		

Table 6.1.3.1.2-2: UL throughput loss for 14800 – 15350 MHz [Absolute ACIR value]

	ACIR (dB)	8	9	10	11	12	13	14	15	20	22	23	25	30
Apple	Average throughput loss in %			0.6					0.3	0.13	0.099	0.079	0.06	0.022
	5%-tile throughput loss in %			0.59					0.22	0.14	0.131	0.1	0.1	0.01
CATT	Average throughput loss in %			0.027					0.018	0.01			0.0055	0.0024
	5%-tile throughput loss in %			0.088					0.0032	0.0001			3.1e-5	9.7e-6
MediaTek	Average throughput loss in %			2.12					1.15	0.60			0.3	0.14
	5%-tile throughput loss in %			8.48					4.05	1.94			0.75	0.16
Vivo	Average throughput loss in %			0.80					0.38	0.18			0.08	0.04
	5%-tile throughput loss in %			5.77					2.82	0.93			0.14	0
Qualcomm	Average throughput loss in %			1.4					0.7	0.4			0.18	0.09
	5%-tile throughput loss in %			7.4					2.8	1.8			0.7	0.4
Ericsson	Average throughput loss in %	0.0088	0.0078	0.0068	0.006	0.0052	0.0046	0.004						
	5%-tile throughput loss in %	6	5.66	5	4.6	4.22	3.6	3.3						
Huawei	Average throughput loss in %			3.57					2.00	1.08			0.56	0.27
	5%-tile throughput loss in %			8.59					5.63	3.58			2.30	1.28

In addition, coexistence simulation results for 3 active UEs and Indoor Probability 0% are summarized in Table 6.1.3.1.2-3.and 6.1.3.1.2-4 below.

Table 6.1.3.1.2-3: UL throughput loss for 14800 – 15350 MHz [Relative ACIR with 3 active UEs]

Company	Throughput loss	Relative ACIR offset									
		0	-2	-3	-4	-6	-8	-9	-10	-12	-15
Nokia	Average throughput loss in % (15 GHz)	0.23		0.33		0.48		0.72		1.08	1.63
	5%-tile throughput loss in % (15 GHz)	1.81		3.40		3.47		5.06		6.14	9.49

Table 6.1.3.1.2-4: UL throughput loss for 14800 – 15350 MHz [Absolute ACIR with Indoor Probability 0%]

Company	Throughput loss	Absolute ACIR						
		8	9	10	11	12	13	14
Ericsson	Average throughput loss in % (15 GHz)	0.02	0.017	0.015	0.013	0.012	0.01	0.009
	5%-tile throughput loss in % (15 GHz)	12.52	11	10	8.2	7.2	6	5

Based on the above simulation results, the required UL ACIR for 14800 – 15350 MHz for urban macro scenarios are in summarized in Table 6.1.3.1.2-5. Many results suggest ACIR around e.g. 13-15dB excluding highest and lowest values.

Table 6.1.3.1.2-5: UL simulation results for 14800 – 15350 MHz

	ACIR (dB)
Company	**Urban macro**
Nokia	-9 (relative)
Apple	22-24
CATT	20
MediaTek	15-17
Vivo	12
Qualcomm	13
Ericsson	11-14
ZTE	-10 (relative)
Huawei	18

6.2 General parameters

6.2.1 Duplex mode

There is no defined 3GPP band for the 14800 - 15350 MHz frequency range. Even though FDD is not precluded, TDD is assumed as a baseline duplexing in this frequency range. SBFD can be a candidate duplexing method for this frequency range. The core requirements for Rel-19 SBFD work item can be tracked through the list of impacted specs captured in the respective Work Item description.

6.2.2 Channel Bandwidth

While a number of channel bandwidth will be specified for this frequency range, 200 MHz is considered as a typical channel bandwidth. Other channel bandwidths compared to 200MHz are not precluded for this range.

6.2.3 Signal Bandwidth

The signal bandwidth for a 200MHz typical channel bandwidth signal is associated with both SCS and spectrum utilization, and can be calculated based on the spectrum utilization:

$$\text{Signal bandwidth} = N_{RB} \times \text{SCS} \times 12$$

with N_{RB}: Number of Resource block for 200 MHz channel bandwidth and SCS to be specified when introducing new band(s) for this frequency range.

6.3 BS parameters

6.3.1 Transmitter characteristics

6.3.1.1 Power dynamic range

There is no power control in downlink and fixed power per resource block is assumed during the study phase. Hence 0 dB power dynamic range was agreed for the LS reply.

6.3.1.2 Spectral mask

Category A limits for Wide Area BS for AAS BS are listed in Table 6.3.1.2-1.

Table 6.3.1.2-1: Wide Area BS operating band unwanted emission limits for AAS BS (Category A)

Frequency offset of measurement filter -3dB point from the carrier frequency, Δf	Limits	Measurement Bandwidth
0 MHz ≤ Δf < 50MHz	$2\text{dBm} - \frac{7}{50}\left(\frac{f\_offset}{MHz} - 0.05\right)$	100 kHz
50 MHz ≤ Δf < min(100 MHz, Δf_{max})	-5 dBm	100 kHz
100 MHz ≤ Δf ≤ Δf_{max}	-4 dBm	1 MHz
NOTE: Δf_{max} is equal to f_offset_{max} minus half of the bandwidth of the measuring filter, where f_offset_{max} is the offset to the frequency Δf_{OBUE} = 100 MHz outside the downlink operating band.		

Note: AAS BS Category B limits for Wide Area BS are not yet specified by regional regulatory bodies.

Medium Range BS and Local Area BS OBUE limits are listed in Table 6.3.1.2-2, 6.3.1.2-3 and 6.3.1.2-4.

Table 6.3.1.2-2: Medium Range BS operating band unwanted emission limits for AAS BS, 40 < $P_{rated,c,TRP}$ ≤ 47 dBm

Frequency offset of measurement filter -3dB point, Δf	Frequency offset of measurement filter centre frequency, f_offset	Limits	*Measurement bandwidth*
0 MHz ≤ Δf < 50 MHz	0.05 MHz ≤ f_offset < 50.05 MHz	$\text{Prated, c, TRP} - 53\text{dB} - \frac{7}{50}\left(\frac{f\_offset}{MHz} - 0.05\right)$	100 kHz
50 MHz ≤ Δf < min(100 MHz, Δf_{max})	50.05 MHz ≤ f_offset < min(100.05 MHz, f_offset_{max})	$P_{rated,c,TRP}$ - 60dB	100 kHz
100 MHz ≤ Δf ≤ Δf_{max}	100.05 MHz ≤ f_offset < f_offset_{max}	Min($P_{rated,c,TRP}$ - 60dB, -16dBm)	100 kHz
NOTE 1: $P_{rated,c,TRP}$ is rated carrier total radiated power declared per radiated interface boundary. NOTE 2: Δf_{max} is equal to f_offset_{max} minus half of the bandwidth of the measuring filter, where f_offset_{max} is the offset to the frequency Δf_{OBUE} = 100 MHz outside the downlink operating band.			

Table 6.3.1.2-3: Medium Range BS operating band unwanted emission limits for AAS BS, $P_{rated,c,TRP} \leq$ 40 dBm

Frequency offset of measurement filter -3dB point, Δf	Frequency offset of measurement filter centre frequency, f_offset	Limits	*Measurement bandwidth*
0 MHz ≤ Δf < 50 MHz	0.05 MHz ≤ f_offset < 50.05 MHz	$-13\text{dBm} - \frac{7}{50}\left(\frac{f\_offset}{MHz} - 0.05\right)$	100 kHz
50 MHz ≤ Δf < min(100 MHz, Δf_{max})	50.05 MHz ≤ f_offset < min(100.05 MHz, f_offset_{max})	-20 dBm	100 kHz
100 MHz ≤ Δf ≤ Δf_{max}	100.05 MHz ≤ f_offset < f_offset_{max}	-20 dBm	100 kHz
NOTE 1: $P_{rated,c,TRP}$ is rated carrier total radiated power declared per radiated interface boundary. NOTE 2: Δf_{max} is equal to f_offset_{max} minus half of the bandwidth of the measuring filter, where f_offset_{max} is the offset to the frequency Δf_{OBUE} = 100 MHz outside the downlink operating band.			

Table 6.3.1.2-4: Local Area BS operating band unwanted emission limits for AAS BS

Frequency offset of measurement filter -3dB point, Δf	Frequency offset of measurement filter centre frequency, f_offset	Limits	*Measurement bandwidth*
0 MHz ≤ Δf < 50 MHz	0.05 MHz ≤ f_offset < 50.05 MHz	$-21\text{dBm} - \frac{7}{50}\left(\frac{f\_offset}{MHz} - 0.05\right)$	100 kHz
50 MHz ≤ Δf < min(100 MHz, Δf_{max})	50.05 MHz ≤ f_offset < min(100.05 MHz, f_offset_{max})	-28 dBm	100 kHz
100 MHz ≤ Δf ≤ Δf_{max}	100.05 MHz ≤ f_offset < f_offset_{max}	-28 dBm	100 kHz
NOTE: Δf_{max} is equal to f_offset_{max} minus half of the bandwidth of the measuring filter, where f_offset_{max} is the offset to the frequency Δf_{OBUE} = 100 MHz outside the downlink operating band.			

6.3.1.3 ACLR

The ACLR should be higher than the value specified in Table 6.3.1.3-1.

Table 6.3.1.3-1: Base station ACLR limit

BS channel bandwidth of lowest/highest carrier transmitted $BW_{Channel}$ (MHz)	BS adjacent channel centre frequency offset below the lowest or above the highest carrier centre frequency transmitted	Assumed adjacent channel carrier (informative)	Filter on the adjacent channel frequency and corresponding filter bandwidth	ACLR limit
200	$BW_{Channel}$	NR of same BW (Note 2)	Square (BW_{Config})	30 dB
	2 x $BW_{Channel}$	NR of same BW (Note 2)	Square (BW_{Config})	30 dB
NOTE 1: $BW_{Channel}$ and BW_{Config} are the BS channel bandwidth and transmission bandwidth configuration of the lowest/highest carrier transmitted on the assigned channel frequency. NOTE 2: With SCS that provides largest transmission bandwidth configuration (BW_{Config}).				

6.3.1.4 Spurious emissions

The Category A spurious emission limits applicable are extracted from TS 38.104 [9], as listed in Table 6.3.1.4-1.

Table 6.3.1.4-1: General BS transmitter spurious emission limits for 14800 - 15350 MHz operation (Category A)

Frequency range	Limit	Measurement Bandwidth	Note
30 MHz – 1 GHz	-13 dBm	100 kHz	Note 1
1 GHz – 2nd harmonic of the upper frequency edge of the DL operating band		1 MHz	Note 1, Note 2
NOTE 1: Bandwidth as in ITU-R SM.329, s4.1 NOTE 2: Upper frequency as in ITU-R SM.329, s2.5 table 1.			

Note: AAS BS Category B limits are not yet specified by regional regulatory bodies.

The AAS BS transmitter spurious emission limits in Table 6.3.1.4-1 are also applicable to Medium Range and Local Area BS.

6.3.1.5 Maximum output power

The maximum base station output power/ sector (e.i.r.p.) was provided as extracted in Table 6.3.1.5-1. It was agreed to be aligned with antenna characteristics.

Table 6.3.1.5-1: Maximum BS output power in 14800 to 15350 MHz

	Macro suburban	Macro urban	Micro urban	Indoor Hotspot
Maximum base station output power/sector (e.i.r.p.) (dBm)	84.3	84.3	74.3	40.0

The Total Radiated Power (TRP) for two polarizations was agreed as shown in Table 6.3.1.5-2 below.

Table 6.3.1.5-2: Total Radiated Power

Parameter	Macro Sub-urban	Macro Urban	Micro Urban	Indoor Hotspot
Total Radiated Power for two polarizations (dBm)	46	46	36	23

6.3.1.6 Average output power

It was agreed the average output power won't be mentioned in the reply LS.

6.3.2 Receiver characteristics

6.3.2.1 Noise figure

The BS typical noise figure is listed in Table 6.3.2.1-1, and BS class definitions can be seen in [9], § 4.4.

Table 6.3.2.1-1: Noise figure

BS class	Noise figure (dB)
Wide Area	8
Medium Range	13
Local Area	16

6.3.2.2 Sensitivity

The OTA sensitivity requirement will be based on the NF and the antenna gain:

$$EIS_{REFSENS} = P_{kT} + 10 * log_{10}(BW) + NF + IM + SNR - G \quad (dBm)$$

Where:

- BW is the configured bandwidth of the FRC,
- NF is the noise figure,
- IM is implementation margin not related to antenna array,
- SNR is the required SNR to reach 95% throughput, and
- G is the antenna gain including RF losses and 3dB off peak margin.

However, the sensitivity is not a critical parameter for sharing and compatibility studies. It was agreed to not mention any value for this parameter in LS.

6.3.2.3 Blocking response

The out-of-band blocking radiated requirement applies from 30 MHz to 2nd harmonic of the upper frequency edge of the operating band, excluding the in-band blocking frequency range, but including the downlink frequency range in case of an FDD operating band as listed in Table 6.3.2.3-1. It is agreed to adopt Δf_{OOB} = 100 MHz for AAS BS.

Table 6.3.2.3-1: OTA out-of-band blocking performance requirement for 14800 – 15350 MHz operation

Frequency range of interfering signal (MHz)	Wanted signal mean power (dBm)	Interferer RMS field-strength (V/m)	Type of interfering signal
30 to 12750	$EIS_{REFSENS}$ + 6 dB	0.36	CW
12750 to $F_{UL,low}$ – 100	$EIS_{REFSENS}$ + 6 dB	0.1	CW
$F_{UL,high}$ + 100 to 2nd harmonic of the upper frequency edge of the *operating band*	$EIS_{REFSENS}$ + 6 dB	0.1	CW

The out-of-band blocking conductive requirements and in-band blocking requirements should be further studied in the WI phase.

6.3.2.4 ACS

According to the simulation results in clause 6.1.3, it is agreed to specify 30 dB ACS.

6.4 UE parameters

6.4.1 Transmitter characteristics

6.4.1.1 Power dynamic range

The minimum controlled output power of the UE is defined as the power in the channel bandwidth for all transmit bandwidth configurations (resource blocks), when the power is set to a minimum value. Based on the study in sub-clause 6.5.2, the UE antenna type for 14800 – 15350 MHz can reuse existing FR1 antenna characteristics so that both nominal maximum and minimum output power refer to existing FR1 bands, i.e., power dynamic range is 56 dB with power class 3 (i.e. 23 dBm maximum output power) UE.

6.4.1.2 Spectral mask

The UE spectral mask is described in TS 38.101-1 [12] clause 6.5.2.2 Table 6.5.2.2-1. Emission mask for 200 MHz BW is based on the CA mask as defined in TS 38.101-1 [12] clause 6.5A.2.2. The SEM requirements in this frequency range may be relaxed than FR1 intra-band CA with 200MHz aggregated bandwidth in the WI phase.

6.4.1.3 ACLR

Considering that the UE needs to meet the Occupied bandwidth (OBW) requirements which is higher than the ACLR needed for co-existence as noted in sub-clause 6.1.3, it was concluded that 24 dB ACLR would be sufficient for 14800 – 15350 MHz. Thus, ACLR of 24 dB can be considered for the frequency range 14800 – 15350 MHz.

The actual ACLR for this frequency range or parts there-of should be further studied in the WI phase.

6.4.1.4 Spurious emissions

The general spurious emissions defined in TS 38.101-1 [12] clause 6.5.3 Table 6.5.3.1-2 with OOB boundary given in Table 6.5A.3.1-1 can apply to the frequency range 14800 -15350 MHz.

6.4.1.5 Maximum output power

Based on the study in sub-clause 6.5.2, the UE maximum output power for the considered frequency ranges could be 23 dBm. Other UE power classes, e.g., 20dBm, 26dBm and 29dBm, are not precluded (corresponding ACLR limit will be adapted accordingly to avoid additional interference).

6.4.1.6 Average output power

NOTE: This parameter was not mentioned in the previous response to ITU-R WP5D.

6.4.2 Receiver characteristics

6.4.2.1 Noise figure

A noise figure of 11 dB was assumed for coexistence simulation in sub-clause 6.1.2. For the frequency range 14800 – 15350 MHz noise figure of 13 dB can be reused.

The actual noise figure for this frequency range or parts there-of to define RF requirements should be further studied in the WI phase.

6.4.2.2 Sensitivity

The sensitivity is not a critical parameter for sharing and compatibility studies. It was agreed to not mention any value for this parameter.

6.4.2.3 Blocking response

The blocking characteristic specified in clause 7.6A Tables 7.6A.2.1-1 and 7.6A.3-1 Bandwidth Class C and clause 7.7 Table 7.7A-1 Bandwidth class C for spurious response of TS 38.101-1 [12] could be applied for 200 MHz BW requirements of the frequency range 14800 – 15350 MHz.

The actual requirements for this frequency range or parts there-of may differ depending on the band plan and possible re-use of RF hardware components.

6.4.2.4 ACS

According to the previous studies and simulation results in sub-clause 6.1.3, adjacent channel selectivity (ACS) is agreed as 24 dBc for 14800 – 15350 MHz. Thus, ACS of 24 dB can be considered for the frequency range 14800 – 15350 MHz.

The actual ACS for this frequency range or parts there-of should be further studied in the WI phase.

6.5 Antenna characteristics

6.5.1 BS antenna characteristics

6.5.1.1 Antenna model

The antenna model for AAS BS is described in subclause 7.1.

6.5.1.2 Antenna parameters

In Table 6.5.1.2-1, representable parameter sets relevant for an AAS base station operating within 14800 - 15350 MHz are provided.

Table 6.5.1.2-1: Antenna array parameters

		Macro suburban	Macro urban	Micro urban	Small cell indoor/ Indoor urban
1	**Base station Antenna Characteristics**				
1.1	Antenna pattern	Table 7.1.3-1			N/A
1.2	Element gain (dBi) (Note 2)	6.4	6.4	6.4	5
1.3	Horizontal/vertical 3 dB beam width of single element (degree)	90º for H 65º for V	90º for H 65º for V	90º for H 65º for V	90º for H 90º for V
1.4	Horizontal/vertical front-to-back ratio (dB)	30 for both H/V	30 for both H/V	30 for both H/V	30 for both H/V
1.5	Antenna polarization	Linear ±45º polarized sub-array	Linear ±45º polarized sub-array	Linear ±45º polarized sub-array	Linear ±45º polarized sub-array
1.6	Antenna array configuration (Row × Column) (Note 4)	16x24	16x24	16x24	4x4
1.7	Horizontal/Vertical radiating sub-array or element spacing (Note 5)	0.5 of wavelength for H, 2.8 of wavelength for V	0.5 of wavelength for H, 2.8 of wavelength for V	0.5 of wavelength for H, 2.8 of wavelength for V	0.5 of wavelength for H, 0.5 of wavelength for V
1.7a	Number of element rows in sub-array	4	4	4	N/A
1.7b	Vertical element separation in sub-array ($d_{v,sub}$)	0.7 of wavelength for V	0.7 of wavelength for V	0.7 of wavelength for V	N/A
1.7c	Pre-set sub-array down-tilt (degrees) (Note 6)	3	3	3	N/A
1.8	Array Ohmic loss (dB) (Note 2)	2	2	2	2
1.9	Conducted power (before Ohmic loss) per sub-array or element (dBm) (Note 3)	17.2	17.2	7.2	8.0
1.10	Base station horizontal coverage range (degrees)	±60	±60	±60	±90
1.11	Base station vertical coverage range (degrees) (Note 1)	90-100	90-100	90-100	0-180
1.12	Mechanical down-tilt (degrees)	6	6	6	N/A
1.13	Base station output power/sector (e.i.r.p.) (dBm) (Note 7)	84.3	84.3	74.3	40.0

Note 1: The vertical coverage range is given in global coordinate system, i.e., 90° being at the horizon. This range includes the mechanical down-tilt given in row 1.12.

Note 2: The element gain in row 1.2 includes the loss given in row 1.8 and is per polarization.

Note 3: Conducted power values are per polarization. The conducted power per sub-array assumes 16 × 24 sub-arrays and 2 polarizations for the Macro Suburban, Macro Urban and Micro Urban cases; the conducted power per element assumes 4x4 elements for the Small cell indoor/ Indoor Urban case. This power is typical power, there is no upper limit for Wide Area Base station (For BS class definitions, see 3GPP TS 38.104 [1], § 4.4).

Note 4: 16 × 24 means there are 16 rows and 24 columns of radiating sub-arrays for Macro Suburban, Macro Urban and Micro Urban cases. 4x4 means there are 16 rows and 24 columns of radiating elements for Small cell indoor/ Indoor Urban case.

Note 5: For the case of 4 elements per sub-array, d_v will be 2.8 wavelengths.

Note 6: The pre-set sub array down-tilt is a fixed design parameter for a base station. It is envisaged as a passive fixed (non-varying) electrical tilt within the sub-array elements.

Note 7: The base station e.i.r.p per sector is calculated as total power (including power from two orthogonal polarizations).

Note 8: Mechanical down-tilt is handled by a coordinate system transformation described in 3GPP TR 36.814 section A.2.1.6.2.

Note 9: θ_{etilt} and φ_{escan} is the BS array antenna beam steering direction used in Table 7.1.3-1, they should be set so that the beam steering direction is within the vertical and horizontal coverage ranges in row 1.11 and row 1.10, respectively.

6.5.2 UE antenna characteristics

6.5.2.1 General considerations

One of the key issues for this range is the UE RF architecture. While existing FR1 system parameters are defined for frequencies up to 7.1GHz, same FR1 principles are already assumed for e.g. 7.1-8.4GHz, which is however below the considered range of 14.8-15.3GHz. At the same time, the lower bound for the FR2 starts at 24.25GHz, which is notably higher than 15.3GHz. A choice for a particular UE RF architecture at these frequency ranges should consider implementation feasibility, e.g. physical constraints in case of handheld devices, and anticipated performance, such as coverage. The capabilities of PA technology in the FR2 frequency range motivated 3GPP to consider a UE architecture which relies on panels performing analog beam-forming, which was also considered as a feasible option from the handheld device implementation perspective. In contrast, panels and analog beam-forming are not feasible for lower FR1 frequencies.

In the context of the UE RF architecture, better UL coverage at FR2 frequencies was one of the key driving factors to consider the UE RF design with panels performing analog beam-forming. An FR2-like array antenna system incorporates analog beamforming into the array antenna to increase the coherent EIRP gain, thus helping to reduce the path loss between the UE and the base station. Furthermore, the FR2 array antenna, LNAs, PAs, beamformers, and PMIC are integrated into a single package, small form factor of which was also considered as a feasible option from the handheld device implementation perspective. As for the frequencies around 10-15GHz, previous work studied feasibility of FR2 principles in hand-held devices operating in that frequency range. One of the main challenges is the size of potential FR2 panel and, as noted in previous work, "*… we can see that the antenna module doubles in size going from 28 GHz to 20 GHz and further doubles at 14 GHz*". Figure 6.5.2.1-1 presents an example of the patch width and ground plane extension based on the microstrip patch array design assuming four elements with half-wavelength spacing.

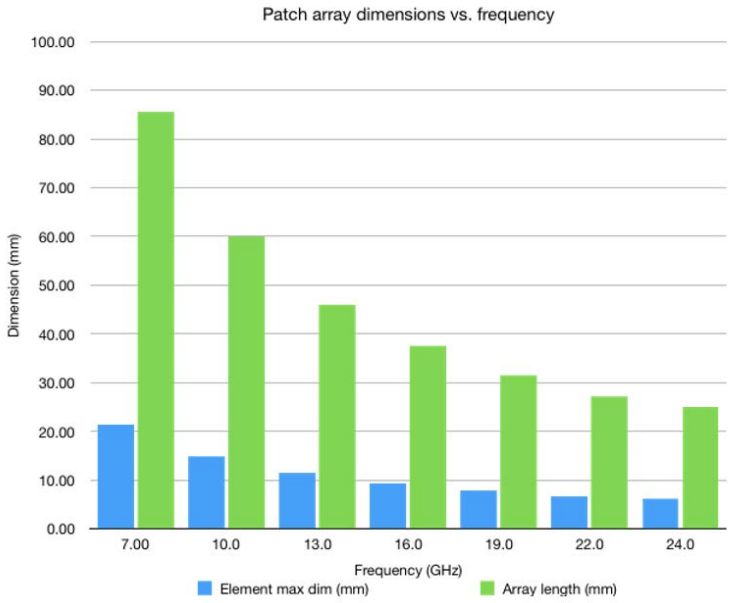

Figure 6.5.2.1-1: Patch array dimensions vs. frequency

For more detailed information on the potential array antenna size operating at the considered frequency of 15GHz, Figure 6.5.2.1-2 below presents several example cases with different antenna arrangements accounting for the typical spacing between elements of the array antenna of half wavelength. As can be seen from the figure for a typical inter-element antenna spacing, the total antenna array size becomes much larger comparing to the FR2 sizes.

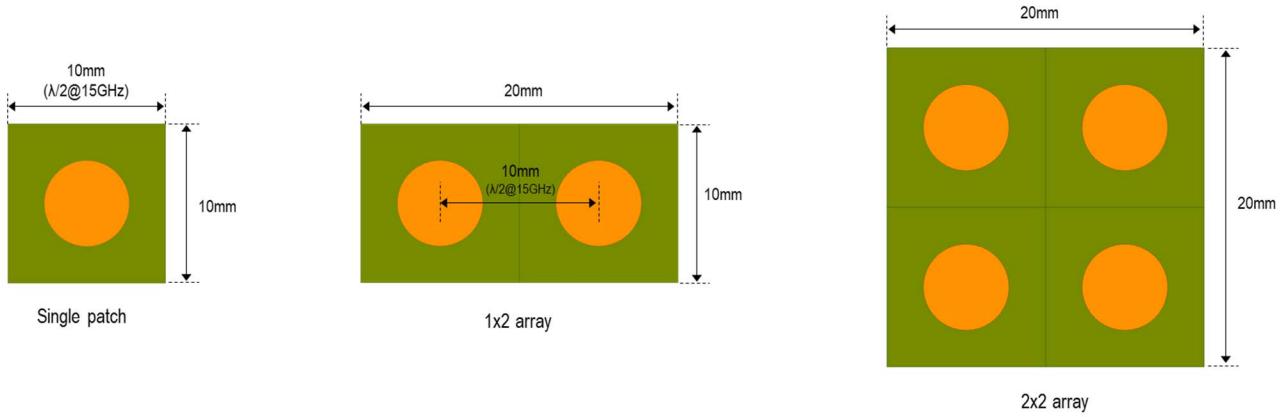

Figure 6.5.2.1-2: Estimated antenna size at 15GHz

Figure 6.5.2.1-3 below illustrates an example of a survey of the internal area used by four different commercially available 5G devices for FR1 (based on individual company contributions in RAN4). The FR2 area is calculated based a single 4x1 reference design, the configuration used as the basis for current FR2 spherical coverage requirements. Additionally, an estimate of the required 12-15GHz antenna array area is provided for comparison, similarly based on a 4x1 microstrip patch array with half-wavelength spacing. So, assuming dedicated apertures, an estimated 4x1 array at 12-15 GHz would represent an additional area growth on the order of 30-70% relative to antenna area usage currently needed to support FR1.

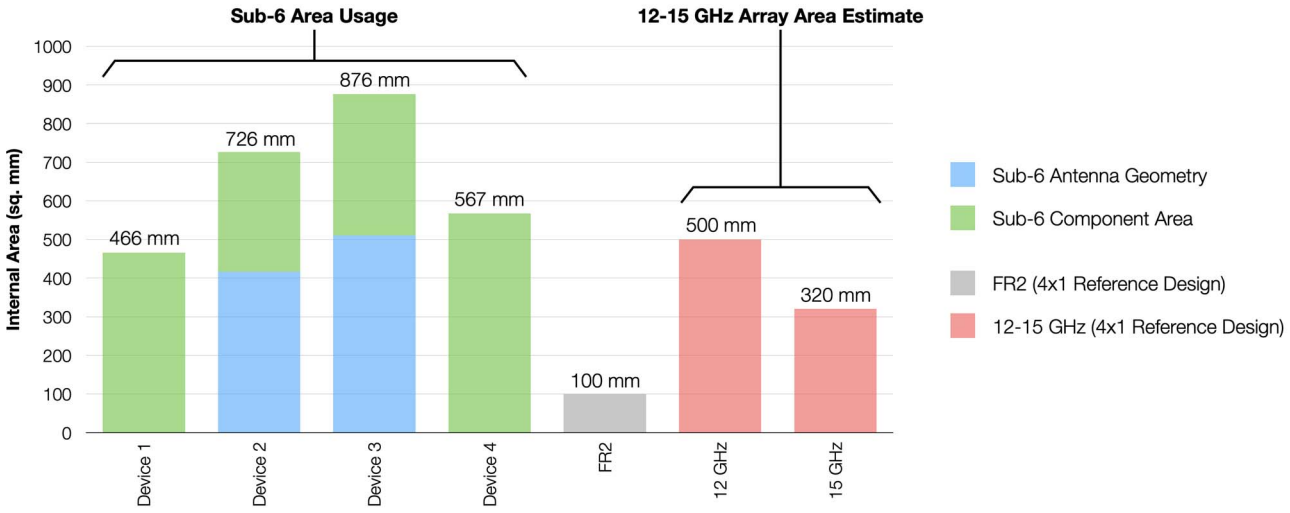

Figure 6.5.2.1-3: A survey of internal area usage for FR1, FR2 and estimated 13-15GHz antennas

In addition, support of analog beamforming in 15GHz might impose a substantial growth and volume requirements dedicated for cellular antennas. Furthermore, the nature of such an array might constrain the dimensions leading to implementation challenges in densely integrated consumer devices that can be of different form factors. For instance, Figure 6.5.2.1-4 shows an example of the PCB of a foldable phone, from which one can see that it might be challenging to mount single patch antennas on four edges or the backside of the smartphone considering the larger array size and the already-packed smartphone space. In other words, it can be difficult for a hand-held to assume that there will be extra space in all required physical dimensions making it challenging, at least from the packing perspective, to put FR2-like panels supporting the 15GHz range.

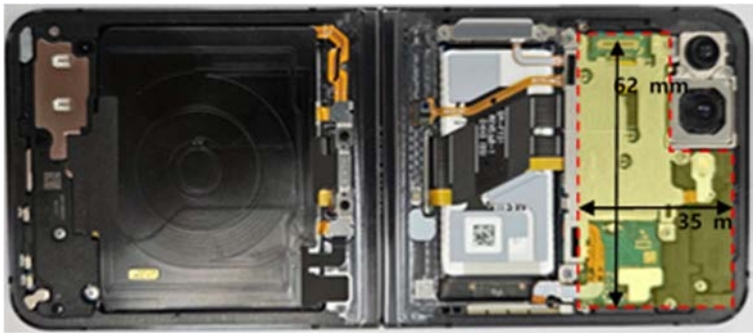

Figure 6.5.2.1-4: Main PCB of a foldable mobile phone.

6.5.2.2 Design with patch antennas

A possible design approach is the adoption of patch antennas (i.e., FR1-like design) which gives more flexibility to the OEM vendors because even if a device implements more than one Tx, there is an additional flexibility on where Tx antennas can be placed. Furthermore, more than one Tx antenna can attain coherent EIRP gain through the corresponding placement of co-directional and co-located antennas when coherent Tx is implemented. Each antenna in such FR1-like system is linked to its own digital chain, allowing for easy support of coherent Tx. It can also reduce the PA power requirement for each antenna element, thus enhancing the overall power consumption of the UE at 15GHz, and it can help increase the coverage distance between the base station and the UE. For instance, Figure 6.5.2.2-1 presents an example of a general mobile device form factor with two patch antennas placed within the device as presented at the distance corresponding to approximately three wavelengths.

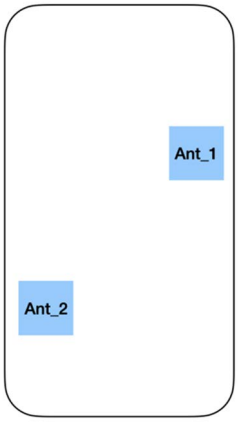

Figure 6.5.2.2-1: Exemplary placement of two patch antennas within a mobile device.

In this example, each patch antenna gain is around 2dB with the Tx power 23dBm. Additionally, Figure 6.5.2.2-2 below presents separately distribution of antenna and EIRP gains for the considered example antennas, where the baseline curve is only one antenna. Gain values are obtained by probing all points in 3D space around considered antennas, which allows us to find the best beam at each point of space independent of the base station location. In other words, these figures illustrate possible gain values, including the best one, regardless of the phone orientation with respect to the base station. As can be seen from this example, from the antenna gain perspective, the average gain comparing to one Tx is around 2.5dB. From the EIRP perspective, the average gain comparing to one Tx is around 5.5dB, which comprises 2.5dB antenna gain and 3dB coming from the fact that there are two Tx antennas each transmitting at 23dBm.

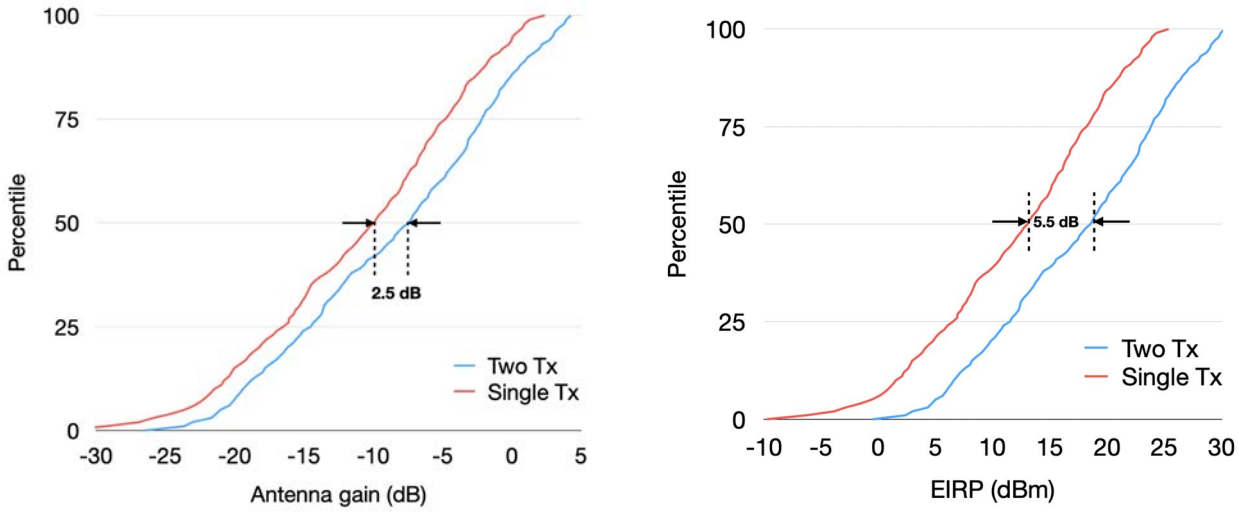

Figure 6.5.2.2-2: Antenna and EIRP gain for the considered two Tx antennas.

An additional aspect for the FR1-like antenna design is the resulting radiation pattern. It is worth noting that unlike at the antenna and EIRP gain, which are not very sensitive for the actual placement of Tx antennas, the radiation pattern may vary a lot. For instance, Figure 6.5.2.2-3 below presents an example resulting beam pattern from two Tx antennas physical location of which is the same as in Figure 6.5.2.2-1. For the sake of better clarity, we present the resulting radiation pattern in 2D and 3D spaces. Since two Tx antennas are placed at the back side of the phone, the resulting radiation pattern has a big negative gain in the opposite direction.

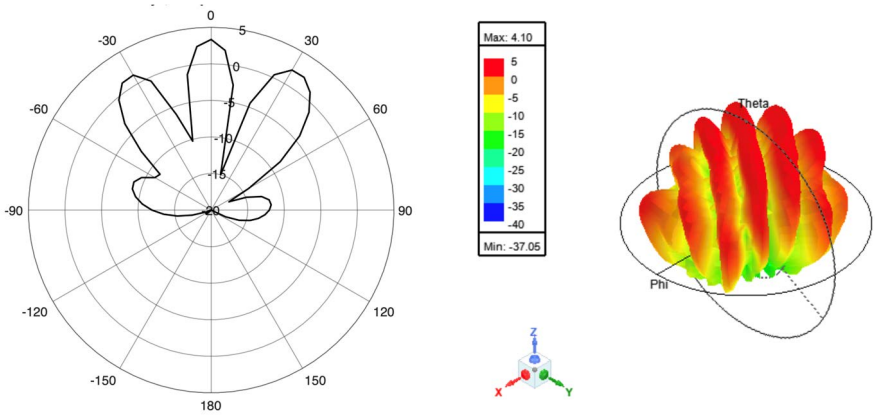

Figure 6.5.2.2-3: Radiation pattern for two Tx antennas presented in Figure 6.5.2.x-2.

On the Rx side, more than one discrete/ FR1-like antenna with digital beamforming can maximize the received signal power to improve the cell edge performance. For a cell-center user, instead of maximizing the received signal power, all antennas can be used jointly to achieve spatial multiplexing gain.

6.5.2.3 Design with metal frame antennas

A simulation with two general metal frame Tx antennas was conducted to estimate the antenna gain and performance for cases of single-Tx and multi-Tx without beam steering assumptions. The antenna placement for the evaluation is captured in 6.5.2.3-1.

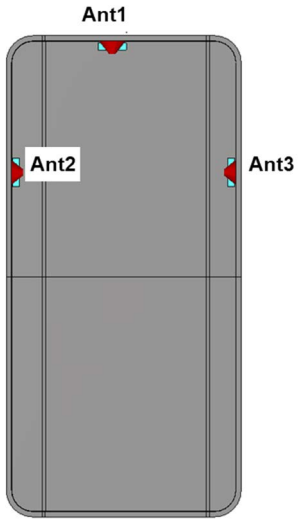

Figure 6.5.2.3-1: Exemplary placement of metal frame antennas within a mobile device.

With the assumption above, simulation results of the above example related to antenna performance are summarized in Figure 6.5.2.3-2 and Table 6.5.2.3-1, which also capture radiation efficiency and directivity in terms of peak antenna gains of each scenario.

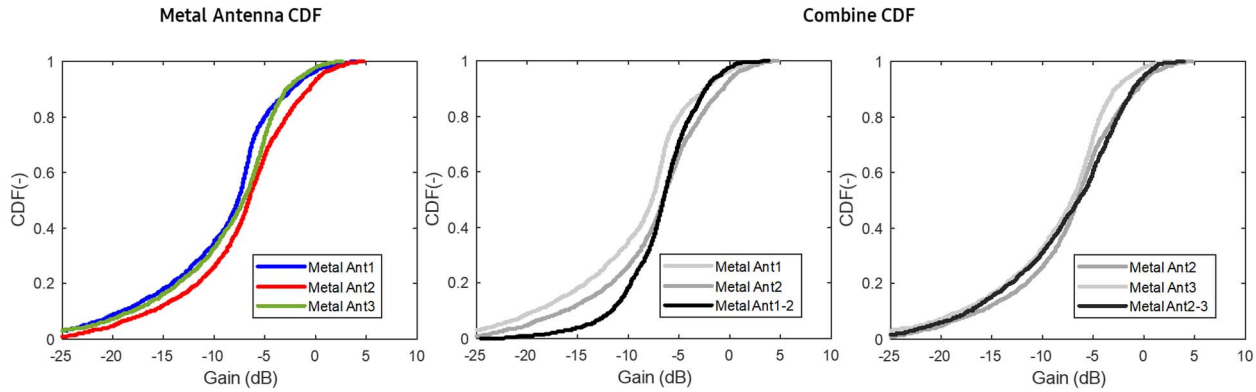

Figure 6.5.2.3-2: CDF of peak antenna gains for metal antennas

Table 6.5.2.3-1: Peak antenna gains for one-Tx and two-Tx

	Ant1	Ant2	Ant3
Gain (dB)	3.9	4.8	2.7
Rad. Efficiency (dB)	-6.3	-4.8	-6.3
Directivity (dB)	10.2	9.6	9.0
	Ant1 + Ant2	Ant1 + Ant 3	Ant2 + Ant3
Combined gain (dB)	3.8	2.6	3.9
Gain drop (dB)	-1.0	-1.3	-0.9

As seen from Figure 6.5.2.3-2 and Table 6.5.2.3-1, in terms of the peak antenna gain with metal frame antennas, it is shown that for the considered example, the single-Tx antenna gain can reach up to 4.8 dB with its directivity and efficiency characteristics at the frequency range around 15 GHz. However, for the case of two-Tx, it is shown that the peak gain of combined two Tx antennas does not show better performance, but rather drops compared to the single-Tx case for the antenna placement in Figure 6.5.2.3-1. This would be coming from two different radiation patterns as depicted in Figure 6.5.2.3-3.

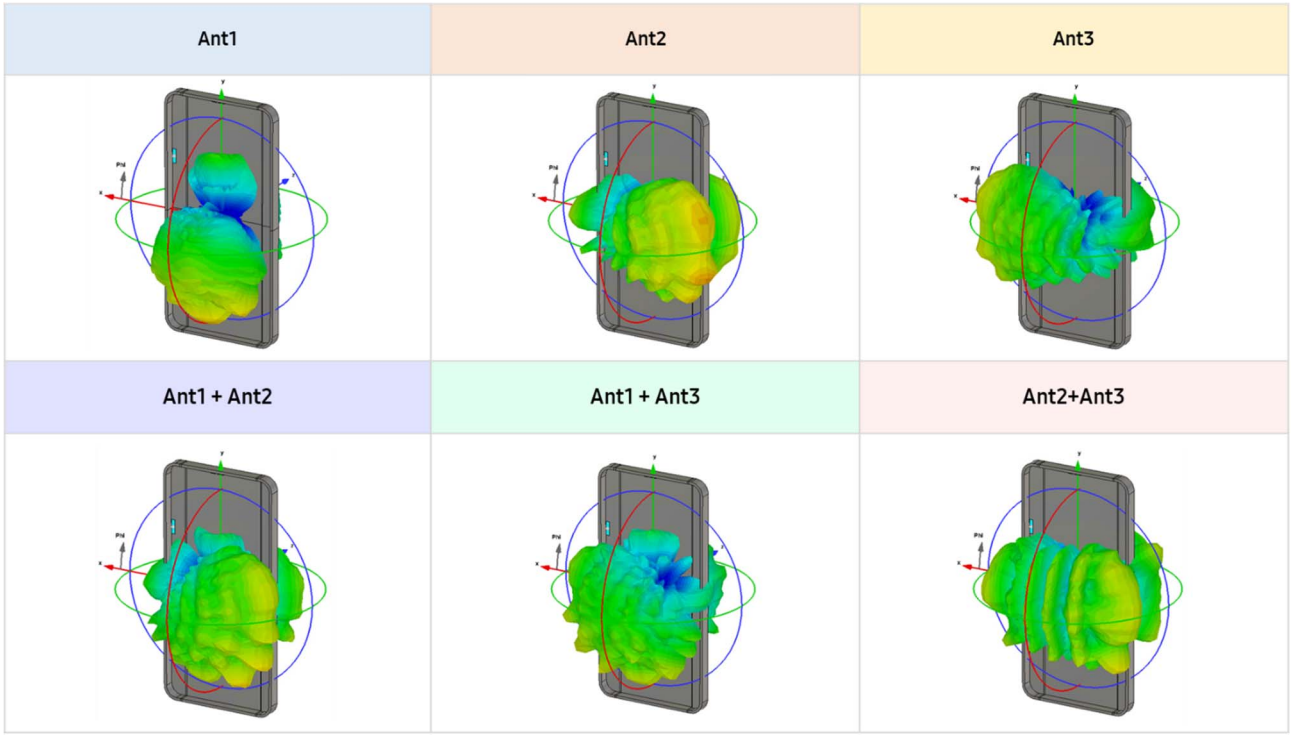

Figure 6.5.2.3-3: Simulated radiation patterns for one-Tx and two-Tx cases

The radiation pattern of antennas in a practical device has different peak direction compared with the boresight direction since the UE ground has much longer electric strength at this frequency range as shown in Figure 6.5.2.3-3. For example, Ant2 would form its peak direction toward Ant3, and similarly, Ant1 has the peak gain at the opposite direction toward the bottom side of UE at this case. On the other hand, if two Tx antennas are adjacent with the same orientation, it may have increased peak antenna gain thanks to the same radiation pattern between two Tx antennas although it would face a different issue such as antenna isolation to keep the fundamental performance.

In this regard, for FR1-like design with metal frame antennas, similar to the design approach with FR1-like patch antenna case, it should be noted that multi-Tx antennas may not help improving peak gain performance unless their placements are not designed carefully in terms of both radiation patterns and isolation.

7 Additional information on AAS

7.1 Array antenna model

7.1.1 Overview

A parameterized array antenna model has been developed over time in 3GPP to model AAS BS radiation patterns. The model has been used for numerous coexistence studies in RAN4, including AAS, NR, HST, IAB, etc. The model has been adopted in other forums outside RAN4 and is also described in RAN1 and in ITU-R in recommendation M.2101 [28].

The model is defined around a set of equations, which rely on a set of input parameters to describe the array antenna. At a high level the model can be described as shown in Figure 7.1.1-1.

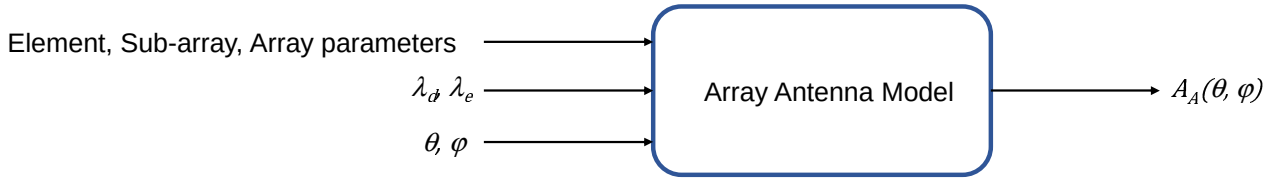

Figure 7.1.1-1: Array antenna model overview

Parameters can be divided into different categories:

- General parameters, which are parameters that will be required for the simulator (spatial angles, considered wavelength).
- Element parameters used to model the radiating elements.
- Sub-array parameters used to model the sub-array.
- Array parameters used to model the array.

The model will produce gain normalized radiation pattern for given θ, φ angles defined in the range $0 \leq \theta \leq 180$ degrees and $-180 \leq \varphi \leq 180$ degrees.

The wavelength, λ_d is related to the design of the array and is fixed by design, while the excitation wavelength, λ_e may vary as function of considered frequency within a specific operating band.

7.1.2 Parameters

The input parameters required to describe the antenna is summarized and described in Table 7.1.2-1.

Table 7.1.2-1: Model input parameters

Category	Parameter	Description	Note
General	λ_d	Design wavelength for array antenna in meters	The wavelength is fixed and selected for a given design frequency. The wavelength will not vary within a given operating band for a given design.
	λ_e	Array excitation wavelength in meters	This wavelength varies within the considered band.
	θ	Vertical angle in degrees	
	φ	Horizontal angle in degrees	
	P_{tx}	Total conducted power in dBm	For a dual polarized antenna, the total conducted power is calculated over $MxNx2$ ports
	θ_{mech}	BS mechanical down-tilt angle in degrees	The mechanical down-tilt angle is a deployment parameter selected to maximize coverage within a given coverage area. The mechanical tilt can be applied as a coordinate transformation as described in TR 36.814, subclause A.2.1.6.2.
Element	A_m	Element front-to-back ratio in dB	
	SLA_v	Element side-lobe suppression in dB	
	φ_{3dB}	Element horizontal half power beamwidth in degrees	
	θ_{3dB}	Element vertical half power beamwidth in degrees	
	$G_{E,max}$	Element peak gain in dBi	This parameter is related to the selection of φ_{3dB}, θ_{3dB} and L_E, where $G_{E,max} = D_{E,max} - L_E$ and $D_{E,max}$ is related to φ_{3dB}, θ_{3dB} and array lattice unit area for the element.
	L_E	Element loss in dB	
Sub-array	M_{sub}	Number of element rows in sub-array	
	$d_{v,sub}$	Vertical element separation in sub-array in meters	
	$\theta_{subtilt}$	Electrical pre-set sub-array down-tilt angle in degrees	The pre-set sub array down-tilt is a fixed design parameter for a base station. It is envisaged as a passive fixed (non-varying) electrical tilt within the sub-array elements. The deployment configuration (including mechanical tilt) for a base station is dependent on the environment. Thus, a same base station with fixed pre-set subarray tilt could also be used across different environments. The value of the pre-set tilt is determined based on the intended deployment scenarios and targeted user distribution and coverage range.
Array	M	Number of sub-array rows in array	
	N	Number of sub-array columns in array	
	d_h	Horizontal sub-array separation in array in meters	
	d_v	Vertical sub-array separation in array in meters	This parameter is related to M_{sub} and $d_{v,sub}$.
	θ_{etilt}	Electrical beam direction down-tilt angle in degrees	
	φ_{escan}	Electrical beam direction scan angle in degrees	
	ρ	Array excitation correlation factor	For wanted signal $\rho = 1$, while for unwanted emission the correlation falls of as function of frequency offset from carrier within the interval $0 \leq \rho < 1$.

The total conducted power, P_{tx} at the Transceiver Array Boundary (TAB) is related to Total Radiated Power (TRP) in logarithmical scale as:

$$P_{tx} = 10log_{10}(2MN) + P_n$$

$$TRP = P_{tx} - L_E$$

Where, P_n is the power per transmitter branch in dBm. Total conducted power is defined as the total power for all ports, including two orthogonal polarizations.

The Equivalent Isotropic Radiated Power (EIRP) is calculated in dBm using the model as:

$$EIRP(\theta, \varphi) = P_{tx} + A_A(\theta, \varphi)$$

The peak EIRP for a bore sight beam can also be derived from parameters as:

$$EIRP_0 = P_{tx} + G_{E,max} + 10log_{10}(M_{sub}) + 10log_{10}(MN)$$

When co-existence is evaluated in RAN4, the focus is on the main beam pointing towards the UE, but for other compatibility scenarios, e.g., with other services, the focus is not necessarily just the main beam. Spatial regions outside the main beam may also be highly relevant. Since the sub-array topology will affect the radiating characteristics in the sidelobe region, the model needs to be extended to provide the ability to model the sidelobe region characteristics correctly with reasonable complexity.

For the case where single element array geometry is considered ($M_{sub}=1$), the extended array model collapses to the original model described in former 3GPP studies.

The antenna element separation is an important parameter that must be selected with care. Obviously, the value is static for a specific base station design, whereas the compatibility analysis may need to cover an entire frequency band. Typically, an array antenna is designed to support given element separations for the highest frequency to avoid grating lobes for lower frequencies, but other design principles can be used for base stations supporting multiple bands or very wide operating bands. When an array antenna is modelled it is essential to separate the design frequency and corresponding wavelength, with the frequency considered (e.g. if bottom, mid and top channel is evaluated within a band).

Some parameters, such as the element beamwidths are related to the peak element gain via the element loss. This means that these parameters must be selected carefully.

Considering base stations are optimized for various factors including performance, cost, and coverage, it is expected that sub array configurations are relevant for all 3GPP bands as well as a set of physical antenna elements are combined to form a logical element. The array antenna model comprises of a basic element pattern which is then combined appropriately based on the equations to form the sub array pattern and the composite pattern. Since dual polarized elements are used for base stations, it is sufficient to model each polarization separately as considered in the specific model. The model equations are selected so that they are simple and representative to model base station performance with sufficient confidence and reasonable complexity. The element pattern is based on a Gaussian beam which has a flat sidelobe level floor. The element pattern can be modelled sufficiently wide to cover most of the regions of interest, especially in the elevation domain. At high elevation angles, the flat sidelobe level is sufficient to model the side lobes of the antenna element which are significantly lower than the main beam. Thus, the proposed extended antenna model to model sub arrays is sufficient to model the beamforming capability of IMT base stations in considered frequency ranges.

Another aspect also to consider is the performance and coexistence simulator complexity. The antenna model provides gain normalized radiation patterns consuming a reasonable amount of simulator resources. If parameters are selected properly, the effect of directivity normalization is reasonable small. Hence, directivity normalization is not used which significantly reduces complexity and saves processing capacity and simulation time.

The antenna model has support to model the array response outside the wanted carrier bandwidth, within adjacent channels and beyond using the correlation factor, ρ. When the wanted signal is considered ρ is equal to 1. For unwanted emissions outside the wanted signal bandwidth values within the range $0 \leq \rho < 1$can be considered. Further details on the frequency response of ρ require further investigations.

7.1.3 Model equations

The AAS BS array antenna model is based on a parameterized Gaussian shaped gain normalized element pattern and vertical sub-arrays. The composite radiation pattern is calcuated as described in Table 7.1.3-1.

Table 7.1.3-1: Array antenna model equations

Description	Equation
Peak normalized element radiation pattern	$A(\theta,\varphi) = -\min\left[-\left(-\min\left[12\left(\frac{\varphi}{\varphi_{3dB}}\right)^2, A_m\right] - \min\left[12\left(\frac{\theta-90}{\theta_{3dB}}\right)^2, SLA_v\right]\right), A_m\right]$
Peak gain normalized element radiation pattern	$A_E(\theta,\varphi) = G_{E,max} + A(\theta,\varphi)$
Sub-array excitation	$w_m = \frac{1}{\sqrt{M_{sub}}}\exp\left(j2\pi(m-1)\frac{d_{v,sub}}{\lambda_d}\sin(\theta_{subtilt})\right)$
Sub-array radiation pattern	$A_{sub}(\theta,\varphi) = A_E(\theta,\varphi) + 10\log_{10}\left(\left\lvert\sum_{m=1}^{M_{sub}} w_m v_m\right\rvert^2\right)$, where $v_m = \exp\left(j2\pi(m-1)\frac{d_{v,sub}}{\lambda_d}\cos(\theta)\right)$
Array excitation	$w_{m,n} = \frac{1}{\sqrt{MN}}\exp\left(j2\pi\left((m-1)\frac{d_v}{\lambda_e}\sin(\theta_{etilt}) - (n-1)\frac{d_h}{\lambda_e}\cos(\theta_{etilt})\sin(\varphi_{escan})\right)\right)$
Composite array radiation pattern	$A_A(\theta,\varphi) = A_{sub}(\theta,\varphi) + 10\log_{10}\left(1+\rho\left(\left\lvert\sum_{m=1}^{M}\sum_{n=1}^{N} w_{m,n} v_{m,n}\right\rvert^2 - 1\right)\right)$, where $v_{m,n} = \exp\left(j2\pi\left((m-1)\frac{d_v}{\lambda_d}\cos(\theta) + (n-1)\frac{d_h}{\lambda_d}\sin(\theta)\sin(\varphi)\right)\right)$

7.2 MIMO modelling

7.2.1 Simulation methodologies

7.2.1.1 Methodology 1

The following simulation methodology was adopted to produce simulation results:

1. For the k-th UE, generate array coefficients, $\mathbf{U}_{k_{n,m}}$, to reflect the UE angles from the BS antenna array in both azimuth and elevation (NOTE 1):

$$\boldsymbol{U}_{k_{n,m}} = exp\left(j2\pi\left((n-1)\frac{d_v}{\lambda}cos(\theta_k) + (m-1)\frac{d_h}{\lambda}sin(\theta_k)sin(\varphi_k)\right)\right)$$

   where, for the k-th UE, θ_k and φ_k are the angles of elevation and azimuth, respectively. The ranges of θ_k and φ_k are $[0, \pi]$ and $[-\pi, \pi]$ radians. The size of the matrix $\mathbf{U}_{k_{n,m}}$ is N×M, where N is the number of rows and M is the number of columns of the antenna array.

2. Assess the angular separation between the K UEs in the cell (NOTE 2).

3. For each UE (NOTE 3), if there is at least another UE which with the minimum angular separation requirement is fulfilled, create a concatenated K×MN channel matrix, $\mathbf{H}_k$ (NOTE 4):

$$\boldsymbol{H}_k = \begin{bmatrix} \boldsymbol{h}_k^T & \dots & \boldsymbol{h}_p^T \end{bmatrix}^T$$

where ^{T} is the transpose operator and $\mathbf{h}_k$ corresponds to the vectorization of $\mathbf{U}_k$ resulting in a vector of size MN×1 (NOTE 5).

4. For each UE, the zero-forcing beamforming (precoding) matrix $\mathbf{W}_k$ (MNxK) is:

$$\boldsymbol{W}_k = \boldsymbol{H}_k^H (\boldsymbol{H}_k \boldsymbol{H}_k^H)^{-1}$$

where $\mathbf{H}_k$ represents the channel matrix with its number of columns corresponding to the number of RX antennas (i.e., UEs) and its number of rows corresponding to the number of TX antennas (BS antenna ports), and ^{H} is the conjugate transpose operator.

1. The entire $\mathbf{W}_k$ matrix can be normalized by diving it by its Frobenius norm, or, doing a column wise normalization by diving each column with its norm (NOTE 6).

2. The actual precoding weights for each UE ($\mathbf{w}_k$) are obtained by selecting the first column of $\mathbf{W}_k$. The size of $\mathbf{w}_k$ is MN×1.

3. Obtain the individual Zero Forcing beam pattern: The precoding weights for each beam $\mathbf{w}_k$ of size MNx1 may be used to obtain the k-th zero forcing beam pattern by reordering the column vector $\mathbf{w}_k$ of size MNx1 into a matrix $\mathbf{W}_k$ of size NxM which can be used as element weight in:

$$A_k(\theta, \varphi) = A_E(\theta, \varphi) + 10log_{10}\left(\left|\sum_{m=1}^{M}\sum_{n=1}^{N} w_{k_{n,m}} \cdot v_{k_{n,m}}\right|^2\right)$$

where w_k refers to the entry in the n-th row and m-th column of weighting matrix $\mathbf{W}_k$ and $v_{n,m}$ is the superposition vector. Note that for AAS with sub-arrays, $A_E(\theta,\phi)$ is updated by $A_{sub}(\theta,\phi)$:

$$A_k(\theta, \varphi) = A_{sub}(\theta, \varphi) + 10log_{10}\left(\left|\sum_{m=1}^{M}\sum_{n=1}^{N} w_{k_{n,m}} \cdot v_{k_{n,m}}\right|^2\right)$$

where $A_{sub}(\theta,\phi)$ calculation follows the method defined in the extended AAS modelling supporting vertical sub-array configurations.

1. The resulting composite ZF beam pattern may be obtained by summing up the individual Zero Forcing beam patterns in linear scale (and transforming them back to dB):

$$A_{ZF}(\theta, \varphi) = 10log_{10}\left(\sum_{k=1}^{K} 10^{\frac{A_k(\theta,\varphi)}{10}}\right)$$

where $A_{ZF}(\theta,\phi)$ refers to the composite ZF beam pattern and $A_k(\theta,\phi)$ refers to the k-th individual zero forcing beam pattern.

NOTE 1: For the computation of $\mathbf{U}_k$, θ_k and φ_k are in Local Coordinate System (LCS) which accounts for the mechanical down-tilt.

NOTE 2: The total 3D angular separation should be considered to determine the fulfillment of the minimum angular separation requirement. Additionally, only the azimuth angular separation may be considered in cases where the elevation angle does not significantly contribute to the total 3D angular separation.

NOTE 3: $\mathbf{H}_k$ must be constructed for each UE separately, since in some instances, one UE can be paired with all other UEs while another UE could be paired with only a single other UE. The next figure depicts this situation: UE_1 can be paired with UE_2 and UE_3 since the min. angular separation is fulfilled (as shown in (a)), UE_2 can only be paired with UE_1 (as shown in (b)), and UE_3 can only be paired with UE_1 (as shown in (c)).

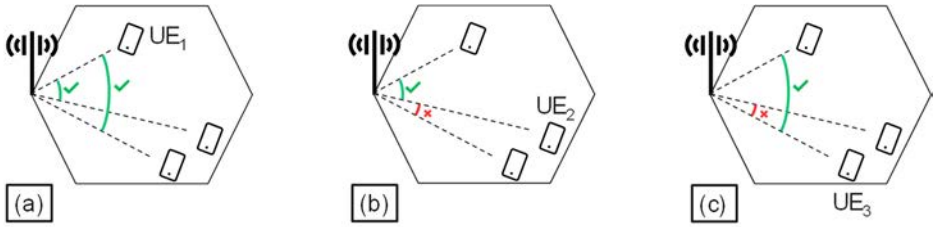

NOTE 4: $\mathbf{H}_k$ only includes the UEs that fulfill the minimum angular separation requirement depending on the size of the BS antenna, so $\mathbf{H}_k$ may have two or three columns (K=2 or 3) in each Monte Carlo snapshot depending on the geometry of the BS and the UEs. For the UEs that cannot be paired with any other UEs (K=1), $\mathbf{H}_k$ is not constructed, and the current beamforming model is used.

NOTE 5: The vectorization must ensure that the vector of size 1×MN correspond to the concatenation of the rows of $\mathbf{U}_k$:

$$\begin{pmatrix} u_{11} & \cdots & u_{1m} \\ \vdots & \ddots & \vdots \\ u_{n1} & \cdots & u_{nm} \end{pmatrix} \rightarrow concatenation \rightarrow [u_{11} \dots u_{1m} \quad u_{21} \dots u_{2m} \quad \dots \quad u_{n1} \dots u_{nm}]$$

NOTE 6: The total power constraint simplifies the design problem and leads to simple and efficient precoders. However, the magnitude of some elements of $\mathbf{w_k}$ may be larger than $\sqrt{1/(MN)}$, which can introduce per-antenna port transmit power larger than $1/(MN)$. In practice, many systems are subject to individual per-antenna port power constraints.

7.2.1.2 Methodology 2

7.2.1.2.1 Beamforming equations

An alternative to a single-user MIMO (a.k.a. point-to-point MIMO) system is MU-MIMO in which an antenna array at the mobile base station simultaneously serves a multiplicity of autonomous user equipments (UEs). These UEs can be single-antenna devices, in which case the multiplexing throughput gains of the MU-MIMO system are shared among the different UEs. A MU-MIMO system is more tolerant of the propagation environments than a single-user MIMO system. For instance, under line-of-sight dominant propagation conditions (implying strong levels of correlation across user channels), the multiplexing gains can disappear for a single-user MIMO system but are retained in the MU-MIMO case provided that the angular separation of the user equipments exceeds the Rayleigh resolution of the array. The co scheduled UEs should lie in uncorrelated or weakly correlated positions. Considering the propagation conditions, , in dominant non-line-of-sight conditions, the multiplexing gains are naturally also retained for the MU-MIMO system. Keeping this in mind, it is worth noting that irrespective of the propagation conditions, the conclusions from standard MU-MIMO techniques like ZF and MMSE to serve multiple user equipments remain consistent. To this end, where necessary, we will assume the existence of a given propagation environment coupled with the appropriate model for generating the propagation channel impulse responses, without specifying or recommending a particular propagation model.

When the mobile base station employs multiuser spatial beamforming techniques like ZF, the antenna array produces spatial nulls in the direction of undesired users. Hence, assuming rank-1 transmission (in 3GPP terminology), if there are K users, then the array forms K analog beams towards the K users where retrieval of the single data streams will occur. Each of the K beams is given by the composite array radiation pattern, as given in Table 7.2.3-1. Yet the separation of users via analog beamforming (BF) alone is not adequate to sufficiently separate the K users signals. To do this, it is preferable to have the users adequately separated say in the azimuth. Spatial beamforming techniques are used in combination with analog beamforming. This will result in nulls in the undesired direction(s).

Consider the simple example below:

Suppose there are say three users communicating with a base station. The three users can be assumed to be located at \phi_{1} = -10 degrees, \phi_{2} = 0 degrees and \phi_{3} = +10 degrees in the azimuthal plane. One can also assume that the base station array (e.g., uniform planar configuration say of size (32x8) is able to steer three independent beams to the three user equipments via the composite radiation patterns generated via the array factor[1] in Table 7.1.3-1 above, with the azimuth main lobe of each beam pointing towards the azimuth angles of -10, 0, and+10 degrees respectively, observed at a fixed elevation angle cut of, say, 90 degrees[2]. Furthermore, one can assume that the base station can implement a multiuser beamforming technique which allows the base station to form nulls in certain undesired directions relative to a desired direction. Then, when serving the user at \phi_{2} = 0 degrees, the base station will form nulls in the direction of the other users (signifying the undesired directions), at \phi_{1}=-10 degrees and \phi_{3} = +10 degrees respectively.

When extrapolating this logic to the case when the base station is serving a higher number of users, e.g., eight users[3], located in eight different azimuth directions, allowing the base station to generate seven nulls in the direction of other users relative to the desired user in the azimuthal plane.

7.2.1.2.2 ZF and MMSE-based beamforming for Rank-1 MU-MIMO Transmission

When spatial beamforming is used in conjunction with analogue beamforming, the beamforming weights may be estimated as below:

7.2.1.2.2.1 ZF based beamforming

Here, we consider ZF-based beamforming for two users, denoted by UE 1 and UE 2 served by a single base station (BS) within the same time-frequency resource. Large numbers of antennas enable the focussing and steering of energy in desired directions. The BS is assumed to have MN antenna elements in total configured in a uniform planar array in the $x-z$ plane in the standard three-dimensional (3D) local coordinate system. For the sake of simplicity, perfect channel estimation at both the BS and UEs are assumed.[4] Both UEs are assumed to have a single antenna. UE 1 and UE 2 is assumed to be located at two discrete azimuth angles, $\phi_{\mathrm{e-scan}}^{1}$ and $\phi_{\mathrm{e-scan}}^{2}$, respectively, with say the same elevation angle, $\theta_1 = \theta_2$. Considering this, the composite antenna array radiation pattern towards UE 1 and UE 2 can be obtained by following the mathematical expressions given in the Table 7.1.3-1 above, where the azimuth angles, $\phi_{\mathrm{e-scan}}^{1}$ and $\phi_{\mathrm{e-scan}}^{2}$, are used Two RF matrices corresponding to UE 1 and 2 as $\boldsymbol{F}_{\mathrm{RF}}^{1}$ and $\boldsymbol{F}_{\mathrm{RF}}^{2}$.[5]respectively are derived. The size of the matrices $\boldsymbol{F}_{\mathrm{RF}}^{1}$ and $\boldsymbol{F}_{\mathrm{RF}}^{2}$is equal to MN x N_t^{RF}. where N_t^{RF} is the number of RF chains at the base station. If every antenna has a transmitter then the size of the beamforming matrices $\boldsymbol{F}_{\mathrm{RF}}^{1}$ and $\boldsymbol{F}_{\mathrm{RF}}^{2}$ is MN x MN respectively.

Even though the UEs may be lying say in one dimension say the azimuth only their impulse response has both an azimuth and elevation component see the impulse response channel matrix in [2].

---

[1] It should be note that the array response is both in the azimuth and elevation.

[2] We assume a broadside array. An elevation angle of 90 degrees is when users are in the elevation boresight.

[3] Whilst antenna numbers can increase due to advancements in semiconductor technology [3], the numbers of users to be nulled must be less than or equal to the number of RF chains

[4] In practice, this is not the case, as *Sounding Reference Signals (SRS)* are used in time-division duplex (TDD) systems, where the UEs would send an uplink SRS signal based on which the BS will estimate the uplink channel and using channel reciprocity, will estimate the downlink channel. In frequency-division duplex (FDD) systems, *Channel State Information-Reference Signal (CSI-RS)* is transmitted from the BS periodically and the UEs will estimate the channel and feedback the channel response via a codebook to the BS [5].

[5] *Mathematical notation*: We note that $\boldsymbol{h}_1$ denotes a vector, while $\boldsymbol{H}$ denotes a matrix. Furthermore, h is denoted as a real scalar value, where as $(\cdot)^T$and $(\cdot)^H$ are used to denote a transpose and a Hermitian transpose operation. Finally, $(\boldsymbol{H})^{-1}$ is used to denote the matrix inverse of a square matrix (same number of rows and columns), $\boldsymbol{H}$.

Note that the exact structure of $\boldsymbol{h}_1$and $\boldsymbol{h}_2$ depends on the radio propagation conditions at the time of transmission from the BS to both UEs. However, this notation is agnostic to the type of conditions and propagation mechanisms present in the channel responses and hence is preferred for use in this document.

Concatenating the equivalent channel responses into a total equivalent channel matrix of appropriate size by stacking the two equivalent user channels, one can write:

$$\widetilde{\boldsymbol{H}} = \left[\, \widetilde{\boldsymbol{h}}_1^T \;\; \widetilde{\boldsymbol{h}}_2^T \,\right]^T \qquad (1)$$

Where $\widetilde{\boldsymbol{h}_1}$ and $\widetilde{\boldsymbol{h}_2}$ are the two equivalent channels and are in turn equal $\boldsymbol{h}_1\, \boldsymbol{F}_{\mathrm{RF}}^1$ and $\boldsymbol{h}_2\, \boldsymbol{F}_{\mathrm{RF}}^2$ respectively.

Now the ZF-based beamforming to null the inter-user interference can be used on $\widetilde{\boldsymbol{H}}$. To this end, the ZF beamforming matrix, $\boldsymbol{W}$, can be calculated as:

$$\boldsymbol{W} = \widetilde{\boldsymbol{H}}^H \left(\widetilde{\boldsymbol{H}}\widetilde{\boldsymbol{H}}^H\right)^{-1}. \qquad (2)$$

This will ensure that if the BS is transmitting the desired signal in the direction of UE 1, i.e., towards $(\phi^1_{\mathrm{e-scan}}, \theta_1)$, a null in the radiation pattern of the BS can be formed towards the unintended direction of UE 2, i.e., towards $(\phi^2_{\mathrm{e-scan}}, \theta_2)$. We note that the ZF beamformer should be normalized to satisfy a total power constraint. There are two different ways to normalize the ZF beamformer, namely via a *vector normalization* or via a *matrix normalization*. Using the example of a vector normalization, the per-user digital beamforming weight vector specific to UE 1 and UE 2 can be written as $\boldsymbol{w}_1$and $\boldsymbol{w}_2$ forming the two columns of $\boldsymbol{W}$. Normalizing these using the vector normalization method yields

$$\boldsymbol{w}_1^{\mathrm{normalized}} = \frac{\boldsymbol{w}_1}{\|\boldsymbol{F}_{\mathrm{RF}}^1\, \boldsymbol{w}_1\|}, \qquad (3)$$

and

$$\boldsymbol{w}_2^{\mathrm{normalized}} = \frac{\boldsymbol{w}_2}{\|\boldsymbol{F}_{\mathrm{RF}}^2\, \boldsymbol{w}_2\|}. \qquad (4)$$

This implies that for UE 1, multiplying the $\widetilde{\boldsymbol{h}_1}\boldsymbol{w}_1^{\mathrm{normalized}} = 1$, while $\widetilde{\boldsymbol{h}_1}\boldsymbol{w}_2^{\mathrm{normalized}} = 0$ and vice-versa for UE 2. Therefore, a null in the azimuth direction can be formed towards UE 2 while serving UE 1.

The array response v_{mn} (in the 3GPP AAS model) can be made to provide maxima at given angular directions by an appropriate choice of the angles in w_{mn} which can be viewed as additional phase terms in the array response. It should be noted that pseudo inverse based on concatenated channels in eqn (1) that are in turn based on w_{mn} alone is flawed and will not provide an exact impact of ZF on the complete array response.

7.2.1.2.2.2 MMSE based beamforming

In the case of MMSE beamforming, the MMSE beamforming matrix, $\boldsymbol{W}$, is given by

$$\boldsymbol{W} = \widetilde{\boldsymbol{H}}^H \left(\widetilde{\boldsymbol{H}}\widetilde{\boldsymbol{H}}^H + \beta \boldsymbol{I}\right)^{-1}, \qquad (5)$$

where $\beta > 0$ is the regularisation constant/factor and $\boldsymbol{I}$ is the identity matrix of the same dimension as $\widetilde{\boldsymbol{H}}\widetilde{\boldsymbol{H}}^H$. By maximizing the SINR at the UEs, the optimal regularisation constant/factor was derived as $\beta = K/\rho$, where ρ is the operating signal-to-noise ratio (SNR) typically computed by taking the ratio of the EIRP with the noise variance (power spectral density) of the UE. Note that optimal regulariser was only obtained for the case of equal conducted transmit power being split across the K user equipments and only applies to rank-1 transmission.

It is noteworthy that when $\rho \to \infty$ (holding the value in K as constant), reflecting high SNR scenarios, the MMSE beamforming matrix in (5) reduces to the ZF beamforming matrix in (2) as $\beta \to 0$.

The normalization of the beamforming vectors of the MMSE approach is identical to the ZF and hence the expressions in (3) and (4) apply with $\boldsymbol{w}_1$ and $\boldsymbol{w}_2$ now derived from the MMSE expression in (5).

7.2.2 Simulation results

7.2.2.1 Methodology 1

7.2.2.1.1 Ericsson

The parameters values listed in Table 7.2.2.1.1-1 and 7.2.2.1.1-2 is used for the simulation.

Table 7.2.2.1.1-1: IMT deployment-related parameters

Parameter	Macro Urban
Base station	
Carrier frequency	6 GHz
Channel bandwidth	100 MHz
BS antenna height	18 m
Cell size	300 m
Sectorization	1 sector [1]
Frequency reuse	1
User Equipment	
UE height	1.5 m
UE density for terminal that are transmitting simultaneously	3 UEs per sector
NOTE 1: This study considers only a single-entry scenario.	

Table 7.2.2.1.1-2: IMT base station beamforming antenna characteristics for IMT

Parameter	Macro Urban
Antenna pattern	Refer to Recommendation ITU-R M.2101 Annex 1
Element gain (incl. Ohmic loss) (dBi)	5.5
Horizontal/vertical 3 dB beamwidth of single element (degree)	90º for H 90º for V
Horizontal/vertical front to back ratio (dB)	30 for both H/V
Antenna polarization	Linear ±45º
Antenna array configuration (Row × Column)	16 × 8
Horizontal/Vertical radiating element spacing	0.5 of wavelength for H 0.5 of wavelength for V
Array Ohmic loss (dB)	2
Base station maximum coverage angle in the horizontal plane (degrees)	±60
Base station vertical coverage range (degrees)	90-120 [1]
Mechanical down-tilt (degrees)	10
NOTE 1: The vertical coverage range includes the mechanical down-tilt. A minimum BS-UE distance along the ground of 35 m should be used for urban/suburban and rural macro environments.	

For the sake of completeness, additional results are provided with an AAS with a subarray configuration. The parameters for this AAS are taken from the WRC-23 studies 5D/1235 and 5D/1461 and are presented in the Table 7.2.2.1.1-3.

Table 7.2.2.1.1-3: IMT base station beamforming antenna characteristics for IMT with subarray configuration

Parameter	Macro Urban
Antenna pattern	Refer to the extended AAS model in 5D/716 (Annex 4.4 - WRC23)
Element gain (incl. Ohmic loss) (dBi)	6.4
Horizontal/vertical 3 dB beamwidth of single element (degree)	90º for H 65º for V
Horizontal/vertical front to back ratio (dB)	30 for both H/V
Antenna polarization	Linear ±45º
Antenna array configuration (Row × Column)	16 × 16
Horizontal/Vertical radiating element spacing	0.5 of wavelength for H 1.4 of wavelength for V
Number of element rows in sub-array	2
Vertical radiating element spacing in sub-array	0.7 of wavelength
Pre-set sub-array down-tilt (degrees)	3
Array Ohmic loss (dB)	2
Base station maximum coverage angle in the horizontal plane (degrees)	±60
Base station vertical coverage range (degrees)	90-100 [1]
Mechanical down-tilt (degrees)	6
NOTE 1: The vertical coverage range includes the mechanical down-tilt. A minimum BS-UE distance along the ground of 35 m should be used for urban/suburban and rural macro environments.	

The IMT network consists of a single site with a single sector. In each snapshot of the Monte Carlo simulation, 3 UEs are uniformly distributed within the sector, and the BS serves each UE with a dedicated beam. These beams can be generated by both the traditional antenna model and as described in subclause 7.2.1.1, assuming a UE minimum angular separation of 10 degrees.

To assess the interference to possible interfered-with receivers, two scenarios are considered, where these receivers are represented by sample points:

1. Equidistant sample points towards the horizon around the IMT BS (Figure 7.2.2.1.1-1a)
2. Equidistant sample points on a hemisphere above the IMT BS excluding the sample points towards the horizon (Figure 7.2.2.1.1-1b)

It is noted that the angular separation between sample points is approximately 15.5 degrees, with scenario 1 having 23 sample points and scenario 2 having 62 sample points.

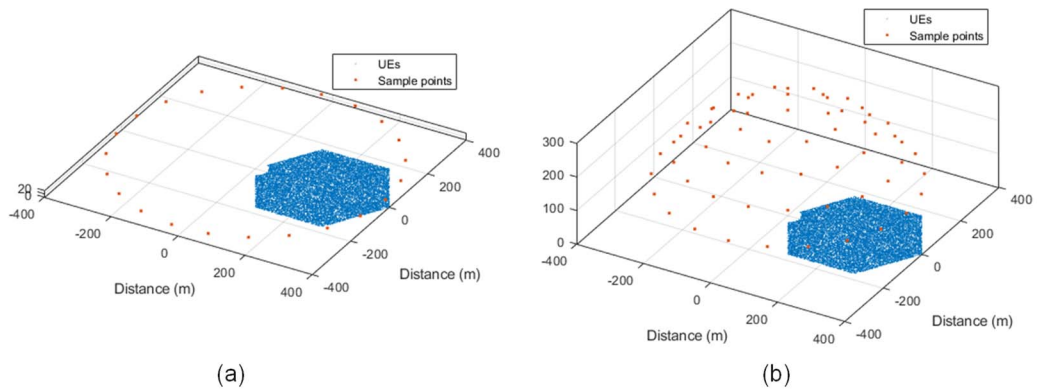

Figure 7.2.2.1.1-1: Equidistant sample points (a) towards the horizon around the BS, and (b) on a hemisphere above the BS

In this section the Monte Carlo simulations results are presented. For each sample point in the considered scenarios, 10.000 snapshots are simulated. The cumulative distribution functions (CDFs) curves of the IMT BS gain towards the sample points of the different scenarios are shown in Figures 7.2.2.1.1-2 to 7.2.2.1.1-5. The CDF results for scenario 1 using a BS without and with subarrays are shown in Figures 7.2.2.1.1-2 and 7.2.2.1.1-3 respectively. The CDF results for scenario 2 using a BS without and with subarrays are shown in Figures 7.2.2.1.1-4 and 7.2.2.1.1-5 respectively. For instance, since scenario 1 has 23 sample points, Figures 7.2.2.1.1-2a and 7.2.2.1.1-3a show 23 pairs of CDFs.

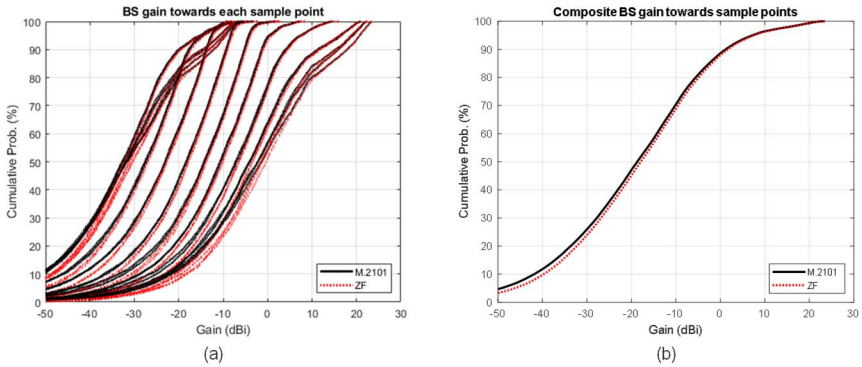

Figure 7.2.2.1.1-2: Scenario 1 (without subarrays) CDFs: BS gain towards (a) each sample point, and (b) all sample points (composite)

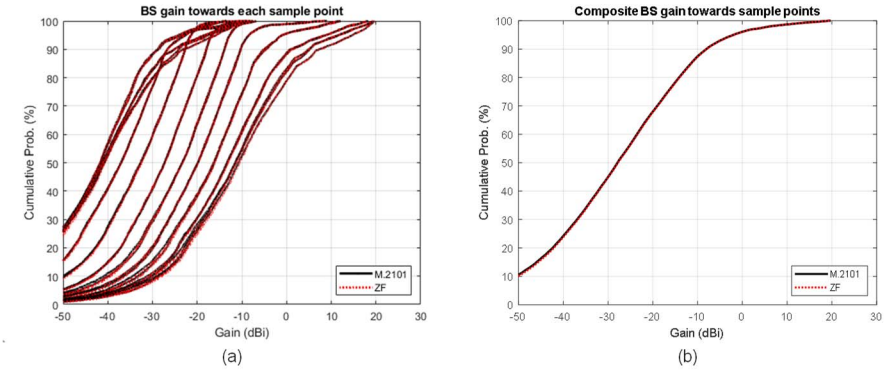

Figure 7.2.2.1.1-3: Scenario 1 (with subarrays) CDFs: BS gain towards (a) each sample point, and (b) all sample points (composite)

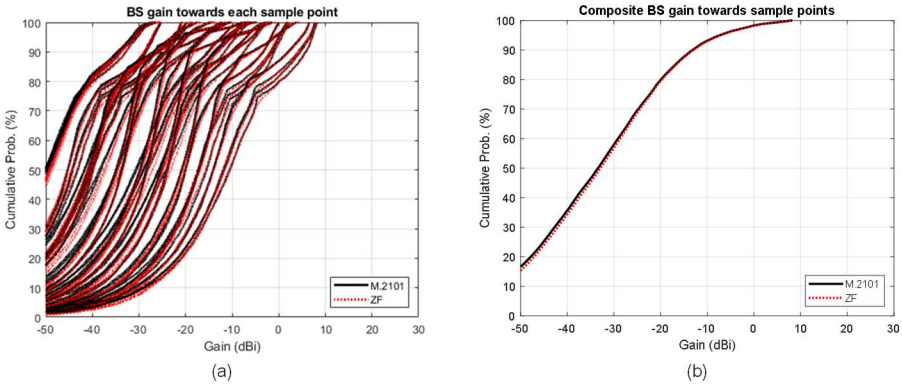

Figure 7.2.2.1.1-4: Scenario 2 (without subarrays) CDFs: BS gain towards (a) each sample point, and (b) all sample points (composite)

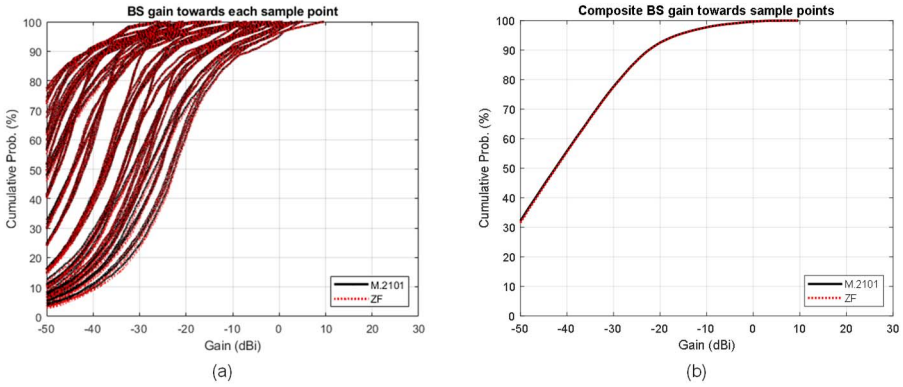

Figure 7.2.2.1.1-5: Scenario 2 (with subarrays) CDFs: BS gain towards (a) each sample point, and (b) all sample points (composite)

To assess the impact on long- and short-term statistics, the 80th percentile and 99.9th percentile are considered respectively. For Figures 7.2.2.1.1-2a, 7.2.2.1.1-3a, 7.2.2.1.1-4a, and 7.2.2.1.1-5a, Table 7.2.2.1.1-1 contains the summary of the average BS antenna gain difference between traditional beamforming model and ZF beamforming model.

Table 7.2.2.1.1-1: Average BS antenna gain difference between traditional beamforming model and ZF beamforming

Scenario	Long-term (80th percentile)	Short-term (99.9th percentile)
Scenario 1 (without subarrays)	0.39 dB	0.14 dB
Scenario 1 (with subarrays)	0.05 dB	~0 dB
Scenario 2 (without subarrays)	0.48 dB	0.06 dB
Scenario 2 (with subarrays)	0.08 dB	~0 dB

Furthermore, the BS antenna gain integrated over parts of or the entire angular sphere around the antenna, i.e., the Total Integrated Gain (TIG), is also evaluated to provide a set of more consistent results by considering all angular directions. The TIG is calculated as follows:

$$TIG \approx \frac{\pi}{2N_\theta N_\varphi}\sum_{\varphi=0}^{N_\varphi-1}\sum_{\theta=0}^{N_\theta-1} G(\theta,\varphi)\sin\theta \qquad \text{(Eq.7.3.2.1.1-1)}$$

where θ and φ represent the elevation and azimuth angles, respectively, N_θ and N_φ are the number of samples on elevation and azimuth, respectively, and G is the antenna gain in linear units at the spherical coordinates (θ, φ).

For this assessment, the BS antenna gain is integrated over the whole sphere and over only the upper hemisphere by limiting the range of θ. The integrated gain is calculated for each individual beam for 10000 snapshots, resulting in three values per snapshot. Note that the integrated gain of the upper hemisphere of the AAS, where $\theta = 90$ degrees is the AAS boresight direction including down-tilt, is not exactly the integrated above the horizon but includes most of it. This is depicted in Figure 7.2.2.1.1-6.

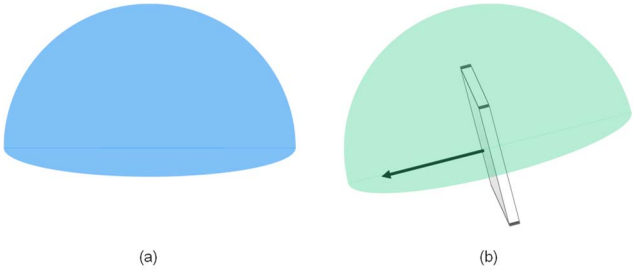

Figure 7.2.2.1.1-6: Upper hemisphere: (a) upper hemisphere above horizon, and (b) upper hemisphere considered in this study

Figures 7.2.2.1.1-7 and Figure 7.2.2.1.1-8 show the BS antenna gain integrated over the whole sphere and over only the upper hemisphere (Figure 7.2.2.1.1-6b), including the horizon, for the BS without and with subarrays, respectively. For simplicity, it is noted that for all the presented results, the integrated gain is always normalized by $\pi/(2N_\theta N_\varphi)$, as indicated in Eq.7.2.2.1.1-1, regardless of the number of samples considered.

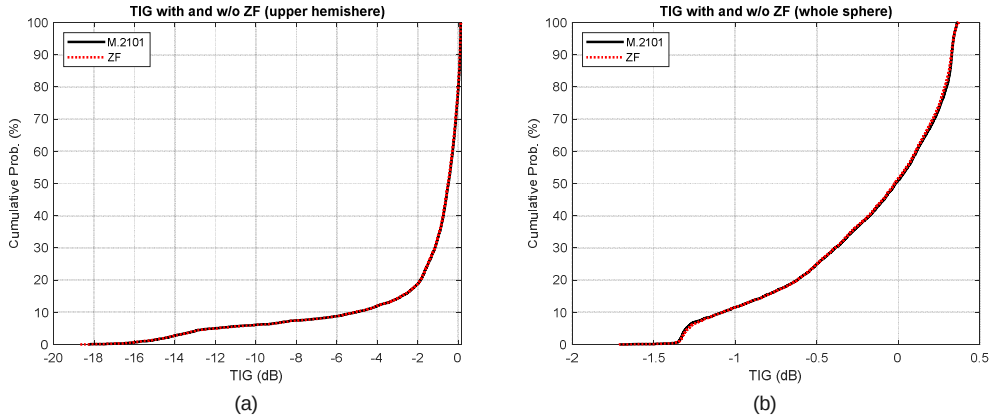

Figure 7.2.2.1.1-7: CDFs of the BS antenna gain without subarrays, integrated over (a) the upper hemisphere, including the horizon, and (b) the entire angular sphere around the antenna

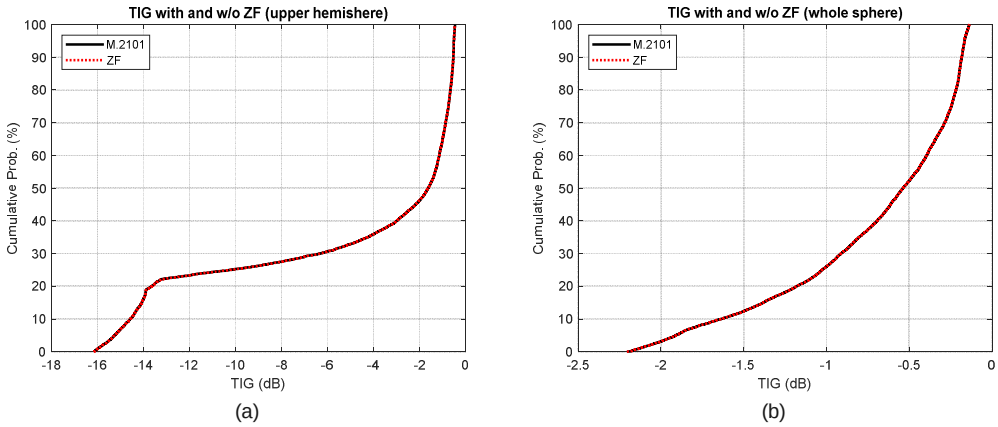

Figure 7.2.2.1.1-8: CDFs of the BS antenna gain with subarrays, integrated over (a) the upper hemisphere, including the horizon, and (b) the entire angular sphere around the antenna

As can be seen, in all cases considered, the TIG difference between the beamforming schemes is negligible.

7.2.2.1.2 Qualcomm

BS AAS parameters and configurations that are considered in our Monte-Carlo simulation campaign are provided in Table 7.2.2.1.2-1, Table 7.2.2.1.2-2, and Table 7.2.2.1.2-3, respectively. In terms of scenario/deployment, we consider a single sector where within each snapshot, 3 UEs are randomly deployed within the coverage region of that sector with a given minimum angular/spatial separation of 10 degrees. The location of those UEs is assumed to be known at the BS and a dedicated beam is generated to serve each UE. In order to investigate the impact of BS emissions above the horizon, probing points in the upper hemisphere have been placed, as visualized in Figure 7.2.2.1.2-1. Black points represent the total probing points, while blue points represent the 3 UEs dropped in each snapshot, taking into account the minimum angular separation among those UEs (i.e., 10 degrees as assumed in this contribution). The probing points are equidistantly distributed on a hemisphere above the horizon with angular separation between them approximately 18 degrees. It is worth mentioning that the objective of our study is to investigate the experienced emissions at the different probing points, since they represent possible incumbent services that will suffer from to the IMT BS unwanted emissions above the horizon.

Table 7.2.2.1.2-1 IMT deployment-related parameters

	Urban macro
Base station	
Carrier frequency	6 GHz-band
Channel bandwidth	100 MHz
BS Antenna height	18 m
Cell size	300 m
Sectorization	1 sector
Frequency reuse	1
User terminal	
UE height	1.5 m
UE density for terminals that are transmitting simultaneously	3 UEs per sector

Table 7.2.2.1.2-2: IMT base station beamforming antenna characteristics for IMT

	Urban Macro
Antenna pattern	Refer to Recommendation ITU-R M.2101 Annex 1
Element gain (incl. Ohmic loss) (dBi)	5.5
Horizontal/vertical 3 dB beamwidth of single element (degree)	90º for H 90º for V
Horizontal/vertical front-to-back ratio (dB)	30 for both H/V
Antenna polarization	Linear ±45º
Antenna array configuration (Row × Column)	16 × 8
Horizontal/Vertical radiating element spacing	0.5 of wavelength for H 0.5 of wavelength for V
Array Ohmic loss (dB)	2
Base station maximum coverage angle in the horizontal plane (degrees)	±60
Base station vertical coverage range (degrees)	90-120 (**Note 1**)
Mechanical downtilt (degrees)	10

Note 1: The vertical coverage range includes the mechanical downtilt. A minimum BS-UE distance along the ground of 35 m should be used for urban/suburban and rural macro environments.

Table 7.2.2.1.2-3: IMT base station beamforming antenna characteristics for IMT with subarray configuration

	Urban Macro
Antenna pattern	Refer to the extended AAS model in 5D/716 (Annex 4.4 - WRC23)
Element gain (incl. Ohmic loss) (dBi)	6.4
Horizontal/vertical 3 dB beamwidth of single element (degree)	90º for H 65º for V
Horizontal/vertical front-to-back ratio (dB)	30 for both H/V
Antenna polarization	Linear ±45º
Antenna array configuration (Row × Column)	16 × 16
Horizontal/Vertical radiating sub-array spacing	0.5 of wavelength for H 1.4 of wavelength for V
Number of element rows in sub-array	2
Vertical radiating element spacing in sub-array	0.7 of wavelength
Pre-set sub-array downtilt (degrees)	3
Array Ohmic loss (dB)	2
Base station maximum coverage angle in the horizontal plane (degrees)	±60
Base station vertical coverage range (degrees)	90-100 (**Note 1**)
Mechanical downtilt (degrees)	6

Note 1: The vertical coverage range includes the mechanical downtilt. A minimum BS-UE distance along the ground of 35 m should be used for urban/suburban and rural macro environments.

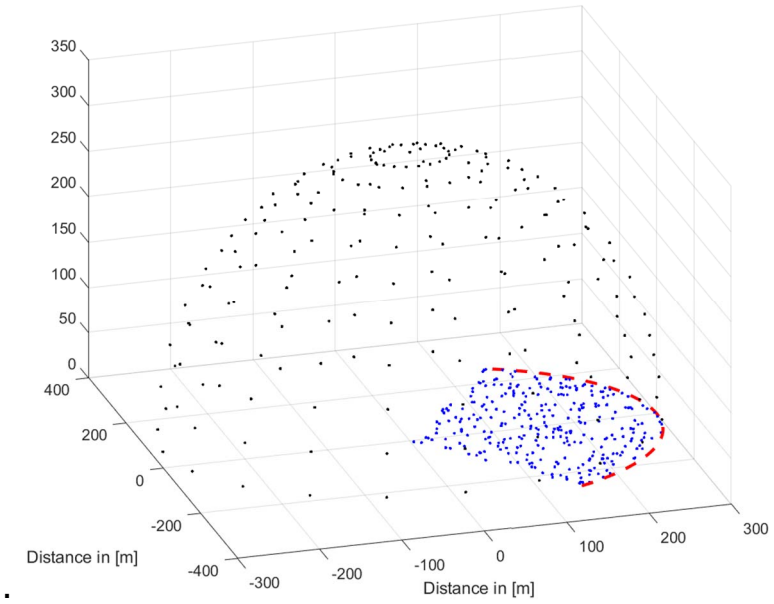

Figure 7.2.2.1.2-1 System layout for a given sector

The CDF curves of the IMT BS gain towards the black probing points are shown in Figure 7.2.2.1.2-2, considering the AAS without subarray structure (left figure) and with subarray structure (right figure). It can be observed the performance degradation observed when ZF is applied is negligible. Such behaviour shows that when considering large number of snapshots in a Monte-Carlo framework, the impact of the spatial beamforming above the horizon has minimal impact on the emissions above the horizon.

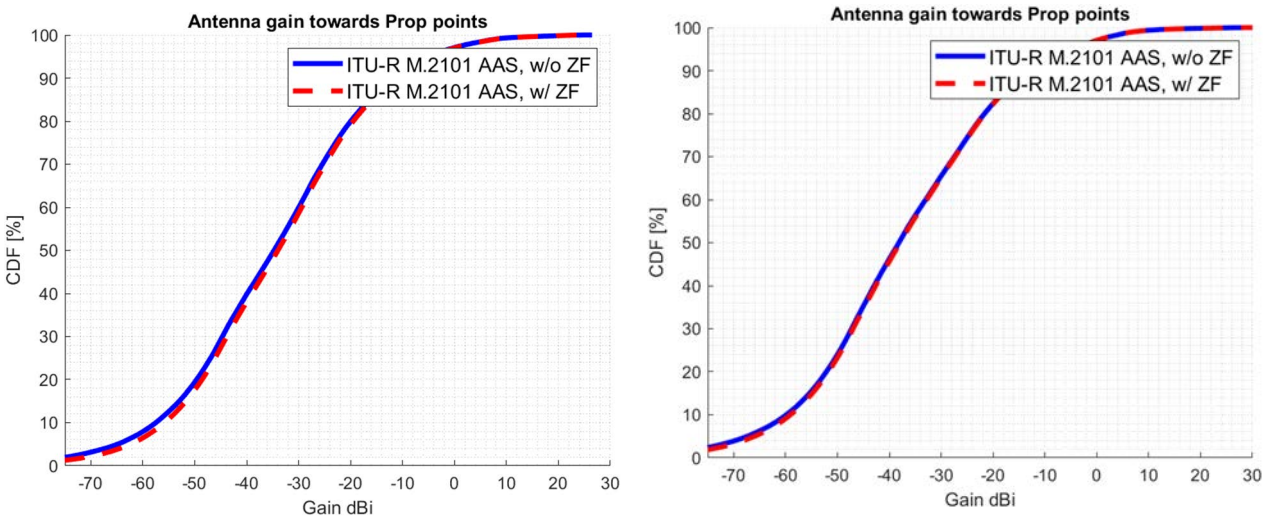

Figure 7.2.2.1.2-2 Composite AAS gain from IMT BS towards probing points considering AAS with (left) and without subarrays (right)

7.2.2.1.3 Huawei

In order to assess the necessity and accuracy of interference comes from IMT systems for ITU-R sharing and compatibility studies, the IMT BS gain towards a number of potential interfered-with receivers located in the upper hemisphere are simulated. The angular separation between sample points is assumed 10 degrees.

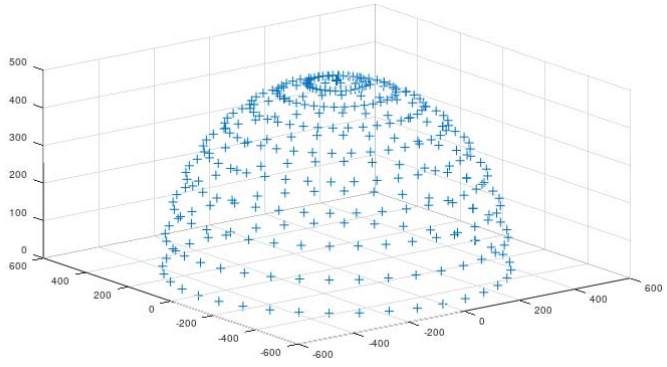

Figure 7.2.2.1.3-1: 10-degree sample points in the upper hemisphere above the BS

Deployment related parameters of BSs and UEs are based on the agreed technical and operational characteristics in the document 5D/716 (Annex 4.4 - WRC-23), and beamforming antenna characteristics are referred to 3GPP liaison statement on parameters for 4400 to 4800 MHZ of terrestrial component of IMT for sharing and compatibility studies in preparation for WRC-27, see 5D/136.

The cumulative distribution functions (CDFs) curves of the IMT BS gain towards the sample points of the different scenarios are shown in Figures 7.2.2.1.3-2 with additional individual per-antenna power constraint. It can be seen that the difference between ITU-R M.2101 and ZF gains are minor.

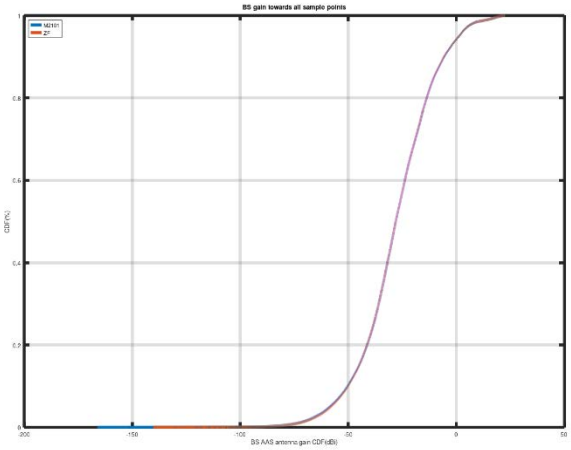

Figure 7.2.2.1.3-2: BS gain towards all sample points (composite) with individual per-antenna power constraint

To assess the impact on long- and short-term statistics, the 80th percentile and 99.9th percentile are considered respectively. Table 7.2.2.1.3-1 contains the summary of the BS antenna gain difference between ITU-R M.2101 model and ZF beamforming model with & without additional individual per-antenna power constraint. Additional individual per-antenna power constraint influences the simulation results very little. In addition, it shows that ZF beamforming get slightly less antenna gain than M.2101 towards to the sample points with individual per-antenna power constraint:

Table 7.2.2.1.3-1: BS antenna gain difference between ITU-R M.2101 beamforming model and ZF beamforming (Method 1)

C band Urban (with subarrays) Scenario	Long-term (80th percentile)	Short-term (99.9th percentile)
M.2101	-13.720	20.861
ZF without individual per-antenna power constraint	-13.587	20.855
ZF with individual per-antenna power constraint	-13.779	20.719
M.2101- ZF difference (dB) (without individual per-antenna power constraint)	-0.133	0.006
M.2101- ZF difference (dB) (with individual per-antenna power constraint)	0.059	0.142

7.2.2.1.4 Nokia

A detailed MIMO system level simulator was used to model the BS radiation for ZF and the ITU MU-MIMO beamforming where modeling included standard MU-MIMO scheduling using NR numerology. ZF MU-MIMO is applied in both azimuth and elevation. For the assessment of impact of these two MU-MIMO schemes, parameters of a 2.6 GHz IMT system were used. The study measures the downlink (DL) signal level (interference) seen at different spatial points for each beamforming technique. Table 7.2.2.1.4-1 describes the main system parameters assumed.

Table 7.2.2.1.4-1: Main IMT system parameters

Parameter	Base Station	UE
Network topology, cell structure and characteristics		
Centre frequency	2.6 GHz	
Channel bandwidth	20 MHz	
Network Configuration (Duplex Mode)	TDD	
Cell radius	0.8 km (suburban macro)	N.A.
Antenna height	25 m	1.5 m
Sectorization	3 sectors	N.A.
User equipment density for terminals that are receiving simultaneously	N.A.	3 UEs per sector
Frequency reuse	1	N.A.
Indoor user terminal usage	N.A.	70%
Antenna characteristics		
Antenna pattern model	Extended AAS model	Isotropic, -3 dBi gain
Element gain **(Note 1)**	6.4 dBi	N.A.
Horizontal/vertical 3 dB beamwidth of single element	90º for H 65º for V	N.A.
Horizontal/vertical front-to-back ratio	30 dB for both H/V	N.A.
Antenna polarization	Linear/±45 degrees	N.A.
Antenna array configuration (Row × Column)	4 x 8 elements	N.A.
Horizontal/Vertical radiating element/sub-array spacing	0.5 of wavelength for H, 2.1 of wavelength for V	N.A.
Number of element rows in sub-array	3	N.A.
Vertical radiating element spacing in sub-array	0.7 of wavelength of V	N.A.
Pre-set sub-array down-tilt	3º	N.A.
Array ohmic loss **(Note 1)**	2 dB	N.A.
Conducted power (before Ohmic loss) per antenna element/sub-array	28 dBm	N.A.
Base station horizontal coverage range	±60º	N.A.
Base station vertical coverage range	90º -100º	N.A.
Mechanical down tilt	6º	N.A.
Maximum base station output power/sector (e.i.r.p.)	72.28 dBm	N.A.

Note 1: The element gain includes the ohmic loss. Therefore, ohmic loss is not needed for the calculation of the BS composite antenna gain and e.i.r.p.

In the simulation, up to 3 of 10 available UEs per cell are MU-MIMO scheduled per slot in DL by a serving cell (21 total cells simulated) over 50 subframes (500 slots) where only the most recent interference measured at each measurement point is saved for each Monte Carlo drop. A minimum separation distance of 10 degrees (in azimuth and elevation) between the BS beams steered towards the served UEs is considered for MU-MIMO scheduling. The measurement points are equidistant from the center on a hemisphere above the IMT cell grid, as illustrated by the blue points in Figure 7.2.2.1.4-1, with the red points indicating the locations of the tri-sector sites. Given 100 Monte Carlo drops, 648 measurement points per drop, then 64800 snapshots of interference radiation are taken (64800 = 100 x 648) for each case modeled.

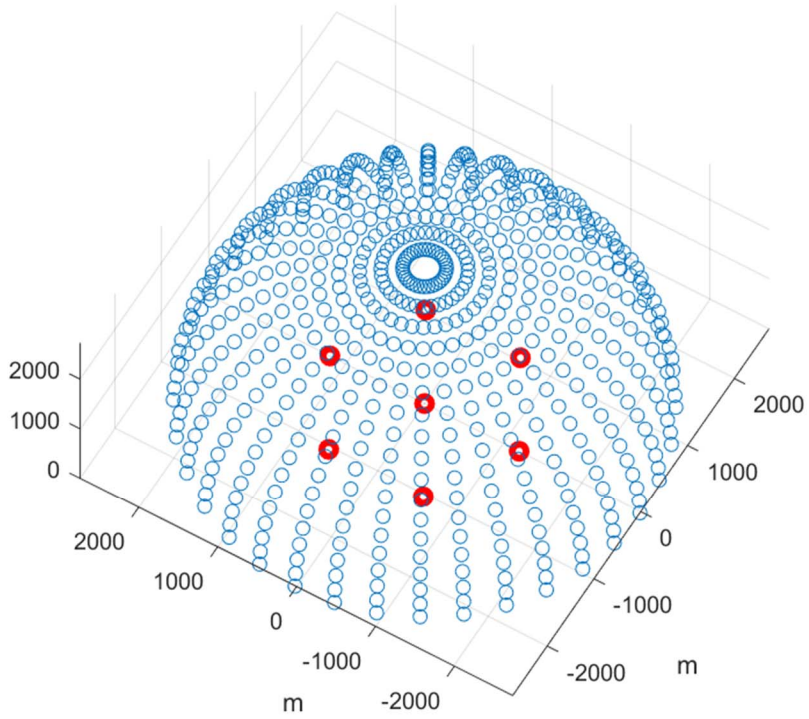

Figure 7.2.2.1.4-1: Measurement points in blue: equidistant from the center on a hemisphere above the IMT cell grid; locations of tri-sector sites in red

Figure 7.2.2.1.4-2 shows interference CDFs for ZF MU-MIMO and ITU MU-MIMO for LOS channel. The delta of CDFs at the 5%-ile, 50%-ile, and 80%-ile points from Figure 7.2.2.1.4-2 are shown in Table 7.2.2.1.4-2 below. Since the interference delta CDF values are less than ~0.3 dB, the considered beam forming techniques have very similar impact to victim services.

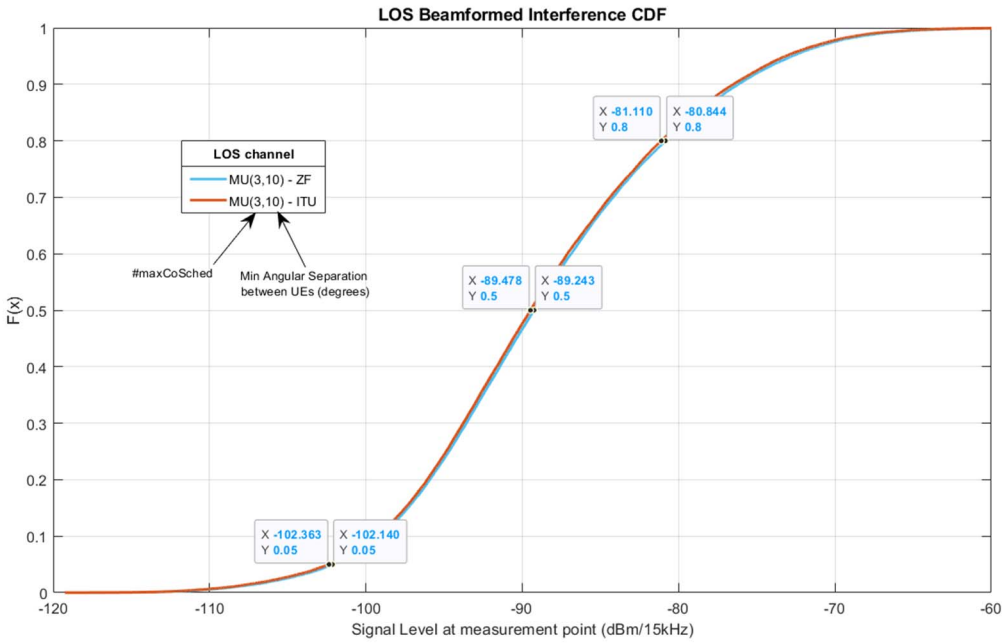

Figure 7.2.2.1.4-2: Interference CDFs for ZF MU-MIMO and ITU MU-MIMO for LOS channel and for minimum separation of 10 degrees for determining pairing

Table 7.2.2.1.4-2: Interference CDF values for ZF and ITU MU-MIMO for LOS channel

Beamforming Type	Interference CDF values (dB)		
	5%-ile	50%-ile	80%-ile
ZF MU-MIMO	-102.13	-89.24	-80.81
ITU MU-MIMO	-102.36	-89.48	-81.08
Delta CDF values	~ 0.23	~ 0.24	~ 0.27

Similar study was conducted considering UMa channel for ZF MU-MIMO. Figure 7.2.2.1.4-3 shows the interference CDFs for ZF MU-MIMO and ITU MU-MIMO for this case. The delta of CDFs at the 5%-ile, 50%-ile, and 80%-ile points from Figure 3 are shown in Table 7.2.2.1.4-3 below. Since the interference delta CDF values are less than ~0.25 dB, the considered beam forming techniques have negligible difference in the impact to victim services.

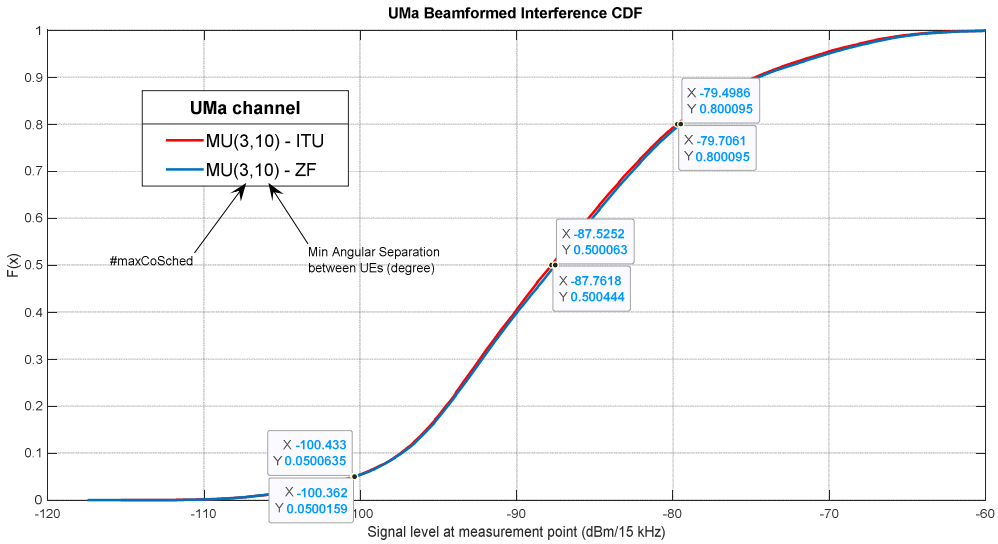

Figure 7.2.2.1.4-3: Interference CDFs for ZF MU-MIMO and ITU MU-MIMO for UMa channel and for minimum separation of 10 degrees for determining pairing

Table 7.2.2.1.4-3: Interference CDF values for ZF and ITU MU-MIMO for UMa channel

Beamforming Type	Interference CDF values (dB)		
	5%-ile	50%-ile	80%-ile
ZF MU-MIMO	-100.36	-87.53	-79.5
ITU MU-MIMO	-100.43	-87.76	-79.71
Delta CDF values	~ 0.07	~ 0.23	~ 0.21

7.2.2.2 Methodology 2

7.2.2.2.1 Spark

We provide below example simulation results for using ZF with two UEs, both are in the azimuth at 0 and 10 degrees respectively and are at the same elevation with a 5 degrees down tilt (angle from the Z axis is 95 degrees). The antenna and other parameters are:

Table 7.2.2.2.1-1 IMT deployment-related parameters

Parameter	Value
Environment	Macro Urban
Carrier frequency	6 GHz
Sectorization	1 sector
Frequency reuse	1

Table 7.2.2.2.1-2 IMT base station beamforming antenna characteristics for IMT

Parameter	Macro Urban
Antenna pattern	Refer to Section 5 of Recommendation ITU-R M.2101
Element gain (incl. Ohmic loss) (dBi)	5.5
Horizontal/vertical 3 dB beamwidth of single element (degree)	90º for H 90º for V
Horizontal/vertical front to back ratio (dB)	30 for both H/V
Antenna polarization	Linear ±45º
Antenna array configuration (Row × Column)	16 × 8
Horizontal/Vertical radiating element spacing	0.5 of wavelength for H 0.5 of wavelength for V
Array Ohmic loss (dB)	2
Base station maximum coverage angle in the horizontal plane (degrees)	±60
Base station vertical coverage range (degrees)	90-120
Mechanical down-tilt (degrees)	10

The cdf of the array gain of the elevation pattern above the horizon for methodology 2 using ZF MU MIMO is shown below for 1000 simulation runs.

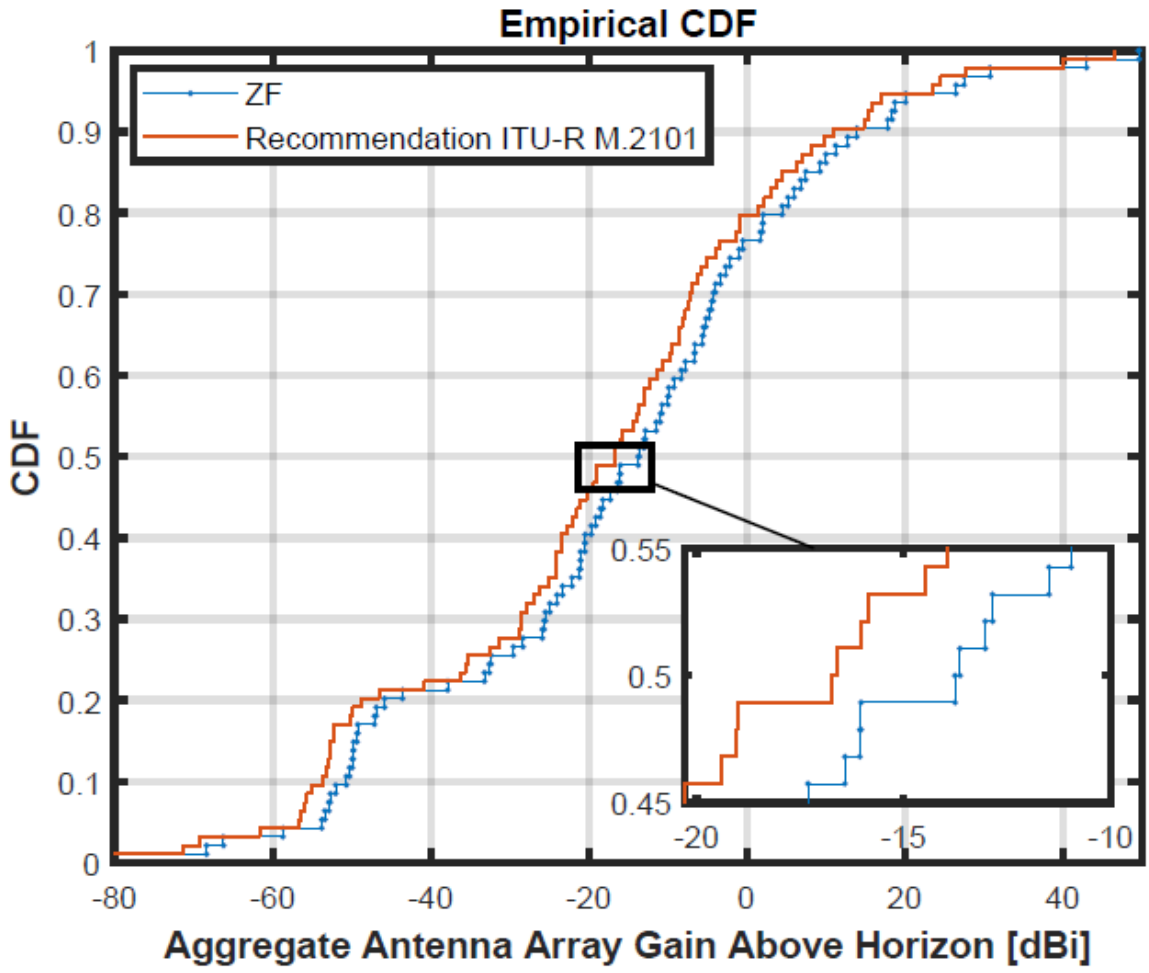

Figure 7.2.2.2.1-1 Aggregate Antenna Array Gain Above Horizon [dBi]

The following observations may be made:

The median gain difference is about 3 dB.

When more UEs are added to the ZF set, the placement of nulls in the azimuth pattern will have a consequential impact on the elevation pattern and will further increase this difference.

The example is for two UEs with a given azimuth placement. The median gain difference will also be sensitive to the actual azimuth angles at which the UEs are placed. The point of this exercise is just to demonstrate the impact of ZF beamforming using the correct formulation of pseudo inverse to accurately assess the aggregate antenna array gain above the horizon. The conclusions presented here can be replicated for a larger number of users in a given sector with the same methodology.

7.2.2.2.2 Huawei

The cumulative distribution functions (CDFs) curves of the IMT BS gain towards the target UE are shown in Figure 7.2.2.2.2-1. It can be seen that this method can also get reasonable target antenna gain compared to M.2101.

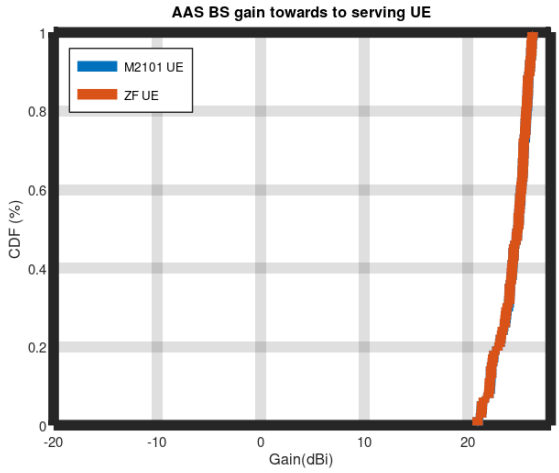

Figure 7.2.2.2.2-1: BS gain towards to target UEs

The cumulative distribution functions (CDFs) curves of the IMT BS gain towards the sample points of the different scenarios are shown in Figures 7.2.2.2.2-2 without additional individual per-antenna power constraint. It can be seen that the difference between ITU-R M.2101 and ZF gains are minor.

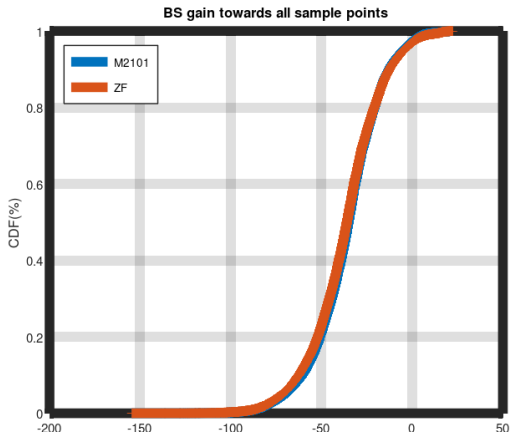

Figure 7.2.2.2.2-2: BS gain towards all sample points (composite) without individual per-antenna power constraint (Method 2)

Table 7.2.2.2.2-1: BS antenna gain difference between ITU-R M.2101 beamforming model and ZF beamforming (Method 2)

C band Urban (with subarrays) Scenario	Long-term (80th percentile)	Short-term (99.9th percentile)
M.2101	-20.810	19.527
ZF (Method 2) without individual per-antenna power constraint	-20.992	19.197
M.2101- ZF (Method 2) difference (dB) (without individual per-antenna power constraint)	0.182	0.33

7.2.3 Summary and Conclusion of MIMO modelling

The simulation results in clause 7.2.2 using the simulation methodologies in clause 7.2.1 have indicated that MU MIMO based ZF BF does not need to be considered for the pure LOS case, and Rec. ITU-R M.2101 methodology remains valid for performing sharing and compatibility studies in WP5D.

7.3 Modelling array antenna gain outside the carrier

7.3.1 General

7.3.1.1 Purpose

This clause aims to provide IMT base station and IMT user equipment technical parameters for analyzing adjacent band compatibility of terrestrial IMT systems with other co-primary services in the ITU Radio Regulations covering aspects related to modelling array antenna gain outside the wanted carrier relevant for modelling spatial characteristics for unwanted emissions.

7.3.1.2 ITU radio regulations on adjacent terrestrial IMT systems with other co-primary services

There are adjacent services in the bands being considered for IMT 2030.

For example: for the case of 4400-4800 MHz, the adjacent band services are:

On the lower edge below 4400 MHz:

- Aeronautical radio navigation;
- Aeronautical mobile;
- Additional possible allocation of EESS (passive) as per Agenda Item 1.19 of WRC-27;

On the upper edge above 4800 MHz:

- Fixed service;
- Radio Astronomy;
- Radio navigation satellite;

For the case of 7125-8400 MHz, the adjacent band services are:

On the lower edge below 7125 MHz:

- Fixed
- Fixed Service Satellite (Earth-to-space)

On the upper edge above 8400 MHz:

- Space Research Service (space-to-Earth)
- Additional possible allocations of EESS (passive) as per Agenda Item 1.19 of WRC-27
- Earth Exploration Satellite
- Radiolocation
- Space Research (active).

For the case of 14.8-15.35 GHz, the adjacent band services are:

On the lower edge below 14.8 GHz:

- Fixed Service;
- Fixed Satellite Service (Earth-to-space)
- Radionavigation

On the upper edge above 15.35 GHz:

- Space research (passive)
- EESS (passive)
- Radio Astronomy

In particular, the frequency range 15.35 – 15.4 GHz is marked as a footnote 5.340 band, which is stating "*All Emissions are Prohibited*" with the exception of those provided by RR 5.511.

It is therefore important that out of band emissions are correctly modelled so that appropriate guidance is provided for the above question to WP 5D.

7.3.2 Adjacent channel modelling

7.3.2.1 Correlation roll-off based model

7.3.2.1.1 Modelling overview

The array antenna model adopted by 3GPP in previous studies creates the composite pattern as a multiplication between the element factor (or sub-array element factor) and array factor. The array antenna model was first introduced in the early days of AAS for BS. Based on the antenna model, the average radiation pattern produced by an array antenna was evaluated and an analytical expression for the average radiation pattern was established.

To generate the array excitation of an instantaneous de-correlated array pattern a random noise is added to the array excitation factor via independent real-valued Gaussian random numbers $x_{m,n}^{q}$ and $y_{m,n}^{q}$ with zero mean value and standard deviation 1, see Table 7.3.2.1.1-1.

Table 7.3.2.1.1-1: Array antenna model equations for instantaneous de-correlated patterns

Description	Equation
Instantaneous array excitation	$w_{m,n}^{q} = \sqrt{\rho} w_{m,n} + \sqrt{1-\rho}\frac{1}{\sqrt{MN}}\frac{1}{\sqrt{2}}\left(x_{m,n}^{q} + jy_{m,n}^{q}\right)$
Instantaneous composite array pattern	$A_A^q(\theta,\varphi) = A_{sub}(\theta,\varphi) + 10\log_{10}\left(\left\lvert\sum_{m=1}^{M}\sum_{n=1}^{N} w_{m,n}^{q} v_{m,n}\right\rvert^2\right)$ Where $v_{m,n}$ is defined in Table 7.1.3-1.
Average of composite array radiation patterns	$A_{A,avg}(\theta,\varphi) = E(A_A^q(\theta,\varphi)) = A_{sub}(\theta,\varphi) + 10\log_{10}\left(1+\rho\left(\left\lvert\sum_{m=1}^{M}\sum_{n=1}^{N} w_{m,n} v_{m,n}\right\rvert^2 - 1\right)\right)$
Note: E(x) denotes expectation (mean) value over the q statistical instantaneous samples.	

The average composite radiation gain pattern for pure LOS channel can be expressed in logarithmical scale as:

$$A_A(\theta,\varphi) = A_{sub}(\theta,\varphi) + 10\log_{10}\left(1+\rho\left(\left\lvert\sum_{m=1}^{M}\sum_{n=1}^{N} w_{m,n} v_{m,n}\right\rvert^2 - 1\right)\right) \qquad \text{(Eq. 7.4.1-1)}$$

where ρ is the correlation factor defined in the interval $0 \le \rho \le 1$. Relevant parameter values for the frequency range 4400 to 4800 MHz can be found in subclause 4.4.1.2 and for 7125 to 8400 MHz in subclause 5.4.1.2, and for 14800 to 15350 MHz in subclause 6.5.1.2.

It can be noticed that the average antenna gain for the wanted signal where ρ is equal to 1, the composite array gain is produced ($G_{E,max}$ + 10log$_{10}$(M_{sub}) + 10log$_{10}$(MN) dBi), while for unwanted emission away from the carrier where ρ is equal to 0 only the gain of the element/sub-array is produced ($G_{E,max}$ + 10log$_{10}$(M_{sub}) dBi). For sharing studies, it would be relevant to consider ρ being represented as a function of frequency offset.

The impact of array signal correlation to directivity and gain response have been evaluated for different array antenna structures considered for 4400 to 4800 MHz, 7125 to 8400 MHz and 14800 to 15350 MHz considering 10 degrees down-tilt beam steering direction. The results are plotted in Figure 7.3.2.1.1-1.

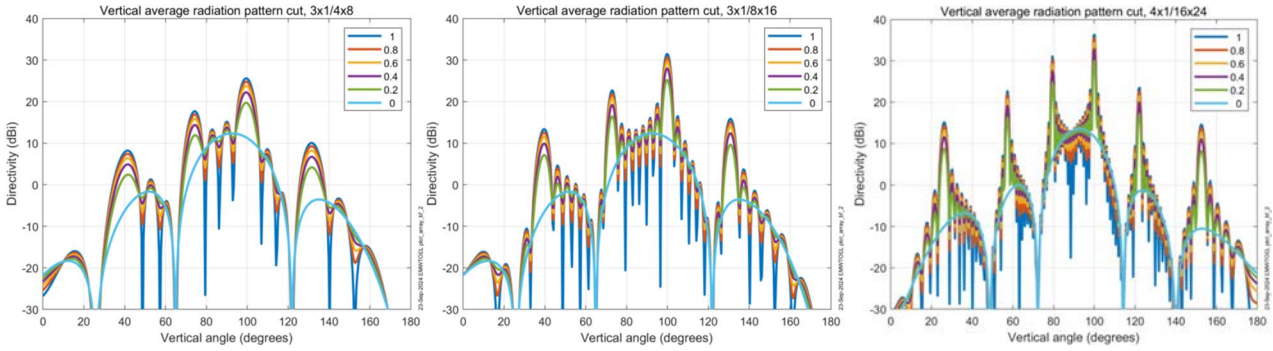

Figure 7.3.2.1.1-1: Vertical average radiation pattern considering different array geometries and correlation factor.

The array factor impact due decorrelation can be analysed for all antenna geometries separately. The array factor drops gradually for low correlation as shown in Figure 7.3.2.1.1-2.

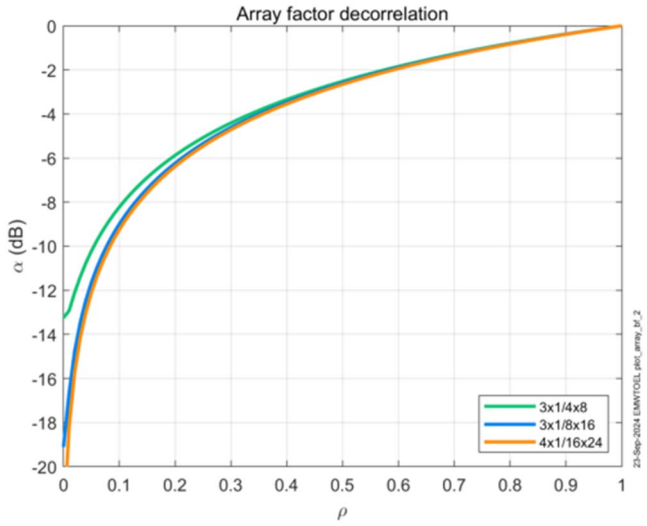

Figure 7.3.2.1.1-2: Array factor decorrelation characteristics plotted as function of correlation.

It can be noticed that the average gain drops gradually when the array correlation reduces. At array correlation 0.5 the array factor has reduced approximately 3 dB.

The characteristic is visualized in Figure 7.3.2.1.1-2 can be used to translate measured directivity drop to correlation factors to use for modelling purposes.

7.3.2.1.2 Correlation roll-off model

Since the array factor gain relies on coherent combining of signals it is not expected that the array factor will operate outside the carrier with full strength in situations outside the carrier where the emission is created as the sum of correlated intermodulation distortion and uncorrelated wide band noise. The Inter-Modulation Distortion (IMD) is coming from non-linear transmitter. The characteristics is typically categorized as distortions due third order (IM3), fifth order (IM5), seven order (IM7), etc. IMD. It is known that the order of IMD will determine the spectral distribution of the distortion. The IMD will also depend on the wanted signal carrier bandwidth, B. The IMD response typically reduces moving away from the edge of the wanted signal.

For the wanted carrier (within the interval $-0.5B \leq f_c \leq 0.5B$, f_c is the carrier centre frequency) full array factor is expected which means that the correlation factor is equal to 1. Moving away from the carrier edge ($f_c > |0.5B|$) the correlation will drop gradually due to the composition of the emission outside the carrier. The emission will be created as the sum of correlated noise due to intermodulation products and non-correlated noise due to wideband transmitter noise. The relation to the induvial noise levels will determine the out-of-carrier correlation properties in the adjacent emission regions. At a certain frequency offset far from the carrier edge the emission noise will be dominated by uncorrelated wideband noise which means that the correlation is equal to 0.

Therefore, it would be appropriate to define a model for the array correlation factor to account for carrier bandwidth and decaying correlation moving away from the carrier edge.

To properly model the AAS base station array antenna gain pattern outside the carrier the correlation factor needs to be modelled as a function of frequency offset to the carrier centre frequency. To capture fundamental aspects of the array antenna gain drop outside the wanted signal a parameterized piece-wise linear roll-off model can be adopted for the correlation factor, as visualized in Figure 7.3.2.1.2-1.

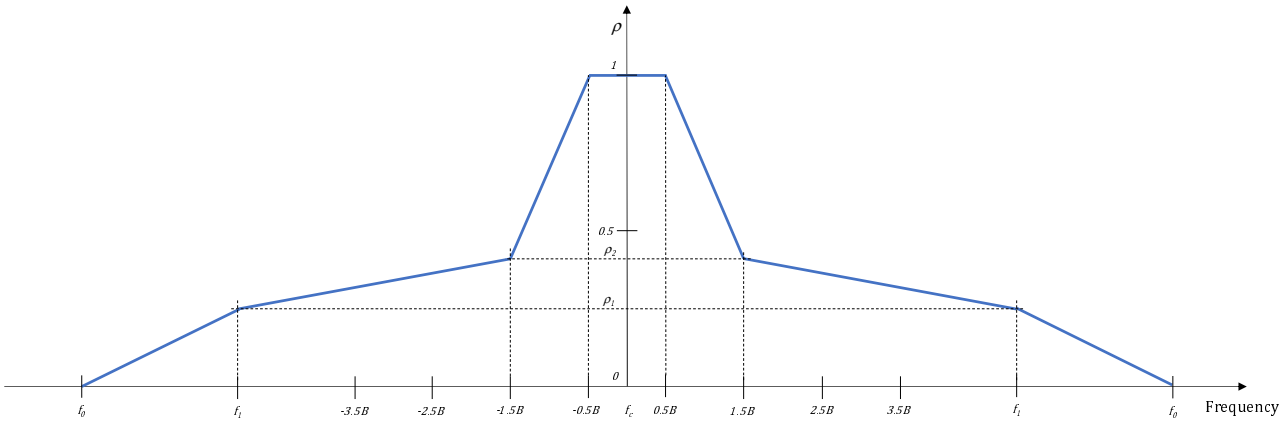

Figure 7.3.2.1.2-1: Array correlation factor roll-off model.

The roll-off is modelled to reduce stepwise moving away from the centre frequency, also the characteristics is assumed to be symmetrical around the wanted carrier. Close to the carrier the correlation is expected to be close to 1, while moving towards *+/-1.5B* reducing to ρ_2. At f_1 the correlation has reduced even more to ρ_1. At f_0 the correlation has reduced to 0, which corresponds to that the array factor gain in 0 dB.

To make the array correlation factor roll-off model useful parameter values for B, f_0, f_1, ρ_1 and ρ_2 needs to be determined.

Using the approach above the antenna model can be extended to capture array antenna gain outside the wanted carrier as outlined in Table 7.3.2.1.1-2:

$$A_A(\theta,\varphi,f) = A_{sub}(\theta,\varphi) + 10\log_{10}\left(1+\rho(f)\left(\left|\sum_{m=1}^{M}\sum_{n=1}^{N} w_{m,n}v_{m,n}\right|^2 - 1\right)\right) \quad \text{(Eq. 7.3.2-1)}$$

Observe that the extended array antenna model only captures effect due to array signal correlation and not effects due to antenna element detuning effects of mismatch effects in transmission lines and Radio Distribution Network (RDN).

7.3.2.1.3 EIRP model

Observe that the array correlation roll-off model presented above only captures decorrelation effects related to the array factor. Keep in mind that even though the array factor totally collapses the sub-array still produce gain far outside the carrier. Typically, the sub-array starts to collapse outside the operating band until the antenna is completely detuned far from the centre of the operating band.

Another aspect to consider when modelling spatial unwanted emission outside the carrier is the suppression of unwanted emission outside the carrier in the adjacent channel regions as well as in the spurious domain. In these regions the emission is suppressed by the ACLR and RF filter suppression.

The radiated emission from a base station to be studied in a sharing situation can be calculated as:

$$EIRP(\theta,\varphi,f) = P_{tx}(f) + A_A(\theta,\varphi,f)$$

where P_{tx} is the total conducted power fed to the antenna at a frequency offset, f is the frequency offset between the carrier centre frequency and the considered frequency. The frequency dependence for the gain pattern $A_A(\theta,\varphi,f)$ as described in Eq. 7.3.2.1.2-1.

The power fed to the antenna can be expressed as a function of frequency offset as:

$$P_{tx}(f) = P - S(f)$$

where is P is the total conducted carrier power fed to the antenna, $S(f)$ is the suppression achieved by $ACLR_1$ (First adjacent channel), $ACLR_2$ (Second adjacent channel), $ACLR_3$ (Third adjacent channel) and additional RF filter suppression (if frequencies outside the operating band is considered) as function frequency offset.

It is evident that the radiated power in the adjacent channel regions and beyond depends on the drop of antenna gain at considered frequency offset and the power fed to the antenna at considered frequency offset. The combined effect should be considered to properly model coexistence situations.

7.3.2.2 Array ACLR based model

7.3.2.2.1 Overview

Out of band emissions are well understood but often for a single transmitter.

It is necessary to distinguish between a *single element ACLR*, and an *array ACLR*. In a non AAS system, where the radiation pattern is "constant" over a sector, the single element ACLR makes sense, since the received power ratio at any point is the same as the transmitted. However, with AAS, the desired signal experiences also an array/beamforming gain that might be different from the array/beamforming gain of the interfering signal received in the adjacent band; this later observation is also dependent if SU or MU MIMO is used (i.e. the array may send distortions in unintended directions).

When an array in AAS base stations is used, the 3GPP specifications provide a method to compute the array ACLR (albeit in a TRP mode) [9]:

"The ACLR (CACLR) absolute basic limits in table 6.6.3.2-2 + X, 6.6.3.2-2a + X (where X = 9 dB) or the ACLR (CACLR) basic limit in table 6.6.3.2-1, 6.6.3.2-2a or 6.6.3.2-3, whichever is less stringent, shall apply."

However, the above method is array pattern agnostic and does not account for beamforming variations due to MU MIMO.

Recent published results, discussed/summarized in this report, show that that array ACLR is spatially sensitive and is also dependent if SU or MU MIMO functionality is utilized. There is thus a need to accurately model the ACLR when AAS is used.

As part of additional information requested by ITU-R WP 5D establish a model for array correlation factor (ρ) roll-off to describe how the array factor collapses moving away from the centre frequency. If the beamforming performance degrades towards a single element radiation pattern, then the frequency when the continuity of array features is regarded as degraded, will also need to be determined.
To address the SI, the questions posed may be devolved into topics below:

1. Establish a model for array correlation factor-ie the correlation of the in-band signal with the out of band signal.

There is no definition of an array correlation factor. Is it the correlation of the in-band signal with out of band signal. But the in-band signal, $P_{inband}(\theta,\phi)$, is spatially sensitive and as discussed below the out of band signal , $P_{oob}(\theta,\phi)$, may also be spatially sensitive. Then the array correlation ρ is also spatially sensitive may be defined as:

$$\rho(\theta,\phi) = E\left(P_{inband}(\theta,\phi)\, P^{T}_{oob}(\theta,\phi)\right) \quad \text{.....(6)}$$

2. How does the array factor collapse when moving away from the centre frequency?

This also means that $\rho(\theta,\phi)$ defined above is a function of frequency separation from the band centre. In this case best to denote this as:

$$\rho_{\Delta f}(\theta,\phi) \quad \text{.....(7)}$$

Where Δf is the frequency separation from band centre

3. If the beamforming performance degrades towards a single element radiation pattern, then the frequency when the continuity of array features is regarded as degraded, will also need to be determined.

Therefore, we would need to characterize and investigate the constituent components of $P_{oob}(\theta,\phi)$ as a function of Δf

The above topics are interrelated but need to be separately discussed as well. The discussion below addresses topics 2 and 3 respectively.

Array performance in adjacent bands is governed by:

- Array performance at different frequencies arising due to adjacent bands.
- Modelling of the impact of PA non linearities
- Modelling of band pass filters

- Putting all of the above together to obtain an end-to-end model

Additionally, one must also consider if the array is supporting a single user or multi-user systems.

7.3.2.2.2 Array performance at adjacent band frequencies

Assume that the lower and upper adjacent bands have a bandwidth of 100 MHz each respectively. Arrays in a band are designed at the centre frequency of a given band ie vertical and horizontal spacing is determined by the centre frequency of the band which for example in band 1 is 4600 MHz shown in Table 7.3.2.2.2-1 below. Likewise for other bands. The lower and upper adjacent bands can be simulated via a proxy array with different spacings e.g for band 1, the lower adjacent band is 4300-4400 MHz with centre frequency 4350 MHz. Therefore, for band 1, changing the vertical spacing to 0.74 lambda and horizontal spacing to 0.53 lambda will effectively simulate the lower adjacent band. Likewise for the upper adjacent band (0.66, 0.474) will simulate the upper adjacent band.

Table 7.3.2.2.2-1: Array performance in adjacent bands

Band	Centre Frequency	0.7 Lambda, 0.5 Lambda (cm)	Centre freq of Lower adj band	Centre freq of Upper adj band	0.7 Lambda, 0.5 Lambda for lower adj band	0.7 Lambda, 0.5 Lambda for upper adj band
1	4600 MHz	4.565/3.26	4350 MHz	4850 MHz	4.827/3.45 (0.74, 0.53)	4.33/3.09 (0.66, 0.474)
2	7762.5 MHz	2.7/1.93	7075 MHz	8450 MHz	2.96/2.118 (0.767, 0.55)	2.48/1.773 (0.64, 0.46)
3	15.075 GHz	1.39/0.99	14.75 GHz	15.40 GHz	1.42/1.012 (0.715, 0.511)	1.36/0.97 (0.68, 0.49)

The following parameter/metrics are impacted [15] when the inter element spacing is changed:

- Nulls
- Maxima
- Half power points
- Minor lobe maxima
- First null beamwidth
- Half power beamwidth
- First side lobe beamwidth

Exact expressions for the above are given below from [15] for a ULA along the z axis and for omni directional antennas. Considering the exact formulas below in Table 7.3.2.2.2-2 and Table 7.3.2.2.2-3 the changes due to inter element spacing in the proxy array will result in some changes to the values of the above metrics. See Figure 7.3.2.2.2-1, Figure 7.3.2.2.2-2 and Figure 7.3.2.2.2-3 for an eight element ULA for 0.5 lambda, 0.7 lambda and 0.8 lambda inter element spacing respectively. However, these frequency/wavelength adjustments are no different to what is present today in systems that have a wide operating bandwidth and antennas are designed at the centre frequency of the band). Note that the results below are not for an array of sub arrays and 3GPP antenna element patterns, but the trends will be similar for the array of sub array case as well.

Table 7.3.2.2.2-2: Broadside array antenna pattern equations

Nulls, Maxima, Half-Power points and Minor Lobe maxima for Broadside Arrays	
Nulls	$\theta_n = \cos^{-1}\left(\pm\frac{n}{N}\frac{\lambda}{d}\right)$, n = 1,2,3…., $n \neq N, 2N, 3N..$
Maxima	$\theta_m = \cos^{-1}\left(\pm m\frac{\lambda}{d}\right)$, m = 0,1,2,3….,
Half Power Points	$\theta_h = \cos^{-1}\left(\pm 1.391\frac{\lambda}{\pi Nd}\right)$, $\frac{\pi d}{\lambda} \ll 1$
Minor Lobe Maxima	$\theta_s = \cos^{-1}\left(\pm\frac{\lambda}{2d}\frac{2s+1}{N}\right)$, s = 1,2,3, $\frac{\pi\lambda}{d} \ll 1$

Table 7.3.2.2.2-3: Broadside array beamwidth equations

Beamwidths for Uniform Amplitude Broadside Arrays	
First Null beamwidth (FNBW)	$\theta_n = \left[\frac{\pi}{2} - \cos^{-1}\left(\frac{\lambda}{Nd}\right)\right]$
Half Power beamwidth (HPBW)	$\theta_h \cong 2\left[\frac{\pi}{2} - \cos^{-1}\left(\frac{1.391\lambda}{\pi Nd}\right)\right]$ $\frac{\pi d}{\lambda} \ll 1$
First sidelobe beamwidth (FSLBW)	$\theta s \cong 2\left[\frac{\pi}{2} - \cos^{-1}\left(\frac{3\lambda}{2Nd}\right)\right]$ $\frac{\pi d}{\lambda} \ll 1$

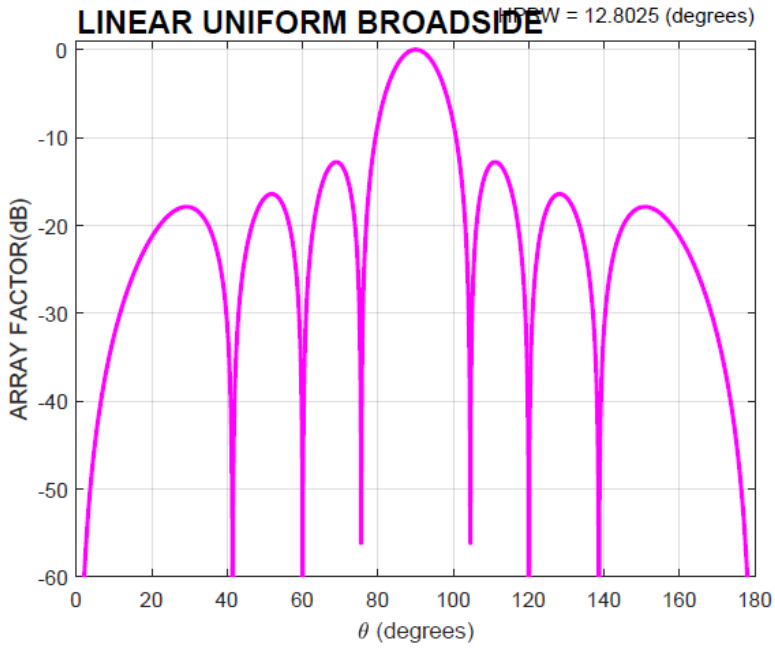

Figure 7.3.2.2.2-1: Eight element ULA response with 0.5 lambda spacing

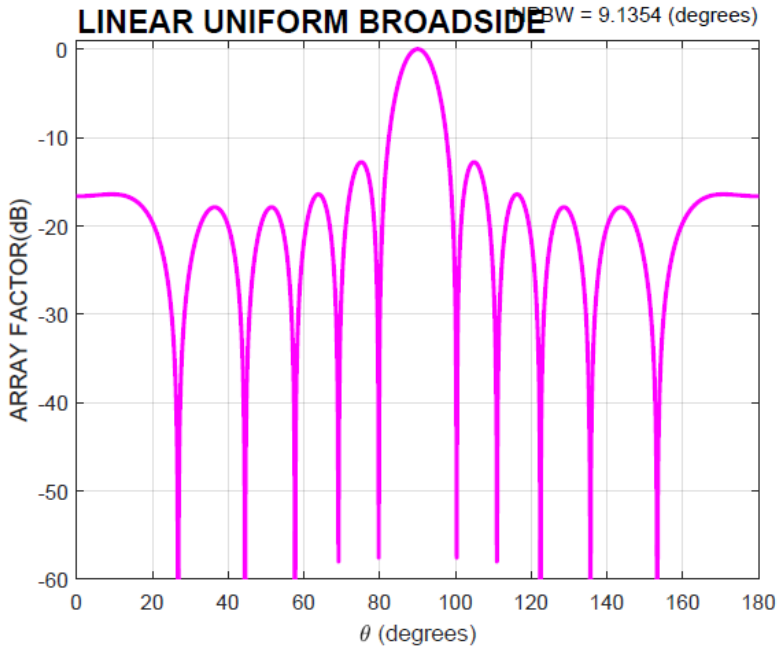

Figure 7.3.2.2.2-2: Eight element ULA response with 0.7 lambda spacing

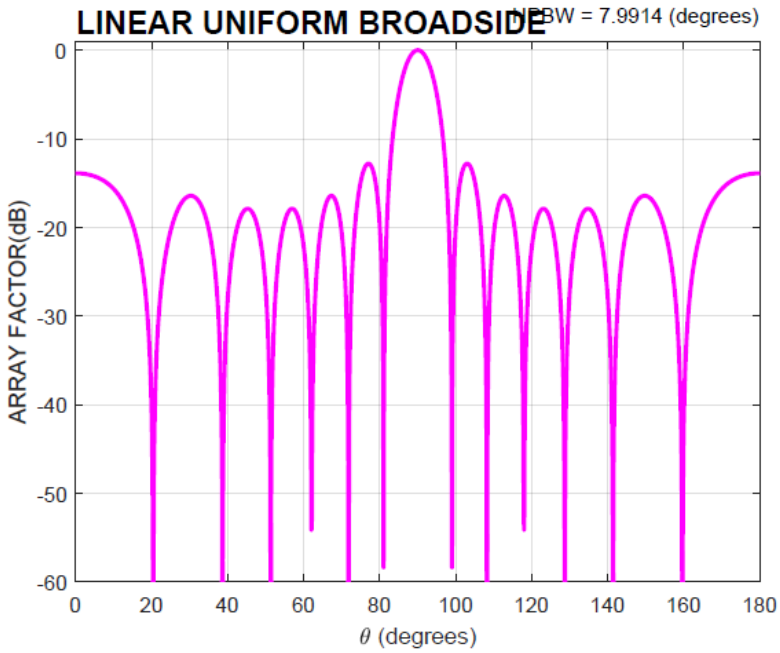

Figure 7.3.2.2.2-3: Eight element ULA response with 0.8 lambda spacing

It is also to be noted that in case of band 2 where the band is very wide (operating bandwidth 1275 MHz) proxy antenna inter element spacings for a carrier at the lower end of the band will almost have a similar impact as the lower adjacent band. Likewise for the upper end of the band.

The above inferences will also remain valid for the second adjacent band.

The above observations will remain valid even if the array is made of sub arrays and the notion that an array may drop down to a sub array in adjacent bands is not valid.

7.3.2.2.3 Modelling of PA non-linearities

Non linearities in hardware in the RF path cause signal distortions- both in band and out of band-(adjacent bands). The nonlinear components in the RF path consist of power amplifiers that are the main cause of nonlinear distortions but other components such as D/A converters, mixers, beam forming circuitry may also contribute to the nonlinear distortions. When antenna arrays are deployed, multiple users may be served by beam forming either in the analog domain or both in the analog and digital domain. Digital beamforming is commonly employed in today's systems- such as zero forcing, MMSE [16]. This results in the placing of nulls in the path of all users except the desired user, but this operation may also cause out of band distortions to fall in unintended spatial directions.

The modelling of PA non linearities has received a lot of interest in the published literature [see 17,18-22 and references therein]. PA behavioural models can be classified as:

- Volterra series based,
- Artificial neural networks,
- Table look up methods,
- Models with linear and nonlinear memory, with and without memory etc.

Ref [17] gives a very good comparison of PA behavioural models in terms of metrics like identification complexity, adaptation complexity, running complexity etc. Measurements on some PAs and the accuracy of the models are presented in [20]. Some commonly used models use polynomials or memory polynomials [18,22], here PA units are modelled via 9th order polynomials whose coefficients are obtained from RF measurements. These papers conclude that the received signal with massive MIMO consists of a desired term with linear gain of the array and also a nonlinear distortion term. Additionally, if the linear response coefficients of the different parallel PAs (in the massive MIMO unit) are different (and they do have small differences), then even the linear signal terms are not fully coherently combining at the receiver. In case of the nonlinear distortion terms, this effect is even more evident as here the phase characteristics of the constituent terms representing the component PAs are different. These two effects manifest in the decrease of the desired instantaneous SINR. When pre-coded multiuser MIMO is used, [21,22] derive analytical models for three different precoder types and for each case derives the received signal. The later now consists of a linear useful signal part and several distortion terms arising from multiuser interference and nonlinear distortion. The conclusion of this paper is:

The choice of a PA behavioural model validated by measurements is needed. Ref [18,19] provide a good framework to model these non-linearities via polynomial models.

The differences in the linear responses of the parallel PAs have a large impact on the system performance. The nonlinear terms do not necessarily adopt the digital predistortion as easily and efficiently. Therefore, the impact of nonlinear power amplifiers is nontrivial both in band and out of band. However, to do this we would need a model for the differences in the PA models in an AAS.

Power Amplifier non linearities should be carefully modelled when considering adjacent channel impacts when MIMO arrays are used. The choice of a PA model should be agreed (say via polynomial models), then it may be validated by measurements and also agree on a model for the differences in the parameters for the distributed PAs.

We may assume for the sake of simplicity there are no differences in the PA model parameters in a distributed PA AAS.

Adjacent band impacts is however not the main focus of [18], but they are considered in [17,18,21]. These papers give the spatial distribution of out of band radiation in the presence of non-linear amplifiers that are modelled by orthogonal polynomials- a special case of the more general Volterra series as described in [17]. Refs [8,21] derive an expression for array ACLR when linear precoding is used with MIMO arrays and a spatial distribution of the ACLR is derived for 1, 2 and 10 users respectively. In particular, [21] develops a framework for rigorous analysis of the spatial characteristics of nonlinear distortion from arrays both in band and out of band. The framework is validated via measurements on a GaN class AB amplifier [23]. It is shown that in the immediate adjacent bands, the third order distortion terms are significant. For a two user MU MIMO case it is shown that the desired signal is beamformed in two directions but the adjacent band distortion signal (arising from PA non linearities) is not beamformed in the same direction as the desired signal. Consideration of this will be important in evaluating the impact of adjacent band victims due to PA non linearities in the operating band.

7.3.2.2.4 Modelling of band pass filters

The filters modelled in some references [15,] use a root raised cosine filter with an excess bandwidth of 0.22. Also, the adjacent channel has the same bandwidth as the operating bandwidth. This is clearly not the case, for all the bands under consideration the operating bandwidths are much larger than the carrier bandwidth. The adjacent channel bandwidth may be saying 100 MHz. However, the framework in [23] can be used to change the bandwidth of the BPF to reflect the operating bandwidth. However, we must specify the bandwidth of the BPF and a model for the BPF.

Annex A (informative): Additional observations for 7125-8400 MHz frequency range

A.1 Impact of higher channel bandwidth on the ACLR/ACS

This Annex presents additional simulation studies to compare the throughput loss% as a function of ACIR for both downlink and uplink transmissions in UMa deployments for both 100MHz and 200MHz, as shown in Figure A.1-1.

NOTE 1: The impact of the higher channel bandwidth on the spectral mask is given in A.2-1.

Note that all the network, BS, and UE parameters follow the adjacent channel coexistence conducted in TR 38.921 [14]. It can be observed that the ACIR required to meet the 5% throughput loss degradation target is nearly identical for the 100 MHz and 200 MHz channel bandwidths. Note that in the above simulations, the conducted power is assumed to be the same for both channel configurations. It is expected that with scaling the conducted power to account for the increased channel bandwidth (i.e., equivalent PSD), the wanted and interfering signal will be scaled accordingly, resulting in comparable ACIR values between the two channel bandwidth configurations. As a result, the BS/ UE ACLR and ACS will not be affected by higher channel bandwidths.

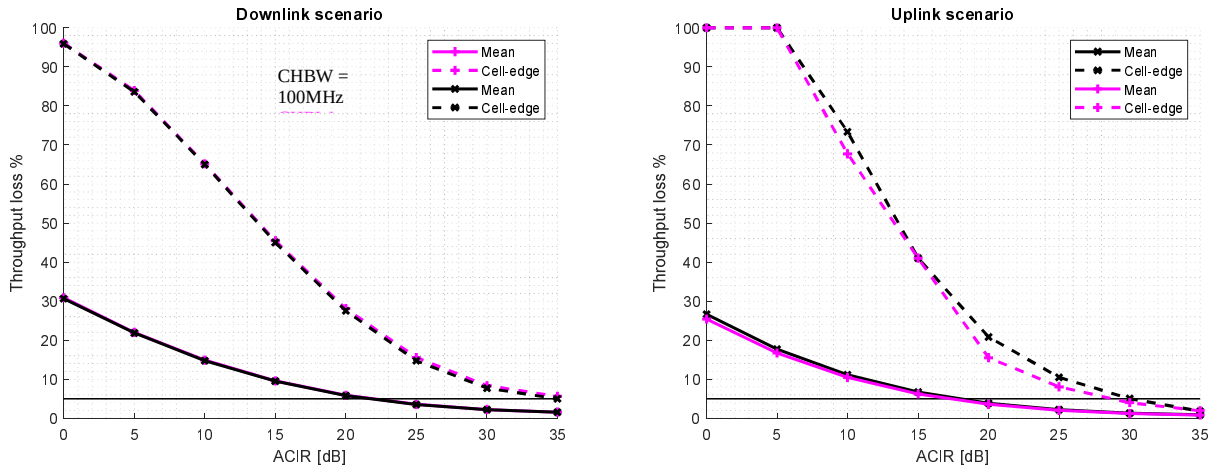

Figure A.1-1 Throughput loss for UMa scenario for 100MHz (black) and 200MHz channel bandwidths (magenta)

A.2 Impact of higher channel bandwidth on spectral emission mask

The BS spectral mask given in Section 5.2.1.2 can be reused for 200MHz channel bandwidth as the BS spectral mask is given as a function of the frequency offset Δf and it is agnostic to the assumed operating channel bandwidth.

The UE spectral mask given in Section 5.3.1.2 can be reused for 200MHz channel bandwidth. Accordingly, the UE spectral mask in Section 5.3.1.2 can be updated to accommodate 200MHz channel bandwidth as given in Table A.2-1.

Table A.2-1: General NR spectrum emission mask

Δf_{OOB} (MHz)	Channel bandwidth (MHz) / Spectrum emission limit (dBm)				Measurement bandwidth
	3	5	10, 15, 20, 25, 30, 35, 40, 45	50, 60, 70, 80, 90, 100, 200	

± 0-1	-13	-13	-13		1 % of channel BW
± 0-1				-24	30 kHz
± 1-5	-10	-10	-10		1 MHz
± 5-6	-25	-13			
± 6-10		-25			
± 5-$BW_{Channel}$			-13		
± $BW_{Channel}$-($BW_{Channel}$+5)			-25		

A.3 Impact of higher channel bandwidth on cumulative in-band and adjacent band emissions.

Based on the observations in sections A.1 and A.2, in case of higher channel bandwidth the amount of emissions in-band and in adjacent-band is expected to be similar or lower compared to the case when 100 MHz channels are used. For the same total transmit power, adopting larger channel bandwidth will lead to lower in-band PSD compared to multiple 100 MHz channels. In terms of adjacent band impact, since the same spectral mask can be reused (as observed in section A.2), the cumulative adjacent band emission is expected to be similar to the case of 100 MHz transmission.

A.4 Impact of higher UE maximum output power on the ACLR/ACS

In order to ensure that the adjacent channel coexistence (i.e., BS and UE ACLR/ACS) derived for PC3 (i.e., UE maximum output power equals 23 dBm) is not impacted when considering higher UE maximum output power (e.g., PC2, with maximum output power equals 26 dBm), we compare the throughput loss % as a function of ACIR for both downlink and uplink transmissions in UMa deployments for both PC3 and PC2 was compared, as shown in Figure A.4-1. Note that all the network, BS, and UE parameters follow the adjacent channel coexistence conducted in TR 38.921 [14]. It can be observed that the ACIR required to meet the 5% throughput loss degradation mark is nearly the same for both PC3 and PC2. As a result, the BS/ UE ACLR and ACS will not be affected by higher UE maximum output power.

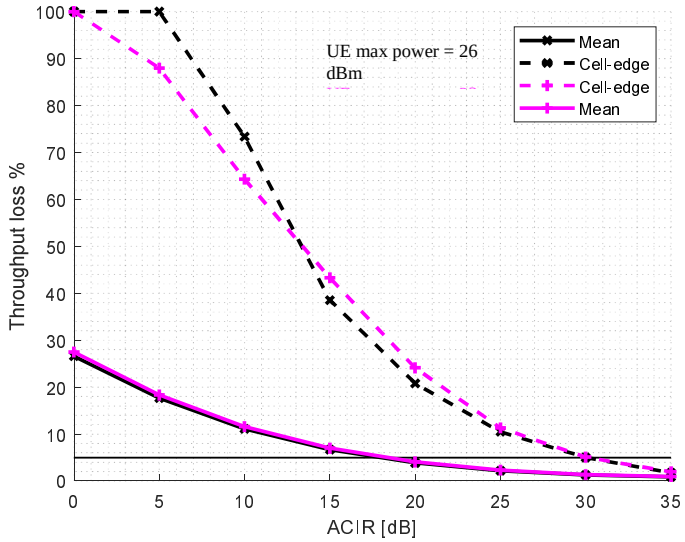

Figure A.4-1 Throughput loss for UL UMa scenario for 23 dBm (magenta) and 26 dBm (black) UE maximum output power

Annex B (informative): Change history

Change history							
Date	**Meeting**	**TDoc**	**CR**	**Rev**	**Cat**	**Subject/Comment**	**New version**
2024-04	RAN4#110bis	R4-2406614				TR skeleton	0.0.1
2024-05	RAN4#111	R4-2408494				Table of contents corrected	0.0.2
2024-05	RAN4#111	R4-2410763				R4-2410722 TP for TR 38.922: Addition of technical background for 4400 to 4800 MHz in clause 4 R4-2410592 TP to TR 38.922: System level simulation methodology and assumptions for co-existence study for 14800 – 15350 MHz frequency range R4-2408083 TP to TR 38.922: Addition of array antenna model description in clause 7	0.1.0
2024-08	RAN4#112	R4-2412608				R4-2412587 TP to TR 38.922: Corrections and clarifications on IMT parameters for 4400 to 4800 MHz frequency range R4-2413278 TP for IMT technology related parameters for 4400 to 4800 MHz R4-2414300 TP for 38.922 on UE IMT parameters for 7125-8400 MHz R4-2414301 TP for BS IMT parameters for range 7125 to 8400 MHz R4-2414303 TP to TR 38.922: Revisions of system level simulation assumptions for study on IMT parameters for 14800 to 15350 MHz frequency range	0.2.0
2024-10	RAN4#112bis	R4-2417200				R4-2417190 TP to TR 38.922: Scope clarification R4-2417102 TP to TR 38.922 Update Clause 1-4 R4-2417103 TP for TR 38.922: Correction on BS IMT parameters for range 7125 to 8400 MHz R4-2417101 Text proposal on 7125-8400 MHz IMT parameters in TR 38.922 R4-2417104 TP for TR 38.922: corrections for 7125 to 8400 MHz frequency range R4-2417105 TP to TR 38.922: Revisions of system level simulation assumptions for study on IMT parameters for 14800 to 15350 MHz frequency range R4-2417106 TP to TR 38.922: Addition of new subclause for MIMO modelling aspects in subclause 7.3	0.3.0
2024-11	RAN4#113	R4-2419346				R4-2420386 TP on coexistence simulation results for 14800 to 15350 MHz frequency range R4-2420387 TP on UE parameters for 14800 to 15350 MHz frequency range R4-2417534 TP to TR 38.922: Corrections and clarifications on IMT parameters for 4400 to 4800 MHz frequency range R4-2417538 TP to TR 38.922: Revisions of system level simulations for study on IMT parameters for 14800 to 15350 MHz frequency range R4-2417874 TP to TR 38.922: Scope clarification R4-2418607 Text proposal on 7125 – 8400 MHz IMT parameters in TR 38.922 R4-2418994 TP to TR 38.922 Updates to Clause 5 R4-2420388 TP on general considerations for the UE antenna parameters for the 14800-15350 MHz frequency range R4-2420389 TP on UE RF design options for the 14800-15350MHz frequency range R4-2420407 TP to TR 38.922: Summary and conclusion for MIMO modelling aspects R4-2420516 TP to TR 38.922: OBUE limits for AAS BS in 7125 to 8400 MHz frequency range R4-2420529 TP for other issues (Adjacent channel modelling) R4-2420390 Discussion on radio and antenna parameters for 14800 to 15350 MHz	0.4.0
2024-12	RAN#106	RP-242945				Presented to RAN for information	1.0.0
2024-12	RAN#106					Editorial corrections	1.0.1
2025-02	RAN4#114	R4-2501512				R4-2502880 TP to TR 38.922 Editorial corrections for 4400 to 4800 MHz frequency range R4-2502881 TP to TR 38.922: Corrections and clarifications on IMT parameters for 7125 to 8400 MHz frequency range R4-2502883 TP to TR 38.922 on parameters for 14.8 - 15.35 GHz frequency range R4-2501862 Co-existence study for 15 GHz R4-2500072 TP to TR 38.922: Simulation results on MIMO modelling R4-2502884 TP to TR 38.922 Editorial corrections for Additional Information on AAS	1.1.0

2025-03	RAN#107	RP-250539				Presented to RAN for approval	2.0.0

Change history							
Date	**Meeting**	**TDoc**	**CR**	**Rev**	**Cat**	**Subject/Comment**	**New version**
2025-03	RAN#107					Approved by plenary – Rel-19 spec under change control	19.0.0
2025-06	RAN#108	RP-250963	0001	1	D	(FS_NR_IMT_4400_7125_14800MHz) Editorial corrections in Annex A title	19.1.0
2025-06	RAN#108	RP-250963	0002		D	(FS_NR_IMT_4400_7125_14800MHz) CR to TR 38.922 on removal of undefined references	19.1.0
2025-06	RAN#108	RP-250963	0004	1	F	(FS_NR_IMT_4400_7125_14800MHz) CR to TR 38.922 on BS antenna pattern for 14800 to 15350 MHz frequency range	19.1.0
2025-06	RAN#108	RP-250963	0005	2	F	(FS_NR_IMT_4400_7125_14800MHz) CR to TR 38.922 on BS blocking response performance requirements for 4400 to 4800 MHz frequency range	19.1.0
2025-06	RAN#108	RP-250963	0006	1	F	(FS_NR_IMT_4400_7125_14800MHz) CR to TS 38.922 on transmission power control model	19.1.0
2025-06	RAN#108	RP-250963	0007	1	F	(FS_NR_IMT_4400_7125_14800MHz) CR to TS 38.922 on corrections and clarifications on IMT parameters	19.1.0
2025-06	RAN#108	RP-250963	0010	1	F	(FS_NR_IMT_4400_7125_14800MHz) CR to TR 38.922 on BS spurious emissions for 4400 to 4800 MHz frequency range and spectral mask for 14800 to 15350 MHz frequency range	19.1.0
2025-06	RAN#108	RP-250963	0011		D	(FS_NR_IMT_4400_7125_14800MHz) CR to TR 38.922 Removal of references to internal TRs and Tdocs	19.1.0
2025-09	RAN#109	RP-252401	0012		F	(FS_NR_IMT_4400_7125_14800MHz) CR to TR 38.922 on correction and clarification on radius of UE dropping within a micro cell	19.2.0
2025-12	RAN#110	RP-253648	0013	1	F	(FS_NR_IMT_4400_7125_14800MHz) CR to TR 38.922: Improvements of description of BS array antenna model in clause 7.1 and 7.3.2	19.3.0

History

Version	Date	Status
V19.2.0	October 2025	Publication
V19.3.0	February 2026	Publication